British Geological Survey

Overseas Geology and Mineral Resources

Number 67

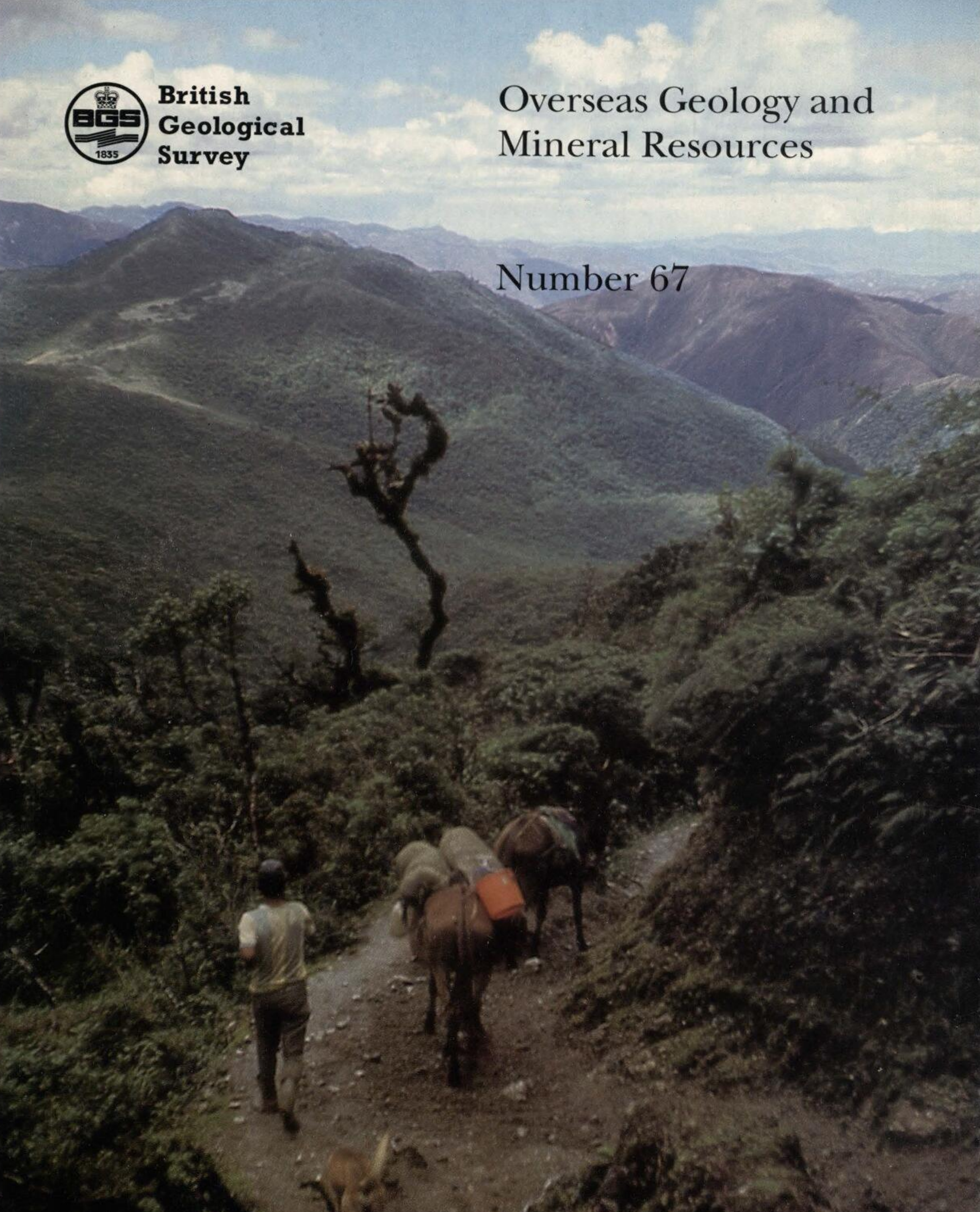

BRITISH GEOLOGICAL SURVEY

Overseas Geology and Mineral Resources

Number 67

The El Oro metamorphic complex, Ecuador: geology and economic mineral deposits

J. A. Aspden, W. Bonilla and P. Duque

CONTRIBUTORS

Whole rock geochemistry
N. J. Fortey and M. G. Gillespie

First published 1995

ISBN 0 85 272242 7

Keyworth, Nottingham British Geological Survey 1995

Bibliographic reference

Aspden J. A., Bonilla W., and Duque P. (1995) The El Oro metamorphic complex, Ecuador: geology and economic mineral deposits. *Overseas Geology and Mineral Resources*, No. 67.

Authors

J. A. Aspden
British Geological Survey
Keyworth
Nottingham NG12 5GG
United Kingdom

W. Bonilla
CODIGEM
Ministerio de Energía y Minas
Quito
Ecuador

P. Duque
Escuela Politécnica Nacional
Casilla 2759
Quito
Ecuador

Contributors
N. J. Fortey and M.G. Gillespie
British Geological Survey
Keyworth
Nottingham NG12 5GG
United Kingdom

Cover photograph
Stunted cloud forest, southern Ecuador
(*C. Mortimer, BGS*)

CONTENTS

PLATES

FIGURES

TABLES

MAPS

The El Oro metamorphic complex, Ecuador: geology and economic mineral deposits

J. A. Aspden, W. Bonilla and P. Duque

ABSTRACT

Reconnaissance 1:100000 scale geological mapping, backed-up by selected geochronological and whole-rock geochemical data, has confirmed that the 2400 km^2 area of the El Oro metamorphic complex in south-west Ecuador comprises rock types/assemblages of differing ages, distinct metamorphic histories and of both continental and oceanic affinities.

To the south of the Zanjón-Naranjo fault the oldest element of the complex (Tahuín semi-pelitic division) is of probable Palaeozoic age and consists of arkosic turbidites. During Late Triassic time these rocks were variably affected by both a dextral transpressional shearing event and by regional Abukuma-type metamorphism the intensity of which increased markedly towards the (present-day) north. At this time a suite of migmatites and granitoids of predominantly S-type character were emplaced (Moromoro granitoid complex) and these rocks are spatially and temporally associated with relatively primitive, mantle-derived gabbroic magmas (Piedras mafic complex).

North of the Zanjón-Naranjo fault is the Palenque mélange division, a regionally extensive, heterogenous unit comprising a matrix of low-grade metasediments, normally greenschists, which contains a variety of large, kilometre-scale, fault-bounded blocks as tectonic inclusions. Several of these inclusions consist of lithologies that are identical to those that occur to the south of the Zanjón-Naranjo fault, however others such as the blueschist/eclogite assemblages of the Raspas ophiolitic complex are clearly exotic.

Together the El Oro metamorphic rocks are interpreted to represent a portion of an accretionary prism complex which elsewhere in the Northern Andes is largely buried by younger volcanic deposits. In Ecuador the eastern limit of this complex coincides with the Baños-Las Aradas fault which also defines the probable western autochthonous limit of the Cordillera Real. Although certain elements of the El Oro metamorphic complex may be far-travelled, others such as the Moromoro granitoids/migmatites and Piedras amphibolites, are considered to be locally derived since they can be correlated with similar lithologies described from the Loja division in the Cordillera Real.

Routine stream sediment sampling over the El Oro metamorphic complex has also been undertaken and the results obtained from 172 samples, analysed for 27 elements plus gold, are presented as point source information.

Within the metamorphic complex itself metallic mineral showings of potential economic interest are relatively limited but gold-bearing quartz veins/stringers occur in Estero Sacachispas; metre-scale rhodonite-bearing quartz lenses are known from Estero Puerto Balsas and stibnite-bearing quartz veins are currently being exploited at Loma Larga. In addition, minor amounts of alluvial gold are worked from the Río Naranjo and its north bank tributaries and to a lesser extent from the Río Arenillas.

Towards the contact with the Tertiary volcano-plutonic complex there are a number of polymetallic occurrences which are actively worked, principally for gold, the most important being Portovelo/Zaruma in the east. Recent discoveries of gold mineralisation at Cerro Pelado, immediately to the north of the abandoned El Antimonio and Guayabo mines, together with small-scale operations at Los Ingleses, Cerro Azul, Daucay and Ligzhu underline the potential importance of the zone. Alluvial gold is widespread and the Los Lilenes deposit is worked commercially. High stream sediment gold values (i.e. >10 ppb and up to >1000 ppb) are common throughout this sector.

Feldspar (for use in the ceramic industry) and brick clays are extracted from the Marcabelí pluton.

INTRODUCTION

Background

The Cordillera Real Project, planned by the British Geological Survey and undertaken by Ecuadorian and British geologists during the period 1986-1993, was a bilateral Technical Co-operation Programme between the governments of Ecuador (Instituto Ecuatoriano de Minería – INEMIN, now renamed Corporación de Desarrollo e Investigación Geológico-Minero-Metalúrgico – CODIGEM, Ministry of Energy and Mines) and the United Kingdom of Great Britain and Northern Ireland (Overseas Development Administration – ODA).

ODA participation in geological development projects in Ecuador began in 1969 and the first residential mission was established in Quito in 1972. On completion of this earlier phase of work in 1980, five ODA geoscientists and their Ecuadorian counterparts had carried out a programme of systematic geological mapping and mineral investigation over western Ecuador which resulted in the publication of four 1:25000 scale: four 1:50000 scale; fifty-one 1:100000 scale geological map sheets and a revised 1:1000000 scale national geological map.

The Cordillera Real Project commenced in March 1986 in response to Ecuador's strategic need for a reliable geological/minerals database in order to attract foreign investment and help establish a viable mining industry. Consequently, systematic geological and mineral studies were extended eastwards to cover the Cordillera Real. In 1990 the Technical Co-operation Programme was amplified to include the reconnaissance geological mapping and stream sediment sampling of the El Oro metamorphic complex. This Project, carried out between June 1990 and March 1993, is the subject of the present report.

In addition to the specific geological, geochemical and geochronological results presented in this report, the Project collection of rock specimens and some 400 thin sections has been donated for teaching purposes to Professor Pablo Duque of the Escuela Politécnica Nacional, Quito. This material is available for study by interested parties.

Description of the area

As shown on the accompanying geological map, the El Oro complex of metamorphic rocks is located in southwestern Ecuador immediately east of the Tumbes region. The national boundary with Perú is disputed. The complex crops out principally in the El Oro Province but extends to the south of the Río Puyango/Pindo, and westwards into Perú. Eastwards towards El Cisne (Figure 1), it extends into Loja Province.

The margins of the complex are irregular, its main outcrop covers an area of about 2400 km^2 and it is approximately bounded in the north and south by latitudes 3°18'S and 3°55'S and in the east and west by longitudes 79°25'W and 80°10'W.

The climate of the area is determined largely by the effect of altitude; which is generally below 1500m, but varies from less than 100m in the north and west to more than 3000m in the extreme east; and the contrasting influences of the Humboldt and El Niño offshore currents. In normal summers the cold, high-salinity Humboldt current of the southern Pacific is displaced northwards between May and November and produces cooler air masses, with dominantly cloudy conditions. Precipitation often falls as drizzle and rainfall decreases from the higher ground in the east towards the south and west, where dry to semi-arid conditions prevail. In winter (December-June), the influence of the warm El Niño current is dominant and hot, water-saturated air which covers the region gives rise to heavy, torrential downpours, interspersed with clear skies. Flooding and landslips are common, humidity is high and insect life abounds, especially in the lower-lying, western parts close to Perú. Field conditions during this period are often difficult and unpleasant.

At higher elevations around Chilla and El Cisne (Figure 1), pockets of stunted cloud-forest remain on the steeper slopes but elsewhere much of the original tropical to semi-arid forest cover has been cleared to give access for agricultural use. Grassland and/or scrub are now dominant, particularly in the drier west and south. Selected climatic data for the area are given in Table 1.

Agriculture is extremely important especially in the flat-lying coastal plain to the north and west. The El Oro province is the principal Ecuadorian producer of export bananas and the second most important national producer of shrimps which are farmed extensively along the coast. Many of the larger cattle ranches are located on the lower hills immediately surrounding the coastal plain. To the south and west of Arenillas dry conditions prevail and there are plans to irrigate this zone using the recently constructed Tahuín dam (Figure 1).

Inland, slopes are often steep and farms tend to be small, with much of the agriculture being at subsistence level. Cattle farming is dominant but goats are commonly herded in the more arid areas. Pineapples are grown extensively in the semi-arid El Prado area but, where rainfall permits, cocoa and coffee are important cash crops, as are tomatoes and peppers in the west. Bananas, maize, citrus fruits, sugar cane, together with lesser amounts of soya beans and peanuts, are extensively cultivated. Chicken farming is of local importance around Balsas.

The larger centres of population (Pasaje, Santa Rosa and Arenillas, Figure 1) are located along the coastal plain. Machala, the provincial capital, is the main financial, military and administrative centre of this region. It is also an important port, particularly for the export of bananas and shrimps. The fast-expanding frontier town of Huaquillas, in the west, is a commercial centre of both local and national importance since it provides the only road link between Ecuador and Perú.

In addition to agricultural support industries, gold mining is of considerable economic significance. The principal hard-rock production comes from the Portovelo/Zaruma and Ayapamba districts and recent discoveries to the south of Bella María, in the Cerro Pelado area (Figure 1), are also being exploited. At Bella María (Los Lilenes) auriferous gravels are currently being worked by Ecuminas/ODIN.

Figure 1. Location Map

Table 1. Selected climatic data from El Oro Province*

	Jan	Feb	March	April	May	June	July	Aug	Sept	Oct	Nov	Dec
RAINFALL (mm)												
STATION MARCABELÍ												
avg.	190	286.3	322.6	275.7	107.7	40.6	7.8	9.4	71.1	21.4	30.2	117.4
min.	31.8	73.6	41.0	40.0	-	-	-	-	-	-	-	-
max.	540.4	555.3	674.4	682.9	303.6	208.4	46.9	31.1	51.1	91.0	187.4	742.9
STATION SANTA ROSA												
avg.	92.4	149.0	148.4	73.5	24.7	12.5	17.8	11.3	15.1	18.6	51.0	23.5
min.	2.1	2.6	-	17.9	-	-	1.5	-	7.6	-	-	-
max.	466.5	377.5	252.5	149.0	64.3	33.3	107	24.8	24.6	57.1	300.5	113.9
STATION ZARUMA												
avg.	212.4	237.0	307.4	221.8	108.9	25.4	6.8	6.5	25.7	40.5	34.7	142.9
min.	48.5	88.8	106.3	37.8	-	-	-	-	-	1.9	-	5.4
max.	361.1	441.0	552.3	484.2	336.2	99.1	27.5	35.6	108.0	143.3	156.1	347.2
TEMPERATURE (°C)												
STATION MARCABELÍ												
avg.	23.2	24.2	24.2	23.2	22.7	23.2	22.8	22.1	22.2	22.2	22.9	23.1
min.	23.2	23.8	23.7	23.2	22.7	22.0	22.0	21.4	22.2	22.0	22.4	22.6
max.	23.2	24.5	24.6	23.2	22.7	24.4	23.6	22.9	22.2	22.5	23.4	23.6
STATION SANTA ROSA												
avg.	25.8	25.9	26.3	26.4	26.0	25.3	25.0	25.5	24.2	26.2	25.3	25.2
min.	25.2	25.3	25.8	25.7	25.7	24.0	24.2	-	-	-	-	-
max.	26.3	26.8	26.8	27.3	26.6	26.1	26.2	26.0	24.3	26.2	25.4	26.2
STATION ZARUMA												
avg.	21.2	21.2	21.4	21.5	21.4	21.3	21.7	22.2	22.4	22.1	22.2	21.9
min.	19.6	19.9	20.3	20.7	20.5	20.0	20.2	21.3	21.8	20.4	20.6	20.6
max.	21.9	23.2	22.6	22.1	22.3	22.2	22.9	23.2	23.7	23.2	23.4	23.1

*Data provided by INAMHI – División de Informática

Access and map coverage

Compared with other parts of Ecuador there is a fairly dense network of roads and tracks that provide reasonable 4-wheel drive access. The all-weather, surfaced, Pasaje-Cuenca road runs along the lower reaches of the Río Jubones valley and skirts the northern edge of the El Oro metamorphic complex. Southwards from Pasaje this road continues, via Santa Rosa and Arenillas, to Huaquillas. Southwards from Arenillas the generally all-weather, Alamor road crosses the southern part of the metamorphic terrain. From Zaracay, (via Santa Rosa and La Avanzada), two all-weather, partially surfaced roads lead to Loja, one via Piñas/Portovelo and the other via Balsas/Chaguarpamba. Apart from these major arterial roads there are also numerous, unsurfaced secondary roads/motorable tracks, some of which are shown in Figure 1. These are variably maintained and can be impassable following heavy rain. In the east, between Chilla and Pasaje, and in the El Cisne – El Prado – Salati area, road access is limited, but these parts are serviced by a reasonable network of mule-tracks and footpaths. Since the completion of the Tahuín dam in the late 1980s road access along the Río Naranjo, to the west of Piedras, is no longer possible.

Complete 1:50000 scale topographic base maps and almost complete, relatively cloud-free, airphotography (nominal 1:60000 scale) coverage of the El Oro metamorphic complex are available. These are indicated on the accompanying geological map and can be purchased from the Instituto Geográfico Militar (IGM) in Quito. Partial Synthetic Aperture Radar Imagery (SAR) coverage also exists for the western part of the area and can be obtained from Centro de Levantamiento Integrado de Recursos Naturales por Sensores Remotos (CLIRSEN), Quito. The 1:100000 scale topographic base map used in this study was prepared by the Project since topographic maps at this scale are currently unavailable in Ecuador.

Due to its situation close to the disputed frontier with Perú much of the El Oro Province is militarily sensitive. The purchase of maps etc., especially those of the western part of the Province, must be accompanied by letters of permission from the appropriate authorities in Quito. Immediately to the east of the disputed Peruvian frontier, to the south of the Arenillas-Huaquillas road and to the west of the Arenillas-El Alamor (Puyango) road (Figure 1), there is an 'exclusion' zone. Special permission must be obtained to enter this area from the military in both Quito and the provincial capital Machala.

Acknowledgements

This study undertaken between June 1990 and December 1993 formed part of the 7-year (1986-1993) Cordillera Real Project, a bilateral Technical Co-operation Programme between the UK and Ecuador. Funding was provided by the Overseas Development Administration of the British Foreign and Commonwealth Office and CODIGEM of the Ecuadorian Department of Energy and Mines. The authors would like to acknowledge the contribution of all CODIGEM staff and especially Carlos Muirragui for his support and encouragement. Particular thanks are due to Fabiola Alcocer, Ramiro Bermúdez, Victor Acitimbay and Manuel Célleri for their loyal and courageous support throughout. The text and map have benefitted from comprehensive reviews by Cedric Mortimer, Martin Litherland and Rob Evans.

J. Aspden would also like to thank all the members of the British Embassy in Quito for their help and the administrative back-up they provided during his 7-year stay in Ecuador.

GEOLOGICAL UNITS OF THE COMPLEX

GENERAL SETTING

The Northern Andes of Ecuador and Colombia strike NNE-SSW and are separated from the NW-SE-striking Central Andes of Perú by the Huancabamba Deflection (Gansser, 1973). According to Megard (1989) one of the major features of this zone of transition, which he refers to collectively as the Huancabamba Andes, 'is the presence of a probable accreted microcontinent … the Amotape – Tahuín terrane', which crops out in northwest Perú and in south-west Ecuador as the El Oro metamorphic complex. More recent work carried out in these areas (Litherland et al., 1994; Aspden and Litherland, 1992; Jaillard et al., 1990), including that of this Project, has resulted in the re-interpretation of the Huancabamba Deflection and, as shown on the accompanying geological map, a more precise definition of the main 'geo-tectonic' elements of this structure is now possible.

In Ecuador, as elsewhere, the contact between the 'Amotape – Tahuín terrane' and the main Cordillera is obscured by younger deposits. However, within the context of the Northern Andes the El Oro metamorphic complex is clearly anomalous. Structural trends are east-west, which contrast markedly with the NNE-SSW strike of the Cordillera Real immediately to the east, and it comprises a variety of low- to high-grade metamorphic rocks, of both continental and oceanic affinity. The complex includes what have generally been considered to be some of the oldest known rocks in Ecuador and, in addition, it contains outcrops of blueschists and eclogites, lithologies that are rare throughout the Northern Andes and, at present, unknown elsewhere in Ecuador.

In the north-west, the complex is covered by largely unconsolidated Late Tertiary to Quaternary deposits of the coastal plain, and along the Jubones valley its northern limit is defined by the east-west-trending Jubones fault. In the east and south it is intruded, and/or overlain, by a major Tertiary volcano-plutonic complex and by the Cretaceous sediments of the Alamor basin.

To the north and east of the main outcrop, for example in the Chaucha and Manú areas, inliers and/or float blocks of metamorphic rocks, have also been recorded (Aspden and Litherland, 1992; Aspden et al., 1988; Feininger, 1987; INEMIN-Misión Belga, 1989; Kennerley et al., 1973). The details of such occurrences remain relatively unknown but the available information suggests that these rocks are lithologically and mineralogically comparable with those found within the El Oro metamorphic complex.

Reconnaissance 1:100000 geological sheet mapping of the El Oro and Loja Provinces was first completed between 1969 and 1981 as part of an earlier bilateral Technical Co-operation Programme between the governments of the United Kingdom and Northern Ireland (ODA) and Ecuador (Dirección General de Geología y Minas – DGGM; Ministry of Energy and Mines). Also, during this period Dr. Tomas Feininger, together with various students from the Escuela Politécnica Nacional in Quito (Almeida, 1977; Sevilla, 1976, Duque, 1975), carried out detailed mapping of the western part of the El Oro metamorphic complex which resulted in the publication of a 1:50000 geological map (Feininger, 1978). This work is indexed on the accompanying geological map.

Late Jurassic to Early Cretaceous	**PALENQUE MÉLANGE DIVISION** Mixed unit comprising metasedimentary matrix and various older (Late Triassic) granitoids and amphibolites, serpentinites and a major HP/LT blueschist complex as tectonic inclusions	
Late Triassic	**MOROMORO GRANITOID COMPLEX** Various granitoids, migmatitic units and plutons of S-type character **PIEDRAS MAFIC COMPLEX** Amphibolitic metaigneous unit	Fragments also occur as tectonic inclusions in Palenque mélange division
Palaeozoic	**TAHUÍN SEMI-PELITIC DIVISION** Unmetamorphosed to high-grade, semi-pelitic sequence	Metamorphosed in Late Triassic

Figure 2. Summary of stratigraphic nomenclature

Some of the information from these earlier studies, especially that from along the frontier zone with Perú has been used to augment that collected during the current study. Equally, some of the geological contacts in the immediate area of Cerro Pelado (Figure 1) are taken from the work of Plateau Mining Company. It is emphasised however, that the interpretation of these data is the sole responsibility of the present authors.

As a result of this earlier work a pre-existing, in part, formal stratigraphic nomenclature had already been established for the El Oro metamorphic complex but in the present study an informal system, summarised in Figure 2, is preferred. Hence the terms division/complex/unit replace those of Group/Formation. In some instances, it has also proved necessary to redefine and/or subdivide, some of the original rock groupings of previous workers but, where possible, names that are in common usage have been retained. These changes are detailed in Figure 3.

Formal stratigraphical nomenclature in the sense of, for example, the North American Stratigraphic Code (NACSN, 1983) and its recommendations for sedimentary and igneous rock unit definition could not be followed because of lack of data on thickness of units, their diffuse and tectonised contacts, their variable metamorphic changes and their irregular forms.

The geology of the El Oro metamorphic complex is illustrated in the accompanying geological map and in the following account is described in terms of two informal ‘sub-provinces’ (Figure 4). Sub-province I, located to the south of the east-west-striking Zanjón-Naranjo fault zone, consists of geologically diverse elements belonging to the Tahuín semi-pelitic division, the Moromoro granitoid complex and the Piedras mafic complex. In spite of this diversity, sub-province I is considered to be a coherent block for which an internally consistent stratigraphy and geological history can be recognised.

North of the east-west-striking Zanjón-Naranjo fault zone sub-province II corresponds to the Palenque mélange division, a heterogenous structural complex that includes various, kilometre-scale, fault-bounded bodies as tectonic inclusions. The northern boundary of this sub-province is the east-west Jubones fault.

GEOLOGY OF SUB-PROVINCE I

Tahuín semi-pelitic division

The Tahuín division consists of a variably metamorphosed, semi-pelitic sequence that shows a rapid increase in metamorphic grade from south to north and is named after the Cordillera of Tahuín, a general name applied to the higher elevations in the western part of the El Oro Province lying to the south of the valleys of the Ríos Naranjo/Arenillas*. It forms an east-west-striking, 10-20 km-wide belt that can be traced continuously for about 80km from the Perú borderland in the west, eastwards into the El Cisne area. The division has been divided into two informal units – El Tigre in the south and La Victoria in the north.

*El Tigre unit (Las Lajas 609/9578) **

The El Tigre unit consists of an unmetamorphosed to weakly metamorphosed sequence comprising poorly sorted, immature, fine- to medium-grained, quartz-rich arkoses, feldspathic quartzites and wackes, with interbedded lutites and siltstones. Apart from river sections, the El Tigre unit is typically deeply weathered but reasonably fresh, semi-continuous outcrops do occur along the Arenillas-Alamor road, between the small settlement of El Tigre, after which the unit is named, and the Río Puyango, and also along the Portovelo-Loja road to the south of El Prado. In the south, the El Tigre unit is overlain unconformably by the Cretaceous sediments of the Alamor basin (Baldock, 1982; Feininger, 1978). This contact is particularly well exposed to the north of the Río Puyango along the Arenillas-Alamor road (Plate 1) but further to the east near El Cisne it has been affected by a series of NNE-SSW-trending faults belonging to the Guayabal fault zone (Figure 4) and precise relationships are more difficult to establish. To the north, the El Tigre unit passes into the metamorphosed La Victoria unit, details of which are discussed below.

In addition to quartz and feldspar (the latter usually altered to sericite), these rocks also contain minor amounts of biotite, muscovite and green or brown tourmaline. Intraformational lutite clasts, which vary from submillimetre to several tens of centimetres in size, are common, especially in the coarser arenaceous beds, some of which are probably composite since they reach several metres in thickness.

Well-preserved, sedimentary structures within the El Tigre unit can be observed in various river sections. For example, in the Quebrada Agua Negra to the west of Marcabelí (**Marcabelí 617/9581**), where the sequence is overturned, massive, crudely graded, quartzose wackes, some of which have erosional bases with sole structures and flute casts, pass into finer-grained, cross-laminated and parallel-laminated siltstones. Flame structures, slump folding and slumped, ‘olistostromic’ horizons (Plate 2) are also present. These features suggest that the El Tigre unit is essentially turbiditic in origin and the absence of volcanic material/detritus in these rocks may indicate derivation from a ‘passive’ margin or cratonic source.

* Where appropriate location/place/river names used in the text and those after which the divisions/units etc are named, are indicated in Figure 1. Grid references (UTM) refer to individual 1:50000 topographic sheets which are indexed on the accompanying geological map

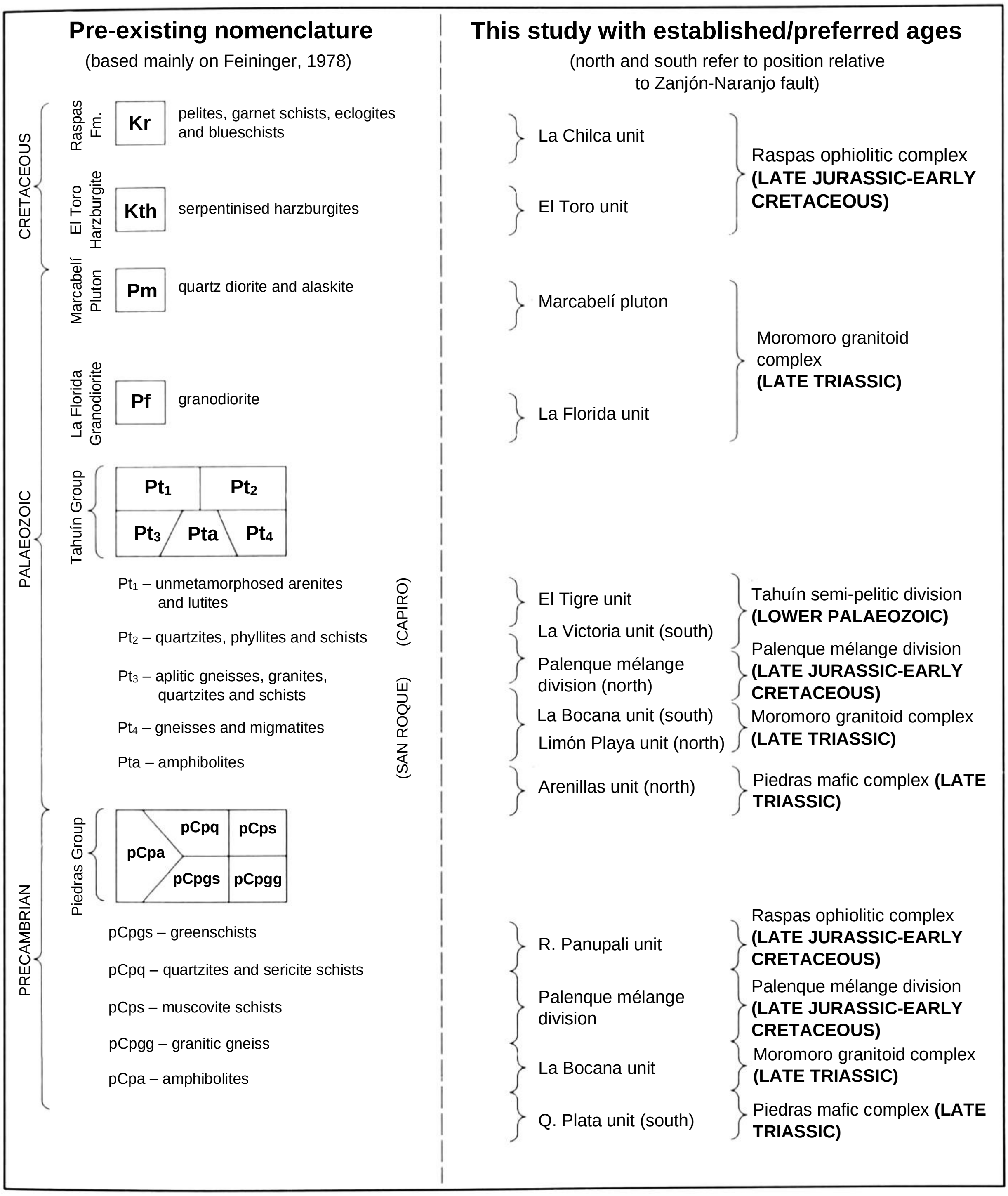

Figure 3. Comparison of pre-existing stratigraphic nomenclature and that used in the present study

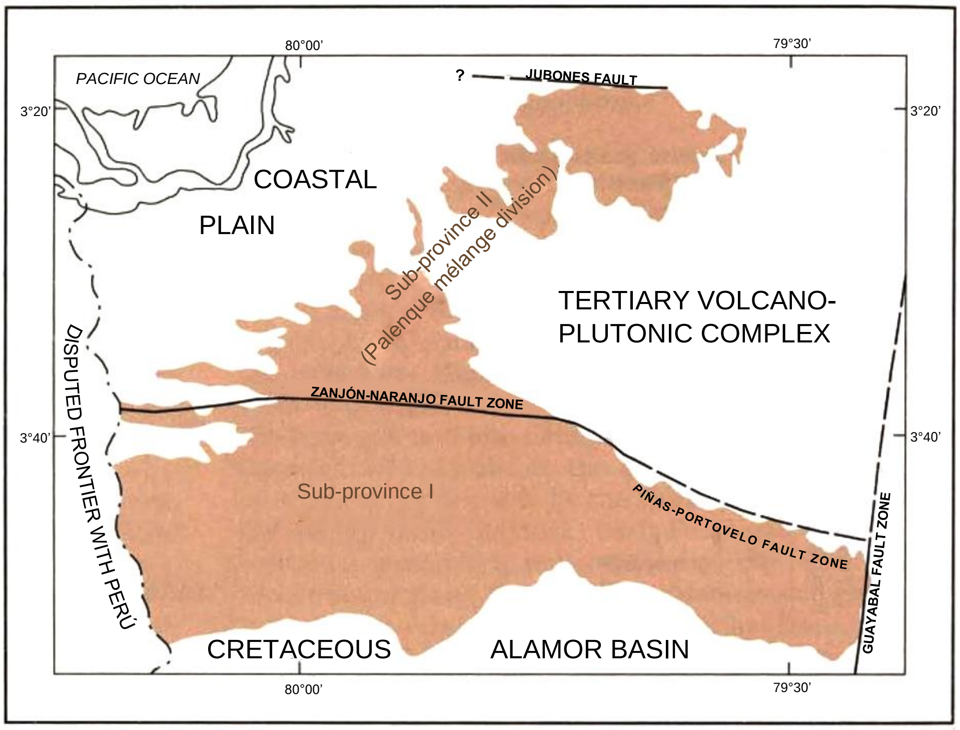

Figure 4. Physiographic setting

Plate 1. Angular unconformity of Cretaceous Alamor basin sequence and El Tigre unit, Tahuín division, new Arenillas-Alamor road c. 1km north-east of Río Puyango road bridge.

Plate 2. Slump folding in turbiditic El Tigre unit, Tahuín division, Quebrada Agua Negra c. 1km south of San José.

La Victoria unit (Las Lajas 604/9582)

The La Victoria unit comprises a variably metamorphosed semi-pelitic sequence that is interpreted to represent the northern equivalent of El Tigre unit. The main Arenillas-Alamor road, immediately to the east of La Victoria provides a section across the La Victoria unit, but outcrops are of varying quality and often weathered. Fresh outcrops occur between Las Lajas and La Victoria, and to the south of La Victoria in the Quebrada Lajas. Further to the east, excellent partial sections are exposed in the Quebrada Primavera, downstream from La Primavera, and also between El Ingenio and Marcabelí, in the Quebrada Marcabelí. In the Río Moromoro, upstream from the junction of the Quebrada El Oso, the unit is almost continuously exposed but access is somewhat more difficult and necessitates overnight camping.

The contact between the La Victoria and El Tigre units is complex and, in part, gradational. However, it is generally marked by the incoming of a regionally developed cleavage and/or the appearance of metamorphic biotite (see also Feininger, 1978). The contact coincides with an important, approximately east-west-trending, 'tectonic' zone which, in the west, is located about 5km south-south-west of La Victoria, in and around the village of Chiriboga. This zone passes eastwards, immediately to the north of Marcabelí and to the south of Capiro, and emerges near the junction of the Ríos Pindo and Amarillo. Further to the east, it is obscured by the El Prado pluton and, in the El Cisne area, by the Guayabal fault zone.

In the south, biotite-bearing slates and phyllites are dominant, bedding is still clearly visible and, in thin section in some of the lower-grade rocks, original clastic textures may still be observed within the more massive, impure, quartzite horizons. Compositionally these rocks appear to be identical to those of the El Tigre unit. Further to the north, the phyllites normally contain small porphyroblasts of sericite after (?)cordierite and/or andalusite. With increasing metamorphic grade, the phyllites are replaced by pelitic schists that are typically composed of biotite ± muscovite, albite and quartz with porphyroblasts of cordierite and/or andalusite. Fibrolite and/or sillimanite (± andalusite, ± garnet) is also commonly developed, especially in the north towards the contact with the Moromoro granitoid complex.

These mineralogical changes, in particular the presence of coarse sillimanite + quartz + plagioclase + muscovite ± biotite ± andalusite ± cordierite ± garnet assemblages, also correspond to the appearance of gneissic/migmatitic lithologies within the La Victoria unit (Plate 3). Many of these gneisses occur either within the Moromoro granitoid complex or are located along its southern contact zone with the La Victoria unit and often contain irregular quartzofeldspathic leucosomes.

Plate 3. Migmatitic paragneiss, La Victoria unit, Tahuín division, near to contact with Moromoro complex, c. 1 km west of San Isidro.

Depositional age of the Tahuín division

The depositional age of the Tahuín division is not well established but it is considered to be Paleozoic, most probably pre-Carboniferous. Approximately 40 samples from the El Tigre unit were examined during this study but none of these contained datable organic remains (Owens, 1992). However, acritarchs and spores recovered from a single sample collected to the south of La Libertad, were assigned a pre-Devonian, possibly post-Ordovician age by Zamora and Pothe de Baldis (1988). A sample of ‘black slate’ collected from below the Cretaceous Cazaderos Formation (Baldock, 1982), in the Río Cazaderos valley, to the south-west of the main Tahuín outcrop in the extreme west of the Loja province, yielded a ‘single possible example of *Emphanisporites* and some unidentified, strongly carbonised, simple spore types which are either laevigate or with a low ornament of cones, spines or baculae. Though no taxa could be positively identified, this is the type of assemblage one could expect to encounter in the Early or Middle Devonian’ (J. E. Whittaker, British Museum-London, personal communication). While the relationship between this sample and the Tahuín division remains uncertain, the presence of a cleavage and its structural position below the Cretaceous Cazaderos Formation, suggest a correlation with the Tahuín division.

In northern Perú at Cerro Amotape, about 140km to the south-west, along strike from the Tahuín division, a similar sequence comprising low-grade quartzites and phyllites has yielded a sparse Devonian brachiopod fauna (Martínez, 1970). Mourier (1988) has reviewed the palaeontological evidence available from this area and points out that, while the Devonian age is uncertain, the discovery of trace fossils (*Cruziana* sp. and *Lophoctenium*) could indicate a lower Palaeozoic age.

The metamorphic age of the Tahuín division, considered to be Late Triassic, is discussed below.

Moromoro granitoid complex (Zaruma 639/9573)

The Moromoro granitoid complex is named after the town of the Moromoro and comprises the La Bocana and La Florida units, and the Marcabelí and El Prado plutons.

La Bocana unit (Marcabelí 622/9592)

The La Bocana unit is a mixed unit that includes a number of different rock types but consist principally of variably foliated fine- to medium-grained, biotite, ± muscovite, ± garnet, ± tourmaline granodiorites, with lesser amounts of migmatites and high-grade paragneisses. It derives its name from the small town of La Bocana and makes up the bulk of the Moromoro granitoid complex. The unit is well exposed in a number of north-south-flowing rivers but the Quebradas Piedras/Primavera, near to the town of La Bocana are almost easily accessible.

Plate 4. Texturally heterogenous granitoid, La Bocana unit, Moromoro complex, Quebrada Palo de Oro. Note the presence of metasedimentary xenoliths, white quartz xenocrysts and irregular zones of diffuse foliation/schlieren

Plate 5. Texturally heterogeneous foliated granitoid, La Bocana unit, Moromoro complex, Quebrada Primavera. Common metasedimentary xenoliths are stretched and flattened parallel to foliation; irregular pale-coloured areas consist mainly of xenocrystic quartz.

Plate 6. Migmatitic granite gneiss, La Bocana unit of Moromoro complex, La Florida area.

Plate 7. Migmatitic granite gneiss, La Bocana unit of Moromoro complex, La Florida area.

In the east, close to El Cisne, the La Bocana unit is truncated by the Guayabal fault zone, and in the north, it is overlain and intruded by a Tertiary volcano-plutonic complex along the Piñas-Portovelo fault zone. Where observed (**La Avanzada 6207/95967; 6266/95961**), the northern contact with the Piedras mafic complex (Quebrada Plata unit, see below) is tectonic. However, the presence of amphibolite xenoliths within the La Bocana unit (**Zaruma 6506/95838; 6477/95895**), and the occurrence of granitic bodies (**Arenillas 5908/95965; La Avanzada 6265/95965**) within the Piedras mafic complex, suggest that this contact was probably originally intrusive.

The main southern contact of the unit with the metasedimentary La Victoria unit is partly gradational but on a regional scale corresponds to a complicated zone of syn- to late-magmatic, dextral shearing (see below) which, especially in the east, has resulted in the tectonic interfingering of lithologies. Where possible, the larger areas of metasediments have been assigned to the La Victoria unit however, as mapped, the La Bocana unit does include at least some paragneisses, many of which are high-grade and show varying degrees of migmatisation.

Plate 8. Unfoliated, late-stage granitic pegmatite cross-cutting foliated granite, La Bocana unit, Moromoro complex, Quebrada Primavera. Note presence of young (Tertiary?) dyke in upper part of photograph.

Plate 9. Irregular pegmatitic apophysis, comprising feldspar, quartz, biotite, muscovite and tourmaline, La Bocana unit, Moromoro complex, Quebrada Primavera.

Further to the south, and contained within the La Victoria unit, are a number of generally strongly foliated, lens-shaped bodies composed predominantly of biotite, ± muscovite, ± garnet granodiorite. These bodies have faulted contacts and often show well-developed, S-C mylonite fabrics (Berthe et al., 1979). These plutons, together with a number of late pegmatitic, generally tourmaline-bearing dykes, which intrude the La Victoria unit, are considered to belong to the La Bocana unit. In the extreme west, a small fault-bounded (c. <500m wide), biotite muscovite granodiorite body, which occurs within the Quebrada Plata unit (see below), to the south of Chacras has also been assigned to the La Bocana unit.

Texturally the La Bocana granodiorites are normally markedly heterogeneous due to the presence of numerous, predominantly metasedimentary, xenoliths that include quartzites, pelitic schists, paragneisses and migmatites (Plates 4 and 5-7). Biotite clasts/schlieren and irregularly shaped clasts of white vein quartz, up to several centimetres across, are also common. Contact relationships between different xenoliths and the granodiorite host vary from being sharp and well defined to diffuse and ghost-like. At outcrop, areas of irregular foliation, and the presence of biotite schlieren, can often be directly attributed to assimilation and/or the break-up of xenolithic material. Mineral assemblages within the metasedimentary, 'restite', xenoliths are variable, but include coarse sillimanite + muscovite + biotite ± andalusite ± cordierite ± porphyroblasts of muscovite (? retrograde after sillimanite) ± garnet, ± K-feldspar. In some areas, for example to the north of La Bocana near Santa Teresita, and westwards towards the Quebrada Tahuín Grande, sillimanite + K-feldspar + muscovite assemblages are present. Also in this area, and to the south of Portovelo in the east, biotite, garnet, ± muscovite granodiorites are widespread. In thin section, some of these granodiorites (e.g. to the south-west of El Blanco, **Marcabelí 611/9594**) contain fresh, euhedral, acicular crystals of coarse sillimanite; whether this mineral is magmatic or xenocrystic in origin has not been established. Irregular apophyses of quartz + feldspar + tourmaline ± biotite ± muscovite pegmatites and late, undeformed, cross-cutting dykes of similar material are common in the La Bocana unit (Plates 8 and 9) and in the extreme west, along the Peruvian frontier, Feininger (1978) recorded the presence of a tourmaline-bearing granodiorite pluton (**Las Lajas 591/9581**).

Downstream of La Florida and La Primavera, in the Quebradas El Guineo and Primavera, several undeformed dykes of intermediate composition cut the La Bocana unit. These intrusions are believed to be related to a younger (Tertiary) event (Plate 8).

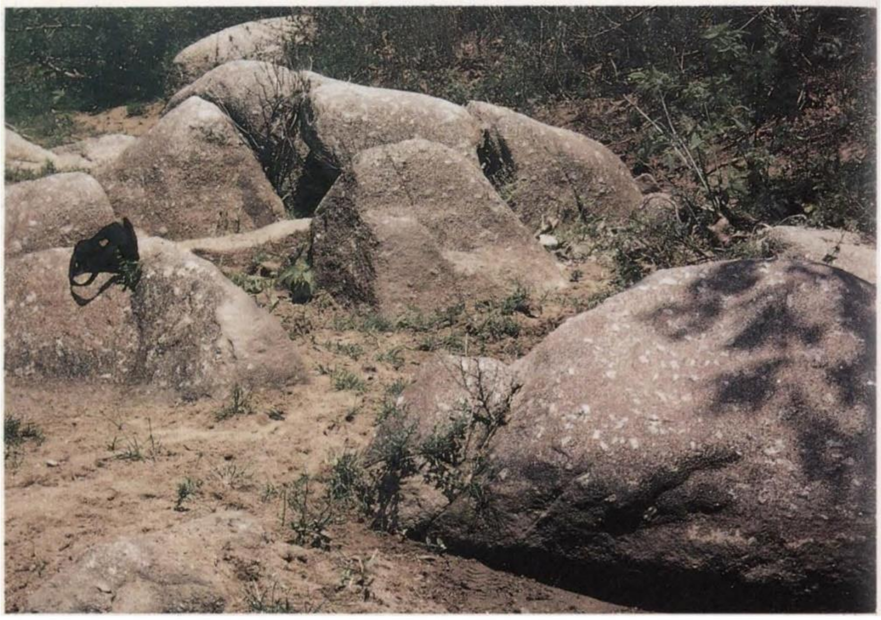

Plate 10. Megacrystic alkali feldspar biotite granite, La Florida unit, Moromoro complex, immediately south of La Florida

La Florida unit (Las Lajas 598/9585)

The La Florida unit takes its name from the small settlement of La Florida situated close to the disputed Peruvian frontier and following Feininger (1978), three plutons belonging to this unit have been mapped in the western part of the Moromoro granitoid complex.

The La Florida unit consists of generally non-foliated, medium- to coarse-grained, alkali feldspar megacrystic, biotite ± garnet granite / granodiorite (Plates 10 and 11). The pale cream-coloured, alkali feldspar megacrysts vary in size and proportion; they are up to 8cm in length and, in hand specimen, frequently display Carlsbad twins. In marked contrast to the La Bocana unit, the La Florida unit is texturally homogeneous and shows good primary igneous textures. It commonly contains metasedimentary xenoliths, which include quartzites, paragneisses and migmatites (Plates 12 and 13). In most cases the contacts of these xenoliths with the host granodiorite are sharp but, in some cases, they are rimmed by irregular, marginal zones of pegmatitic tourmaline + quartz ± biotite ± muscovite. Late dykes of leucocratic two-mica aplites are also present.

Irregular patches of La Florida-type granodiorites, with diffuse/gradational contacts, occur within the La Bocana unit and suggest a similar age and related origin for these granitoids.

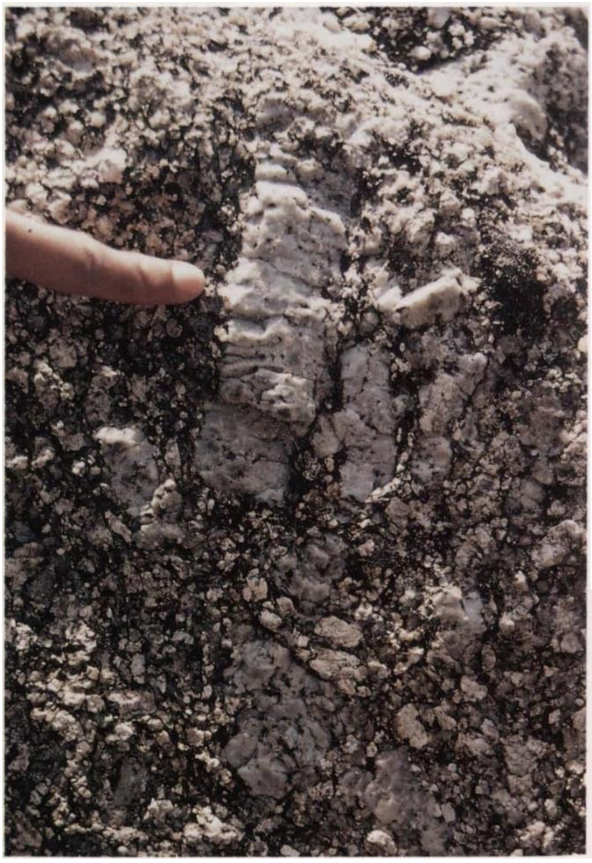

Plate 11. Megacrystic alkali feldspar biotite granite, La Florida unit, Moromoro complex, immediately south of La Florida.

Plate 12. Xenolith of migmatitic granite gneiss in La Florida unit, Moromoro complex, Quebrada Palmales.

Plate 13. Metasedimentary xenoliths with chilled margins, La Florida unit, Moromoro complex, c. 2km south of La Florida

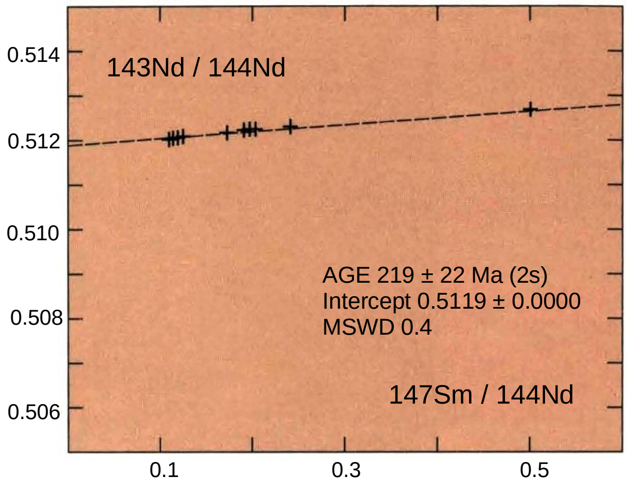

Figure 5. Sm/Nd isochron diagram for garnet-bearing paragneiss, La Bocana unit, Moromoro complex, Río Piedras.

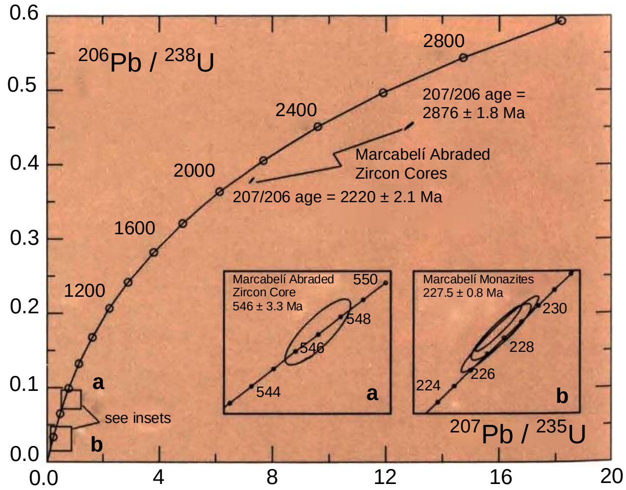

Figure 6. U/Pb concordia diagram for Marcabelí pluton; the crystallisation age of 227.5 ± 0.8 Ma is given by the monazite analyses and strongly abraded zircon cores indicate inheritance of Archean and Proterozoic xenocrysts.

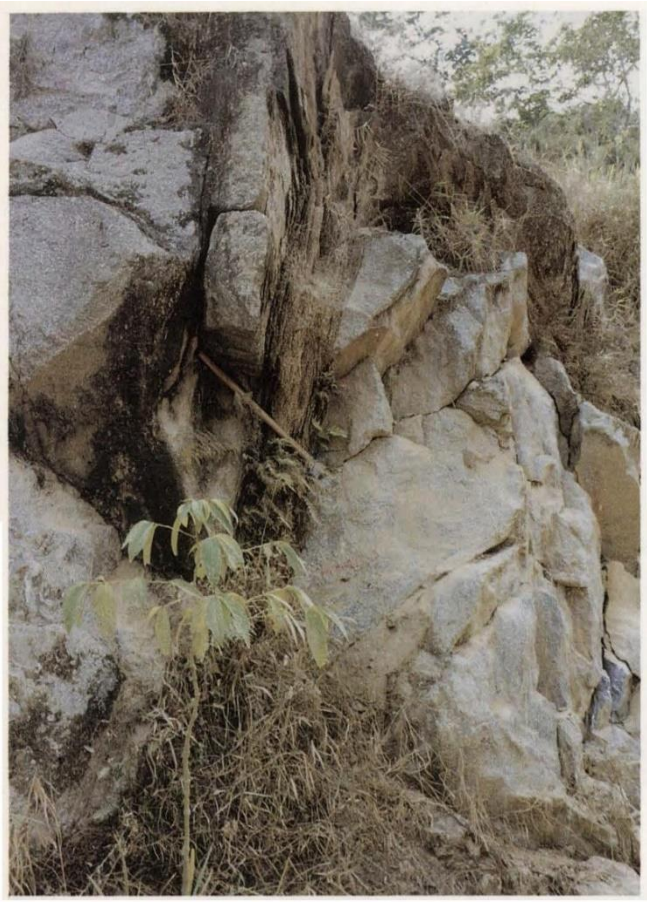

Plate 14. Steep, east-west-trending, ductile shear zone in Marcabelí pluton, c. 1km west of San Roquito.

Marcabelí and El Prado plutons (Marcabelí 621/9582; Zaruma 658/9577)

The Marcabelí and El Prado plutons are located within the Tahuín division and straddle the contact between the La Victoria and El Tigre units. No age dates are available for the El Prado pluton, but its general east-west trend and the occurrence of compositionally and texturally similar granitoids to those observed in the Marcabelí pluton suggest that these two bodies are similar in age. Although in places both plutons are cut by discrete, generally steep, east-west-trending shear zones (Plate 14), they are essentially undeformed, especially in the south where they intrude and contact metamorphose the El Tigre unit. Locally, andalusite is widely developed (Río Balsas, **Marcabelí 6256/95805**). The northern contacts of the plutons have been affected by shearing and their precise limits, and relationship to, the granodiorites of the La Bocana unit require clarification.

The Marcabelí and El Prado plutons are often deeply weathered but consist principally of medium-grained, biotite ± muscovite granodiorites. Both plutons are composite and contain a variety of plutonic phases, the nature of which and their interrelationships remain uncertain. In the west, exposed along the south bank of the Río Puyango (**Marcabelí, 617/9576**), the Marcabelí pluton includes a leucocratic, two mica, topaz-bearing facies. In other areas (to the west of Marcabelí in the Río Marcabelí, **Marcabelí 6194/95811**) medium-grained, hornblende, biotite granodiorites that carry hornblende-bearing xenoliths are exposed. Similar hornblende-rich xenoliths also occur in the Quebrada Milagro (**Marcabelí 6286/95852**), whilst further to the east, exposed in a small quarry near Balsas (**Marcabelí 630/9583**), weakly foliated biotite muscovite granodiorites are present. Similar mineralogical/textural variation can also be observed within the El Prado pluton, which in places (Quebrada Usulaca, **Zaruma 651/9583**), also carries topaz and xenolithic material of igneous origin. Near the village of El Prado and further to the west in the Quebrada Chaupi (**Zaruma 661/9578**) more mafic, hornblende-bearing granodiorites and dioritic variants occur.

Table 2. K-Ar determinations for the Moromoro granitoid complex

Rock type	Area sampled (topographic sheet and grid ref.)	Mineral	K %	Atom 40 %	Rad ^{40}AR (nl/g)	Age (Ma)
LA BOCANA UNIT						
Biotite garnet gneiss	Q. Lobos, near El Carmen (La Avanzada 6194/95950)	Biotite	8.51	-	-	210 ± 8*
Migmatitic, biotite orthogneisses	Q. Piedras, Sta. Teresita area (La Avanzada 6212/95956)	Biotite	6.26	28.24	54.375	211 ± 6
		Muscovite	7.04	11.08	61.822	213 ± 6
		Muscovite	5.68	14.82	48.492	207 ± 6
Biotite muscovite granodiorite	Q. El Negro SSW of La Bocana (Marcabelí 6218/95912)	Biotite	7.47	8.67	66.548	216 ± 6
		Muscovite	8.45	32.94	76.941	220 ± 6
Late tourmaline muscovite granite pegmatite	R. Piedras, La Bocana (La Avanzada 6219/95927)	Muscovite	8.51	15.30	65.994	189 ± 5
MARCABELÍ PLUTON						
Biotite granodiorite	R. Puyango at mouth of Q. Marcabelí (Marcabelí 6173/95771)	Biotite	7.78	-	-	214 ± 6*
Biotite muscovite granodiorite	Balsas quarry (Marcabelí 6308/95837)	Biotite	7.50	72.05	61.798	201 ± 12
		Muscovite	8.41	9.72	74.353	214 ± 6
Biotite muscovite granodiorite	Road to R. Puyango SW of Marcabelí (Marcabelí 6188/95775)	Biotite	7.65	7.06	70.042	221 ± 6
		Muscovite	7.00	74.92	55.487	193 ± 13

Data from Aspden et al., 1992 and *Feininger and Silberman, 1982

In both the Marcabelí and El Prado plutons, undeformed basic dykes and minor intrusions are present. In some areas these rocks are remarkably fresh (e.g. the blocks of 'basaltic' material seen in the village of El Prado) and, in view of the fact that the main El Prado pluton is normally strongly weathered, such intrusives are very probably younger and unrelated to the Moromoro granitoid complex.

Age of La Bocana unit and Marcabelí pluton

The available K-Ar biotite and muscovite mineral ages from the La Bocana unit and the Marcabelí pluton are listed in Table 2. With the exception of a somewhat younger date of 189 ± 5 Ma, obtained from a float block of late tourmaline muscovite granite pegmatite, the La Bocana ages range between 207 ± 6 and 220 ± 6 Ma (mean 213 ± 6 Ma). A Sm/Nd whole-rock/garnet isochron age of 219 ± 22 Ma (MSWD = 0.4) has also been obtained from garnet-bearing paragneisses within the La Bocana unit, collected from the Río Piedras near to Santa Teresita (Aspden et al., 1992 and Figure 5). The K-Ar data from the Marcabelí pluton range from 193 ± 13 to 221 ± 6 Ma (mean 209 ± 9 Ma).

Recently, a U/Pb (monazite) age has confirmed a slightly older, Late Triassic age for the Marcabelí pluton of 227.5 ± 0.8 Ma, and inherited zircon ages which range from 0.546 to 2.876 billion years indicate the presence of a component of reworked crustal material (Noble et al., 1994) (Figure 6).

Piedras mafic complex (La Avanzada 620/9598)

The Piedras mafic complex is named after the area which surrounds the small settlement of Piedras. In sub-province I, rocks belonging to this intrusive complex have been assigned to the Quebrada Plata unit.

Quebrada Plata unit (La Avanzada 634/9596)

Lithologically the Quebrada Plata unit comprises variably textured, massive to gneissic, fine- to coarse-grained, generally mafic, saussuritised metagabbros (now mainly amphibolites) consisting of pale green hornblende and/or actinolite, plagioclase (oligoclase-andesine), epidote and minor amounts of quartz, opaques, ± sphene, ± rutile, ± clinozoisite. In the east, along the Zanjón-Naranjo fault zone, the unit includes some greenschists and in the south, along the contact with the La Bocana unit, pegmatitic amphibolites are common.

The area around the lower reaches of the Quebrada Plata provides both river and road sections across this unit. Excellent outcrops also occur in the Quebrada Piedras, north of Santa Teresita and in the Río Zaracay (**La Avanzada, north of 6266/95961**). In the case of the Quebrada Piedras, outcrops are now being progressively drowned by the rising waters of the Tahuín reservoir.

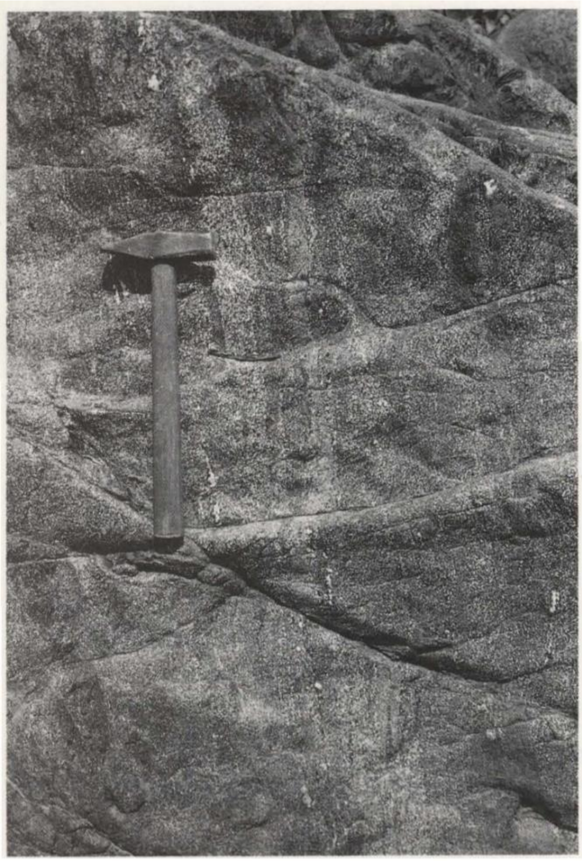

Plate 15. Relict igneous banding, Quebrada Plata unit, Piedras complex, Río Piedras

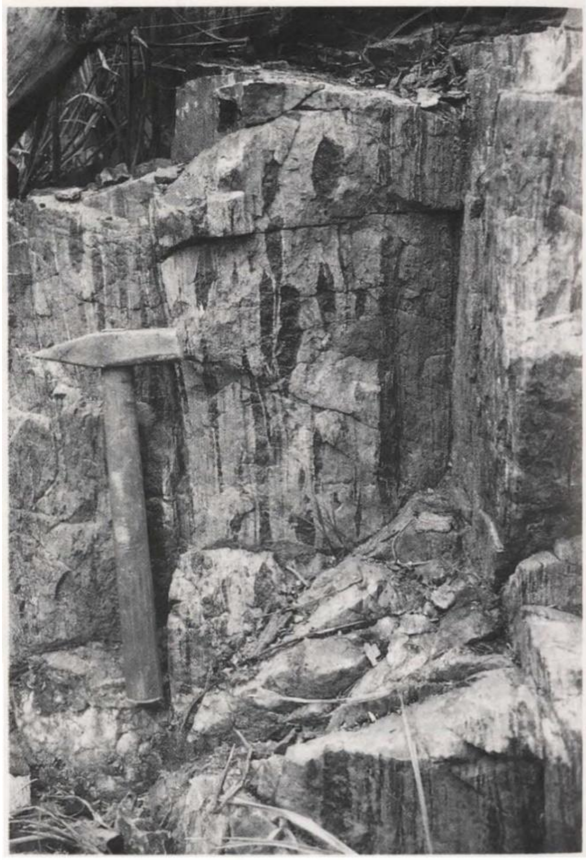

Plate 16. Vertical banding with concordant mafic enclaves, Quebrada Plata unit, Piedras complex, Quebrada Piedras

The Quebrada Plata unit strikes east-west and forms a narrow, generally less than 3km wide, but regionally persistent, belt that can be traced almost continuously for about 60km from the Peruvian border, in the west, to Portovelo, in the east. Where observed, its southern contact with the Moromoro granitoid complex is tectonic and its northern contact coincides with the Zanjón-Naranjo fault zone.

In the Río Piedras (**La Avanzada 620/9597**) hornblende-rich mafic enclaves and relict igneous banding can be observed (Plates 15 and 16). In this same river, and also in the Río Zaracay (**La Avanzada 625/9597**), as one approaches the Zanjón-Naranjo fault from the south, the generally massive, but weakly foliated lithologies, which are typical of the unit, become increasingly mylonitic. The rocks develop a marked, generally nearly vertical, mineral lineation due to the growth of acicular actinolite, now largely epidotised. The end product of this process is a distinctive, finely banded, black to dark green tectonite, in which late-contemporaneous, generally ductile, conjugate sets of Z-folded, kink bands are developed (Plate 17). Elsewhere along the Zanjón-Naranjo fault (**La Avanzada 6266/95967; 6350/95965**) these tectonites occur together with, or are replaced by, more massive greenschists (? retrograde amphibolites) composed of actinolite, epidote, quartz, albite, sphene, ± rutile. In hand specimen, these rocks often resemble serpentinites due to the development of serpentine minerals on joint/fracture surfaces.

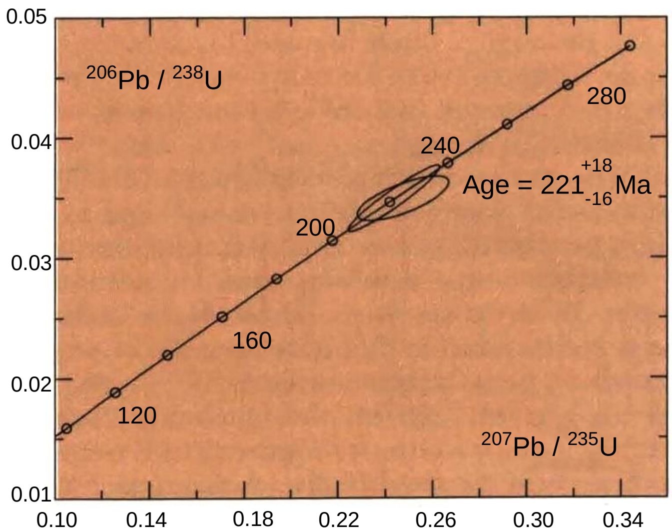

Figure 7. U/Pb zircon concordia diagram for Quebrada Plata unit, Piedras complex, Río Piedras. The two concordia analyses are of strongly abraded magmatic zircons and give a crystallisation age of 221^{+18}_{-16} Ma.

According to Feininger (1978), the Quebrada Plata unit (part of his Piedras Group, see Figure 3) was originally metamorphosed to amphibolite facies and has subsequently been affected by at least one retrograde event. The observations noted above suggest that this latter event was probably related to movements(s) along the Zanjón-Naranjo fault zone.

In the extreme west, along the frontier with Perú (**Arenillas 590/9596**), two, narrow (<500m), fault bonded lenses of biotite muscovite granodiorite and serpentinite crop out within the Quebrada Plata unit. The granodiorite has been assigned to the La Bocana unit of the Moromoro granitoid complex. The serpentinite is of uncertain age and origin but it is tentatively correlated with similar (unnamed) serpentinite lenses which occur further to the north in the Palenque mélange division (see below). Another lens of serpentinite was also mapped by Feininger (1978) to the west of Piedras village, near El Porvenir (**La Avanzada 611/9597**), in an area that is now partially covered by the Tahuín reservoir.

Age of Quebrada Plata unit

Various attempts to date the Quebrada Plata unit have been made using the K-Ar method (Table 3). Previously these rocks were widely quoted as being Precambrian in age, based on a single amphibole determination of 743 ± 13 Ma obtained for a sample from the Portovelo area (Kennerley, 1980, and Table 3). During the present study resampling of this unit in the same area has yielded ages of 647 ± 37 Ma and 224 ± 3 Ma for amphibole mineral separates and these differences cast doubts on the validity of accepting a Precambrian age (Aspden et al., 1992).

U/Pb zircon studies of the Quebrada Plata unit from the Río Piedras section (Plate 15) have provided an age of 221^{+18}_{-16} Ma (Figure 7). According to Noble et al. (1994), the analysed zircons are of magmatic origin and hence this age, which is similar to those obtained from the La Bocana unit and the Marcabelí pluton, is considered to be the age of crystallisation for the mafic complex.

Plate 17. Finely Banded greenschist tectonite with centimetre-scale (Z) kink bands, Quebrada Plata unit, Piedras complex, union of Ríos Naranjo and Piedras, Zanjón-Naranjo fault zone.

Table 3. K-Ar determinations for the Piedras mafic complex

Rock type	Area sampled (topographic sheet and grid ref.)	Mineral	K %	Atom 40 %	Rad ^{40}AR (nl/g)	Age (Ma)
QUEBRADA PLATA UNIT						
Amphibolite	near Portovelo (Zaruma 653/9588)	Hornblende	0.084	-	3.001	743 ± 13 †
Amphibolite	c. 1km SW of Portovelo (Zaruma 6519/95882)	Hornblende	0.05	75.43	1.389	647 ± 37
		Hornblende	0.07	88.72	0.602	224 ± 34
Amphibolite	west of Piedras (La Avanzada 620/9598)	Hornblende	0.238	-	-	196 ± 8 *
ARENILLAS UNIT						
Amphibolite	Arenillas (Arenillas 604/9607)	Hornblende	0.444	-	-	74 ± 1 *
		Hornblende	0.370	91.23	1.062	72 ± 15
Amphibolite	Arenillas road bridge (Arenillas 6049/96072)	Hornblende	0.358	76.17	1.051	74 ± 6
		Hornblende	0.358	81.36	1.080	76 ± 7

Data from Aspden et al., 1992; *Feininger and Silberman, 1982 and † Kennerley, 1980

Summary of conditions and age of metamorphism south of the Zanjón-Naranjo fault zone (Sub-province I).

Within sub-province I of the El Oro metamorphic complex, the Tahuín division has been affected by a single, generally prograde, regional metamorphic event. Although insufficient detailed petrographic and structural data are available to enable the various mineral isograds to be plotted accurately it is apparent that metamorphic grade increases from south to north and varies from weak to incipient in the El Tigre unit, to upper amphibolite facies in the La Victoria unit. The junction between the El Tigre and La Victoria unit corresponds to an east-west-trending, tectonic zone which marks the appearance of a regional cleavage and the development of mineral assemblages typical of the biotite zone (biotite ± chlorite + muscovite + quartz) in the low-pressure metamorphic facies series (for review see Yardley, 1989). Further to the north, in the La Victoria unit, mineral assemblages which are first typical of the cordierite zone (cordierite + biotite + quartz) and then of the andalusite zone (cordierite + andalusite + biotite) can also be recognised. The first (lower) sillimanite zone is marked by the incoming of fibrolite which occurs near the first appearance of andalusite. However, as the contact with the Moromoro granitoid complex is approached, sillimanite coarsens and becomes more abundant.

Within the Moromoro granitoid complex (principally the La Bocana unit), and occurring either as tectonic enclaves or xenolithic/migmatitic restite material, are various, generally high-grade paragneisses, considered to represent equivalents of the La Victoria unit. These gneisses often contain coarse sillimanite + feldspar ± garnet ± cordierite ± biotite ± muscovite ± quartz assemblages and belong to the second (upper) sillimanite zone.

The total absence of kyanite, staurolite, and the presence of garnet only in the highest grades, indicates that the metamorphism which affected the Tahuín division was of a temperature-dominated, low-pressure, Abukuma-type (Miyashiro, 1961). The mineralogy and field relationships of the La Victoria and La Bocana units indicate that during this event temperatures were sufficiently elevated to melt the pelitic sediments of the La Victoria unit (i.e. the upper sillimanite zone). Peak metamorphism probably occurred in the Late Triassic and was contemporaneous with emplacement of the Moromoro and Piedras complexes.

GEOLOGY OF SUB-PROVINCE II

Palenque mélange division (Santa Rosa 636/9626)

The rocks of the El Oro metamorphic complex between the Zanjón-Naranjo fault zone and the Jubones fault are interpreted to represent a structural complex or regional mélange zone, collectively referred to as the Palenque mélange division. They comprise sub-province II (Figure 4) of the metamorphic complex which is named after the area surrounding the village of Palenque, located about 6km south-east of Pasaje.

In the west, the division is buried beneath the largely unconsolidated, Late Tertiary and Quaternary deposits of the coastal plain and in the east, it is intruded, and in part overlain, by a volcano-plutonic complex of presumed Tertiary age. Inliers of metamorphic rocks have been noted, or reported, from several localities (e.g. south of Cerro Azul village along the Paccha road; the Río Daucay, upstream of Playas de Daucay; the headwaters of the Río Chilola, west of Cerro Chillacocha), but insufficient information is available to show these on the accompanying geological map.

The matrix of the Palenque mélange division comprises dominantly metasedimentary rocks which contain a number of large, regionally extensive, fault-bounded blocks as tectonic inclusions. Lithologically and mineralogically some of these inclusions can be correlated with rock types/assemblages that occur in sub-province I but the division also includes various serpentinite lenses and the oceanic and associated high-pressure rocks of the Raspas ophiolitic complex. Geologically these inclusions are distinct and therefore exotic with respect to the metasedimentary matrix.

PALENQUE MÉLANGE DIVISION – MATRIX

No single road/river crosses the Palenque mélange division in its entirety but in the north, fresh and accessible exposures of the matrix rocks occur in the Río Huizho, east of Pasaje (**Uzhcurrumi 640/9632**). The matrix consists mainly of fine- to medium-grained, low- to medium-grade metasediments. Dark-coloured, blue to black to green, semipelitic, schistose phyllites and slates are dominant but quartz-sericite schists, feldspathic schists, metagreywackes, green to black to grey cherts, greenschists and rare amphibole (tremolite) schists are also present.

In outcrop sedimentary structures are rarely observed and the rocks are normally strongly sheared and/or brecciated. They include broken, mixed and pseudoconglomeratic horizons in which lensoid clasts of generally coarser metasedimentary material of variable dimensions (generally <1m) occur within a finer-grained matrix. In the north, along the Jubones fault, the rocks are strongly sheared and/or brecciated and silicified; white quartz veins are common. To the west of Valle Hermoso, in the Río Viron and Río Viron Chico, biotite-rich metasediments, which often carry cordierite, occur in the zone of contact with the Tertiary volcano-plutonic complex. In the south, along the La Palma-El Guayabo fault zone, to the east of El Guayabo, andalusite, and possibly cordierite, are also widely developed as contact minerals. In this same area, immediately to the north of the Raspas ophiolitic complex, various tectonic inclusions of greenschist, serpentinite and amphibolite, too small to be shown on the accompanying geological map, can be observed within the matrix of the Palenque mélange division.

Although mineralogically variable the matrix rocks typically consist of quartz, biotite, muscovite, chlorite, albite, ± graphite, ± actinolite, ± epidote, ± minor garnet. A single example of pale green, tremolite schist, which contains accessory epidote and opaque minerals, has been recorded from the Río Casacay (**Chilla 6445/96309**).

PALENQUE MÉLANGE DIVISION – TECTONIC INCLUSIONS

Raspas ophiolitic complex

The Raspas ophiolitic complex has an east-west strike length of about 45 km and a maximum width of about 6km. Its northern and southern limits are defined by the La Palma-El Guayabo fault zone and by the Tahuín dam/Zanjón-Naranjo fault zones respectively. Since the completion of the Tahuín dam some of the lower-lying areas of the complex, adjacent to the Río Naranjo valley in the west, have been submerged.

The petrology of the western part of the Raspas ophiolitic complex, which contains the best-known examples of eclogites and related high-pressure rocks in the Northern Andes, has been previously described by Duque (1992, 1975); Feininger (1980); and Duque and Feininger (1974). In the following account the complex has been divided into three informal units – Río Panupali, El Toro and La Chilca.

Río Panupali unit (La Avanzada 633/9598)

The Río Panupali unit forms the outer shell of the Raspas ophiolitic complex and comprises pale to dark green, foliated to massive greenschists composed of actinolite, albite, quartz, chlorite, epidote, ± garnet, ± glaucophane, ± sphene, ± calcite, ± opaques (dominantly sulphides).

Apart from the Río Panupali, which provides a complete, almost continuously exposed section across this unit, excellent outcrops of these rocks can also be seen in the Quebrada Sambotambo (**La Avanzada 635/9597**) and, in the west, in the Río Arenillas, downstream from the Tahuín dam.

These rocks were considered by Feininger (1978) to be Precambrian in age (part of the Piedras Group, see Figure 3) but their general field relationships, and the presence of glaucophane and garnet in some samples indicate that they are an integral part of the Raspas ophiolitic complex.

El Toro unit (La Avanzada 611/9601)

The El Toro unit comprises variably serpentinised harzburgites and is particularly well exposed in a series of quarries located immediately to the east of the Tahuín dam in the area of El Toro. The principal outcrop of the unit is crescent-shaped and in the western part of the Raspas ophiolitic complex it separates the outer Río Panupali unit from the inner core of the La Chilca unit. The El Toro unit probably extends at least as far west as the Arenillas-Alamor road beneath the deposits of the coastal plain where it is exposed in a small isolated hill in an abandoned serpentinite quarry.

Lithologically the El Toro unit ranges from massive, medium-grained harzburgite, with an estimated modal composition of olivine (70%), orthopyroxene (12%), amphibole (8%), antigorite (5%), chlorite (3%) and magnetite (2%), through variably foliated and serpentinised harzburgite, to highly schistose, fine-grained, antigorite serpentinite (Feininger, 1980).

La Chilca unit (La Avanzada 617/9600)

The La Chilca unit takes its name from La Chilca village in the east. Lithologies of this unit are normally deeply weathered away from river sections but they form the central core of the Raspas ophiolitic complex and have an east-west strike length of about 20km and maximum north-south width of about 3km.

The La Chilca unit (previously referred to as the Raspas Formation, Feininger, 1978) contains a variety of high-pressure metamorphic rocks but consists principally of pelitic schists with lesser amounts of blueschists and eclogites. Detailed lithological and petrological descriptions of these rocks have been given by Duque (1992) and Feininger (1980) and the following summary is based largely on this earlier work.

Coarse-grained pelitic schists and minor amounts of micaceous quartzites make up about 70% of the La Chilca unit. When fresh, the pelitic schists are pale, silver-grey in colour. Mineralogically the schists consist of quartz, phengitic muscovite, paragonite and garnet, with lesser amounts (generally <10%) of graphite, rutile, pyrite, Mg-chloritoid, ± kyanite.

Blueschists and eclogites (Plates 18 and 19) occur in approximately equal proportions within the La Chilca unit. The blueschists are typically fine to medium grained, dark blue phyllites which carry small (<2mm) garnet porphyroblasts and can contain more than 50% modal glaucophane. In addition, varying amounts of paragonite, phengite, muscovite, epidote, rutile, ± quartz, ± apatite, ± pyrite are present, and secondary minerals include chlorite, ± sphene, ± albite, ± calcite.

The eclogites of the La Chilca unit are normally seen as loose blocks and have only rarely been observed in outcrop (e.g. in ‘Eclogite Canyon’, Río Raspas, **La Avanzada 618/9601**), (Feininger, 1980). The rocks are dark in colour, ranging from fine to medium grained and are variably foliated. They are composed of omphacite, garnet and barroisite often with lesser amounts of clinozoisite, rutile, quartz, ± apatite, ± pyrite. In ‘Eclogite Canyon’ and occurring as layers several meters thick within the eclogites, are amphibole gneisses, consisting of barroisite (>50%), garnet, zoisite, kyanite, rutile, pyrite, ± omphacite, ± paragonite, ± quartz, ± apatite, ± muscovite.

Minor amounts of greenschists (that are mineralogically identical to those of the Río Panupali unit), amphibole pegmatites, garnetites (garnet >50%) and blocks of jadeite also occur within the Raspas unit.

a

b

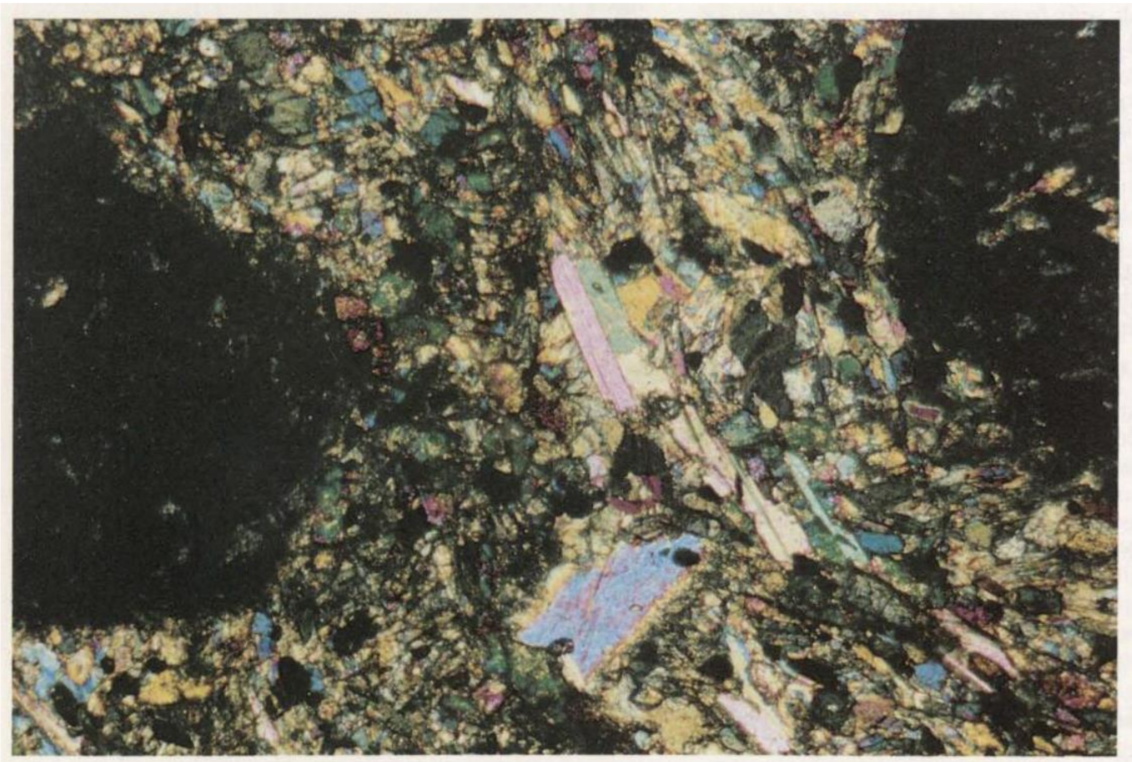

Plate 18. Photomicrographs of La Chilca unit blueschist, Raspas ophiolitic complex; large garnet porphyroblasts show evidence of recrystallisation together with blue amphibole and blades of muscovite. **(a)** Plane polarised light, **(b)** crossed polarisers. Field of view c.8.3mm. (*P. Henney*, *BGS*)

a

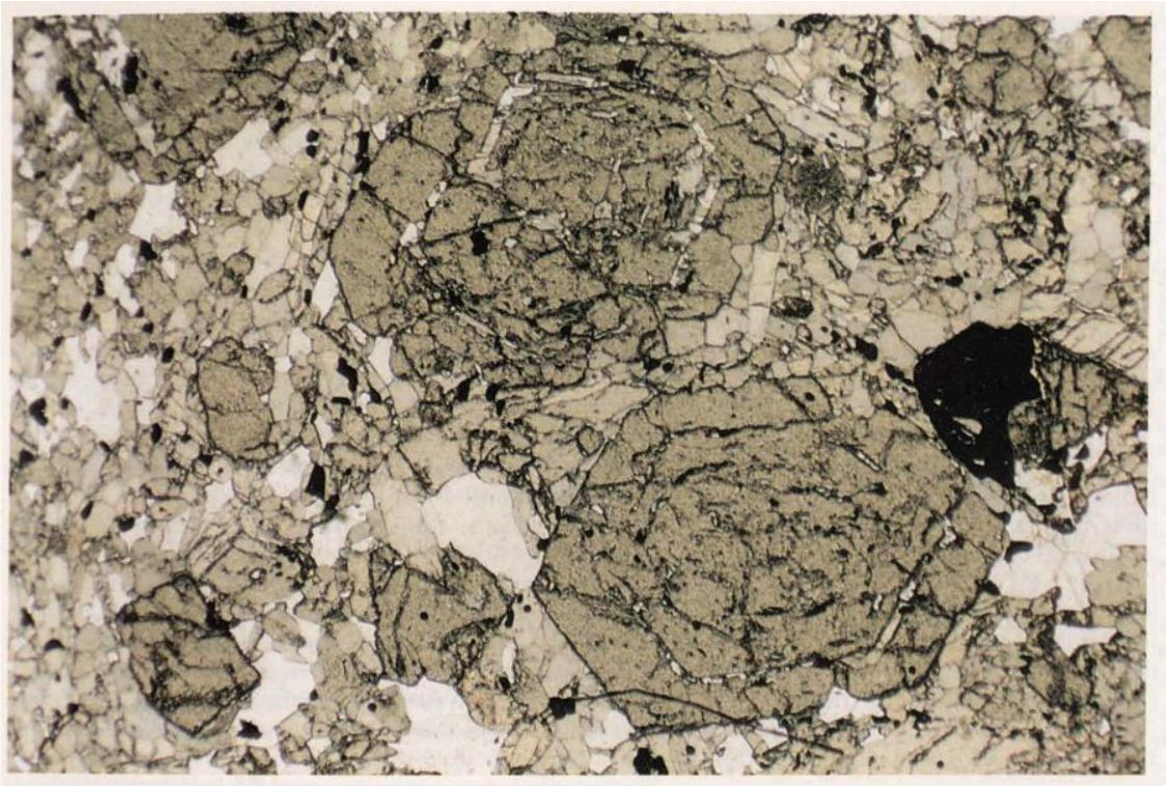

b

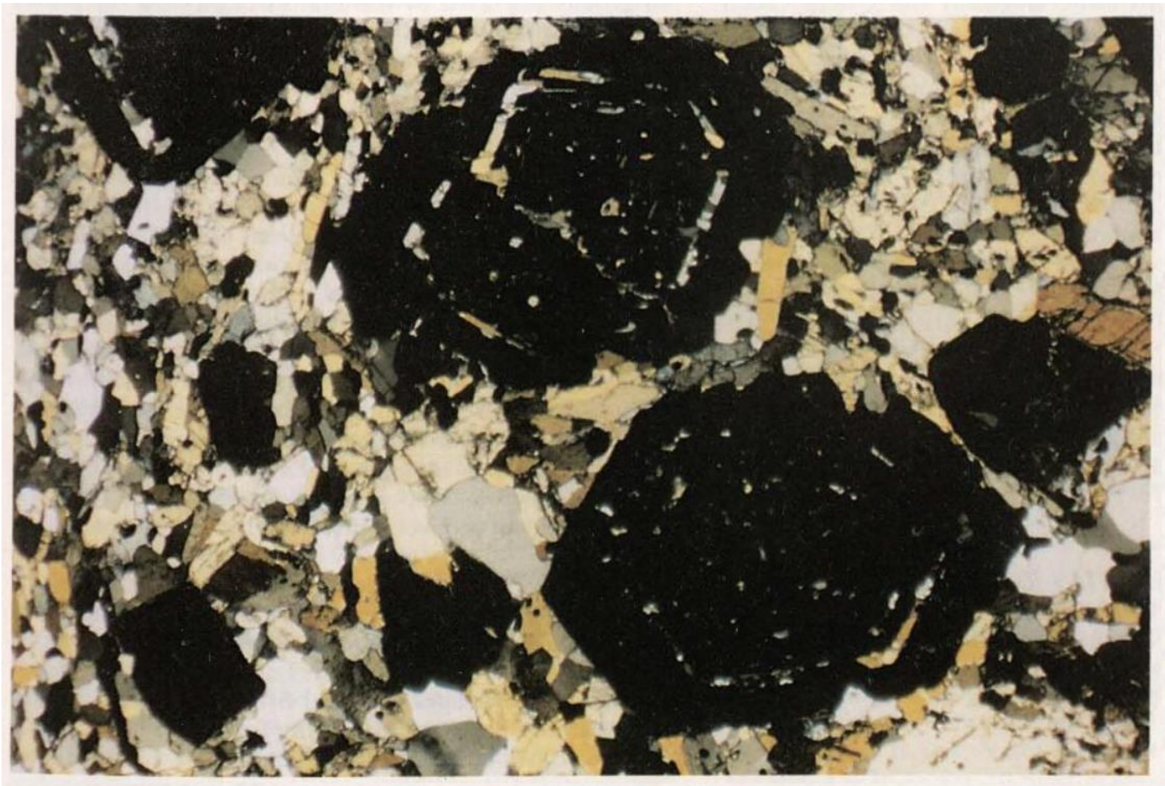

Plate 19. Photomicrographs of La Chilca unit eclogite, Raspas ophiolitic complex; large euhedral porphyroblasts of garnet together with omphacite pyroxene and pale blue amphibole (?crossite). Garnets show multiple inclusion trails indicating episodic growth. Groundmass includes quartz, minor clinozoisite, rutile and apatite **(a)** Plane polarised light, **(b)** crossed polarisers. Field of view c.8.3mm. (*P. Henney, BGS*)

Age of La Chilca unit

A single K/Ar (phengite) determination from a pelitic schist of the La Chilca unit, collected from the Río Raspas, gave an age of 132 ± 5 Ma (Feininger and Silberman, 1982). This date is in general agreement with those obtained from Colombian blueschists (125 ± 15 to 120 ± 5 Ma) (Aspden and McCourt, 1986), and is interpreted to represent a probable cooling (? emplacement) age for the ophiolitic complex below the blocking temperature of phengite.

Metamorphism of the Raspas ophiolitic complex (La Chilca and Panupali units)

According to Duque (1992) (cf. Feininger, 1980) the eclogites, blueschists, pelitic schists and greenschists of the La Chilca and Río Panupali units formed at about 9kb and 465° C. All these rocks represent the prograde products of high-pressure/low-temperature metamorphism and were probably formed in an active subduction zone for which a palaeogeothermal gradient of about 13.8°C/km has been calculated (Duque, 1993).

Limón Playa and Quera chico units

Two large fault-bounded inclusions composed of granodiorite/migmatite and medium- to high-grade paragneisses, have been mapped within the Palenque mélange division. Immediately to the north of the Raspas ophiolitic complex is the Limón Playa unit (**La Avanzada 618/9604**) and, in the north-east, is the Quera Chico unit (**Chilla 651/9627**).

The Limón Playa unit has a maximum width of about 4km, an east-west strike length of about 20km, and consists of a series of fault-bounded granitic/migmatitic lenses which are now tectonically intercalated with amphibolites of the Arenillas unit (see below). Between the small settlement of Limón Playa in the south and La Avanzada in the north, fairly continuous outcrops of these rocks are exposed in the Río Santa Rosa.

The Quera Chico unit is named after a small agricultural area located in the Río Quera. Although the unit outcrops over a large area (>100km^2) it is generally poorly exposed and/or deeply weathered and the only (partial) vehicular access is provided by the unsurfaced Chilla road in the extreme north-east. Elsewhere, access is by a network of mule tracks which lead from the main Pasaje-Uzhcurrumi road in the north, and connect the various scattered farming communities located in the Ríos Cune (**Chilla 653/9630**), Quera (**Chilla 650/9628**), Casacay/Dumari (**Chilla 645/9628**) and Huizho (**Chilla 641/9629**), with Dumari, Chilla and the Palenque area. Owing to the steep terrain, the rivers which cross the Quera Chico unit are usually choked with large boulders. Access is often difficult and sections of continuous outcrop are relatively rare. In the north the unit is fault-bounded but in the south, it is intruded and/or overlain by Tertiary plutonic/volcanic rocks. It should be noted that the southern contact of the unit, to the west of Chilla, is not well defined and further work, preferably supported by geochronological studies, is required in this area.

Lithologically and mineralogically the Quera Chico and Limón Playa units are similar and comprise variably foliated biotite ± muscovite ± garnet granodiorites, migmatitic granodiorites, migmatites and medium- to high-grade paragneisses. The paragneisses are typically composed of quartz, plagioclase, (?) alkali feldspar, biotite, ± cordierite, ± sillimanite (± fibrolite), ± minor garnet, ± minor apatite, ± minor tourmaline. Within the granodiorites, gneissic/migmatitic xenoliths of sedimentary origin predominate. Biotite schlieren and clasts of white vein quartz are also relatively common. In the Limón Playa unit xenoliths of amphibolitic material are widespread (Río Santa Rosa, 'Agua Potable' dam, **La Avanzada 617/96068**), and in some areas, what is interpreted to be hybrid granitoid due to the assimilation/mixing of the amphibolite and granodiorite magma, can be observed (Río Santa Rosa, **La Avanzada 6173/96069**).

Age of Limón Playa unit

The age of the Limón Playa unit is interpreted to be 200 ± 19 Ma based on U/Pb zircon data. Younger ages of 78 ± 1 and 82 ± 1 Ma obtained from monazites are thought to relate to a later period of metamorphism and regional deformation (Noble et al., 1994).

Unnamed granitoid units

Three other tectonic inclusions of strongly sheared, deeply weathered, biotite muscovite granodiorite, have been mapped within the Palenque mélange division. These bodies have not been given specific names but are located to the south of the Jubones fault in the extreme north and immediately to the north of the Zanjón-Naranjo fault in the extreme west.

In addition, to the east of Aserrío, exposed in the Río Raspas approximately 300m downstream of the junction of the Río Colorado (**Santa Rosa 635/9623**), an outcrop of similar mylonitic, biotite granodiorite was noted within a mixed serpentinite/black phyllite sequence. This occurrence is too small to show on the accompanying geological map.

Arenillas and Taqui units

These mafic amphibolite units are named after the town of Arenillas in the west (**Arenillas 604/9607**) and the prominent hill of Peña de Taqui in the north-east (spelt Tarqui on the 1985 edition of the 1:50000 topographic base map) (**Chilla 657/9628**). Both form narrow, but laterally persistent, east-west-striking bodies and are spatially associated with the Limón Playa and Quera Chico 'granitoid' units.

In the south, the Arenillas unit can be traced a minimum of 14km along strike from the town of Arenillas in the west, eastwards into the Río Santa Rosa. In the west, the unit consists of a series of lens-shaped, fault-bounded slivers that are now tectonically intercalated with the Limón Playa unit. These relationships are well exposed along the new Arenillas-Santa Rosa highway to the east and north of the road bridge over the Río Arenillas (**Arenillas 606/9605**) and suggest that the Arenillas amphibolites were possibly originally intruded by the Limón Playa unit. In places the Arenillas unit is brecciated and net-veined by quartz-rich material, features which could also relate to this event.

The Taqui unit is located along the northern edge of the Quera Chico unit with which it is in tectonic contact. In the east, the unit has a maximum width of about 1.5km and can be traced for a minimum of 7km to the west where it is exposed in the Río Quera (**Chilla 651/9627**). It is generally finer grained and more brecciated than the Arenillas unit and, although both amphibolites consist essentially of plagioclase and hornblende, minor mineralogical differences are apparent in thin section. The Arenillas unit contains brown, markedly pleochroic hornblende, together with minor amounts of zircon, clinopyroxene, quartz and epidote. In contrast, the amphibole of the Taqui unit, possibly in part actinolite, is pale green in colour; clinopyroxene has not been recorded in these rocks, but accessory sphene and rutile are present.

Age of the Arenillas unit

The age of the Arenillas unit has not been established but based on its correlation with the Quebrada Plata unit it is considered to be Late Triassic. The K-Ar (hornblende) mineral ages obtained from these amphibolites range from 72 ± 15 to 76 ± 7 Ma (Table 3) and are interpreted to be reset (see also Aspden et al., 1992). These ages are similar to the ‘young’ monazite ages recorded from the Limón Playa unit.

Unnamed serpentinite units

Tectonic inclusions of serpentinite occur within the Palenque mélange division and are particularly common in the north-east where they form a discontinuous, approximately east-west-trending belt that can be traced from the Palenque/Hacienda San José (**Chilla 639/9625**) area in the east, westwards towards San Joaquín and Ugarte. Two small serpentinite lenses are also present in the south, in the eastern part of the La Palma-El Guayabo fault zone which defines the northern limit of the Raspas ophiolite complex.

In addition to the unnamed serpentinites of the Palenque mélange division, immediately to the south of the Zanjón-Naranjo fault zone, along the frontier with Perú, a small serpentinite lens is exposed within the Quebrada Plata unit to the south of Chacras. According to Feininger (1978), this serpentinite can be traced eastwards for several kilometers but, its presence is unconfirmed, for example in the Quebrada Obrajales (**Arenillas 594/9595**), to the west of Palmales where amphibolite of the Quebrada Plata unit is currently being quarried for roadstone.

Lithologically these inclusions are composed mainly of serpentinites but they may also contain irregular patches of silicified and/or black graphitic phyllites, minor cherty horizons and some greenstones (e.g. Río Palenque, near Hacienda San Gregorio, **Santa Rosa 637/9626**). As noted above, a block of mylonitic granodiorite of unknown extent was observed in the unnamed serpentinite unit to the east of Aserrío.

Mineralogically the serpentinites consist dominantly of antigorite with lesser amounts of chrysotile, but relict crystals of olivine and (?)ortho-pyroxene can be distinguished. Accessory minerals include spinel, calcite, ± rutile, ± sphene.

Origin and age of the tectonic inclusions north of the Zanjón-Naranjo fault zone

Lithologically and mineralogically the granitoids and paragneisses of the Limón Playa and Quera Chico units are identical to rocks which occur in the La Bocana unit and in the higher-grade portions of the La Victoria unit, to the south of the Zanjón-Naranjo fault zone. Equally, the Arenillas and Taqui units are petrologically and (in part) geochemically (see below) similar to the amphibolites of the Quebrada Plata unit. The close spatial association between granitoid and amphibolite within the Palenque mélange division also mirrors that shown by the La Bocana and Quebrada Plata units. These observations together with the U/Pb data, indicate that the Limón Playa and Quera Chico units, and the Arenillas and Taqui units, can be correlated with, and were probably tectonically derived from, the La Bocana and Quebrada Plata units respectively.

The derivation of the serpentinites of the Palenque mélange division is less certain but the most obvious source, especially for those bodies located in the La Palma-El Guayabo fault zone, would be the El Toro unit of the Raspas ophiolitic complex.

Attempts to date the matrix of the Palenque mélange division have been unsuccessful but it is assumed to be of probable (?)latest Jurassic to Cretaceous age. The K/Ar (phengite) date of 132 ± 5 Ma (Feininger and Silberman, 1982), obtained from the La Chilca unit of the Raspas ophiolitic complex, would be in agreement with this general age range.

WHOLE-ROCK GEOCHEMISTRY

Background

A total of 59 whole-rock samples, the locations of which are shown in Figure 8, have been analysed from the El Oro metamorphic complex by X-ray fluorescence spectrometry (XRFS). The analyses were carried out in two series; those samples prefixed with 'SH' codes (4 samples) were analysed at the University of Keele (UK) whilst the other samples were analysed by the British Geological Survey, Analytical Chemistry Group, Nottingham. For all the samples, the major elements are reported as weight percentages (wt%) of SiO_2, TiO_2, Al_2O_3, Fe_2O_3 (total Fe treated as ferric), MnO, MgO, CaO, Na_2O, K_2O and P_2O_5. The percentage loss on ignition (LOI) is also recorded. The suite of trace elements analysed, reported as parts per million values (ppm), varied between the two series. The majority of samples included determinations for As, W, Bi, V, Cr, Co, Ni, Cu, Zn, Rb, Sr, Y, Zr, Nb, Mo, Ag, Sn, Sb, Ba, La, Ce, Pb, Th and U. However, in the 'SH' series As, W, Bi, Co, Mo, Ag, Sn, Sb and U were not analysed.

The following summary is taken largely from an unpublished report by Fortey and Gillespie (1993) 'Assessment of geochemical analyses of igneous rocks from Ecuador'.

Moromoro granitoid complex

The whole-rock analyses obtained from the Moromoro granitoid complex (La Bocana unit 10 analyses; Marcabelí pluton 7 analyses and El Prado pluton 5 analyses) are listed in Table 4. The normative compositions of these rocks, together with various geochemical indices, are given in Table 5.

Based on these analyses the Marcabelí and El Prado plutons consist principally of granodiorites and lesser amounts of monzogranites whereas the granitoids of the La Bocana unit fall mainly within the monzogranite field, but also include quartz-rich granitoids and granodiorites (Figure 9).

According to Chappell and White (1974) and Pitcher (1983), field, mineralogical and chemical criteria can be used to distinguish granites incorporating high proportions of crustal material (S-type) and granites essentially of mantle origin (I-type). Isotopic data are also valuable but were not available to the present investigation. Two of the geochemical diagrams used are the Al/(Na + K + Ca/2) v. SiO_2 and the K_2O v. Na_2O shown in Figures 10 and 11 respectively. In Figure 10 most of the samples plot within the S-type field and it can be seen that, although the La Bocana samples show a range of composition, they are normally strongly peraluminous. In contrast, the Marcabelí and El Prado plutons are only slightly peraluminous and two samples plot within the meta-aluminous, (I-type) field. In Figure 11 the granitoids straddle the S-I-type field boundary with the majority of the La Bocana samples falling on the S-type side and the Marcabelí and El Prado granites on the I-type side.

Similar differences can also be seen on the ACF plot (Figure 12) where, with one exception, the Marcabelí and El Prado analyses, being richer in CaO, tend to plot within the area plagioclase-hornblende-biotite, whereas the main group of La Bocana samples spans the plagioclase-biotite tie line. This diagram is constructed using an assumption that 85% of the total iron is in the ferrous state but since most of the variation between units is in the relative proportions of CaO and Al_2O_3-K_2O-Na_2O, then this assumption can be justified.

These diagrams suggest that the Marcabelí and El Prado plutons are similar in composition and comprise dominantly I-type granitoids, but that they may also contain S-type variants. In contrast, the La Bocana unit appears to be mainly S-type in character but it may also contain I-type granitoids which, geochemically, appear to be similar to those of the Marcabelí and El Prado plutons. As mentioned earlier, the Marcabelí pluton contains zircon cores which have inherited ages ranging from 0.546 to 2.876 billion years (Noble et al., 1994). These crystals can only have been derived from an older crustal source and their presence would therefore indicate that recycling of at least some pre-existing continental material occurred during the formation of the Marcabelí pluton.

The use of a rock/ORG (ocean ridge granite) normalised trace element 'spider diagram' has been discussed by Pearce et al. (1984). According to these authors, enrichment of large ion lithophile (LIL) elements is a common feature of both subduction-related (volcanic arc granites), and within-plate (rift-related) granites, but is subdued, or absent, in ocean ridge granites. Within-plate granites also display enrichment in Ta and Nb, and have values for Ce, Zr and Y above 1, or close to 1 (for attenuated lithosphere settings). Volcanic arc granites typically have Ta and Nb close to 1, and the other elements less than 1. However, the degree of LIL element enrichment in volcanic arc granites varies depending on the nature of the arc setting. The authors cite data for a granite from Chile which displays particularly strong LIL element enrichment combined with Ta and Nb values near to 2; using these elements this granite is difficult to distinguish from certain within-plate granites. Collision related granites are similar to the Chilean granite but show a marked depletion in Zr and Y, which may be sufficient to distinguish them geochemically. The current analyses do not include the full suite of elements used by Pearce et al. (1984), but they are sufficient to determine at least the general form of the normalised 'spider diagrams' for the Moromoro granitoid complex.

Although the La Bocana samples show a minor degree of scattering, the rock/ORG 'spider diagrams' are remarkably similar for the La Bocana, Marcabelí and El Prado samples (Figures 13, 14 and 15) and indicate LIL element enrichment together with values of Nb and Ce close to 1, and Zr and Y less than 1. Hence, using the criteria of Pearce et al. (1984), it is suggested that the Moromoro granitoid complex can be interpreted as being either subduction or collision related.

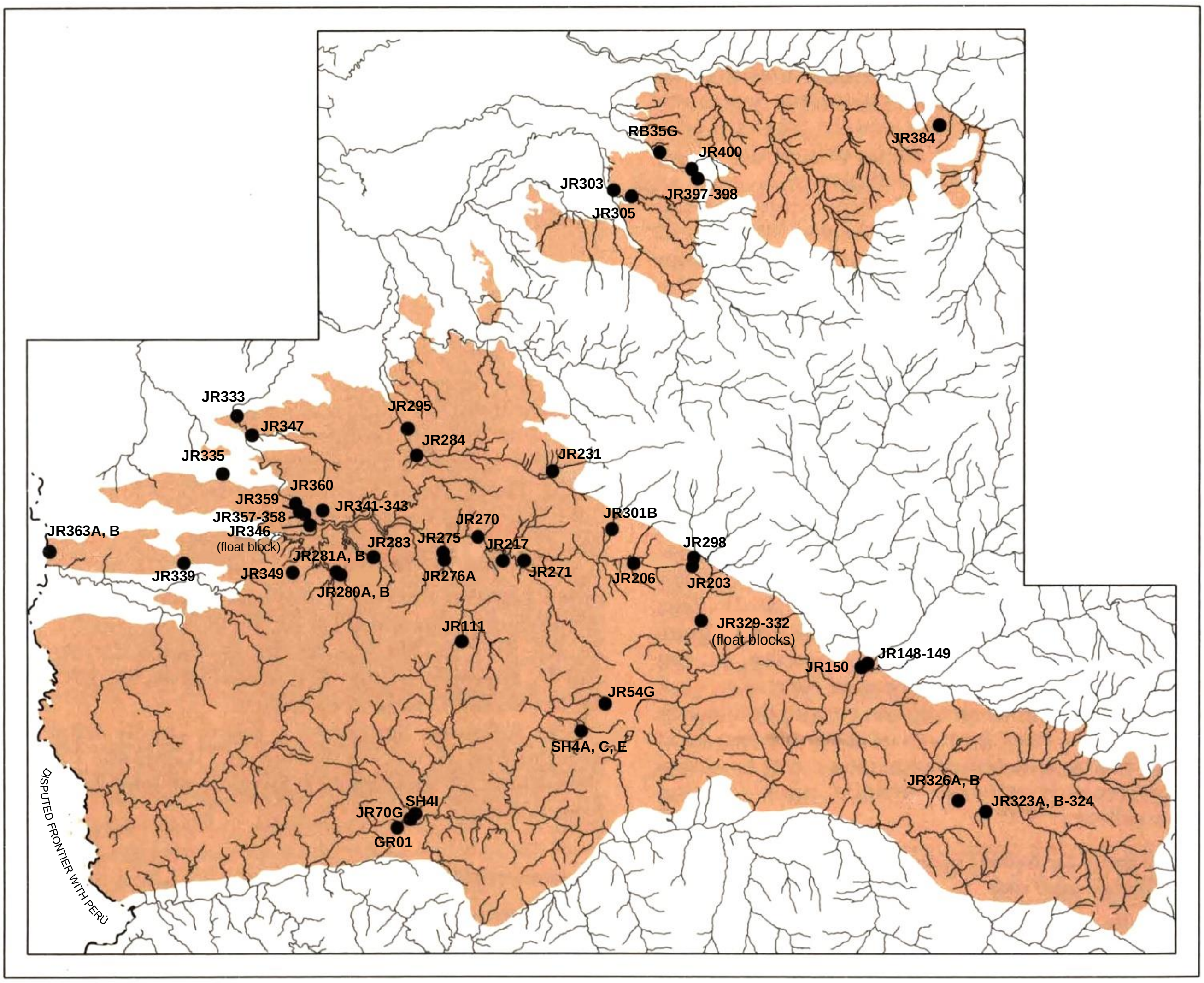

Figure 8. Location map of whole-rock samples.

Pearce et al. (1984) also used the Rb v. Y + Nb discriminant plot to distinguish between granites formed in various tectonic (plate) settings. According to this diagram (Figure 16) the Moromoro granites can all be considered as volcanic arc granites. However, the La Bocana unit extends closer to the within-plate granite boundary and generally contains less Rb than the Marcabelí and El Prado samples, perhaps suggesting a more continental setting.

In summary it is concluded that the Moromoro complex consists predominantly of granitoids of S-type character but that it also includes some I-types and that these rocks were probably formed in either a subduction or collisional setting.

Piedras Mafic Complex

In the following account the Arenillas and Taqui units, which occur as tectonic inclusions within the Palenque mélange division, are considered as part of the Piedras mafic complex from which they are thought to have been derived. A total of 15 whole-rock analyses are available from the Piedras mafic complex (Quebrada Plata unit 11; Arenillas unit 3; and Taqui unit 1) and these are listed in Table 6. The normative mineral compositions of these rocks, together with various geochemical indices are given in Table 7.

Although susceptible to alkali mobility during alteration, the K_2O v. SiO_2 and $Na_2O + K_2O$ v. SiO_2 plots are valuable general classification diagrams and indicate that the Piedras mafic complex, with the exception of the Taqui sample, consist of basalts belonging to the low-K (tholeiitic) series (Figures 17 and 18). In order to avoid the problem of potential alkali loss, Winchester and Floyd (1977) suggested that altered and/or metamorphosed igneous rock could be discriminated by using relatively immobile trace element ratios and based on their plot of Zr/Ti v. Nb/Y. From Figure 19 it can be seen that the above samples fall within the basaltic-andesite field.

On the AFM diagram (Figure 20) the analyses form a fairly well-defined group with a tendency towards iron enrichment. Geochemically the Quebrada Plata and Arenillas units appear to be virtually identical, which supports the correlation made earlier in this report. However, on a number of plots the Taqui sample is somewhat anomalous in that it is enriched in TiO_2, Sr and Zr as well as K_2O, and possibly slightly depleted in MgO (Figures 21, 22 and 24). Since only a single analysis is available from the Taqui unit the significance of these differences remains uncertain.

Table 4. Moromoro granitoid complex whole-rock analyses

	LA BOCANA UNIT										MARCABELÍ PLUTON							EL PRADO PLUTON				
Sample	**111**	**280A**	**280B**	**281A**	**281B**	**283**	**329**	**330**	**331**	**332**	**GR01**	**SH4A**	**SH4C**	**SH4E**	**SH4I**	**54G**	**70G**	**323A**	**323B**	**324**	**326A**	**326B**
SiO_2	73.08	73.56	71.52	73.31	70.21	64.71	72.64	69.19	76.78	80.36	76.75	72.04	71.87	72.73	72.98	66.40	72.18	70.72	70.29	62.94	70.67	71.94
TiO_2	0.37	0.74	0.73	0.62	0.76	0.74	0.35	0.62	0.37	0.33	0.03	0.49	0.45	0.54	0.34	1.00	0.32	0.47	0.46	0.60	0.44	0.45
Al_2O_3	14.42	11.13	11.90	12.97	14.27	17.05	14.68	14.92	12.25	10.59	13.53	14.17	14.37	13.60	14.67	14.71	14.72	14.56	14.70	16.30	14.54	14.62
Fe_2O_3T	2.58	5.40	5.74	5.06	5.34	6.35	2.59	4.11	2.88	2.41	0.96	3.20	3.15	3.58	2.57	5.62	2.54	3.41	3.30	5.88	3.01	3.12
MnO	0.05	0.11	0.16	0.13	0.09	0.12	0.05	0.07	0.05	0.04	0.04	0.07	0.07	0.07	0.06	0.10	0.06	0.06	0.06	0.10	0.07	0.07
MgO	0.96	2.14	2.27	1.51	1.76	2.40	0.77	1.35	0.83	0.64	0.10	0.99	1.02	1.10	1.10	2.45	1.14	1.66	1.58	2.80	1.17	1.21
CaO	1.62	1.60	1.42	1.07	1.61	2.28	2.11	2.14	0.78	0.64	0.39	1.82	2.15	1.94	2.23	4.41	2.32	2.35	2.35	5.43	1.94	2.09
Na_2O	2.92	1.82	1.75	1.68	2.13	2.21	3.99	3.75	1.88	1.81	4.39	3.14	3.37	2.94	3.74	3.23	3.72	3.15	3.19	2.94	3.34	3.35
K_2O	3.22	2.38	2.42	2.59	2.66	2.71	2.18	2.33	2.56	2.42	3.94	3.04	2.63	2.93	2.76	1.68	2.79	3.09	3.11	1.98	3.65	3.35
P_2O_5	0.11	0.23	0.09	0.09	0.11	0.08	0.25	0.35	0.14	0.17	0.05	0.16	0.16	0.12	0.11	0.2	0.1	0.14	0.15	0.12	0.16	0.17
LOI	1.09	0.73	1.09	1.46	1.59	1.88	0.82	1.15	1.49	0.92	0.50	0.92	0.96	0.84	0.79	0.71	0.76	0.79	0.74	0.66	0.59	0.51
Total	100.42	99.84	99.09	100.49	100.53	100.53	100.43	99.98	100.01	100.33	100.68	100.04	100.2	100.39	101.35	100.51	100.65	100.40	99.93	99.75	99.58	100.88
As	0	3	3	5	3	2	2	4	3	4	0	-	-	-	-	0	0	2	1	4	2	2
W	5	2	2	3	2	5	4	3	4	3	2	-	-	-	-	2	2	2	2	4	5	5
Bi	1	0	0	0	0	0	0	0	0	0	0	-	-	-	-	1	0	0	0	0	0	0
V	39	85	94	74	93	115	25	44	42	31	1	46	44	57	40	83	30	41	42	107	33	38
Cr	55	83	85	100	77	100	29	36	55	47	35	37	31	32	25	58	29	40	45	46	31	37
Co	5	15	18	13	15	14	5	8	8	6	0	-	-	-	-	13	6	8	9	15	6	7
Ni	7	36	35	16	22	23	4	11	11	7	1	12	9	12	12	16	8	21	16	10	9	9
Cu	9	19	20	18	36	14	0	11	14	7	1	17	6	6	9	19	8	14	15	26	7	9
Zn	41	88	83	63	68	85	35	60	42	42	20	55	54	58	42	62	35	50	52	89	53	56
Rb	101	92	91	80	89	92	83	118	99	89	158	132	123	132	118	60	110	136	138	72	154	154
Sr	184	129	119	131	168	198	128	126	81	89	17	123	123	104	104	144	99	114	120	274	139	132
Y	20	23	25	28	29	34	13	18	20	16	28	27	23	25	25	24	22	13	15	20	21	23
Zr	117	187	216	275	236	218	115	194	212	251	49	166	167	188	119	217	116	164	169	130	152	159
Nb	7	13	13	11	11	11	8	11	8	5	7	8	9	10	7	7	6	8	7	5	9	8
Mo	0	0	1	0	1	0	0	0	0	0	0	-	-	-	-	1	0	0	0	3	0	0
Ag	0	0	1	0	1	1	1	0	0	0	0	-	-	-	-	2	0	0	0	4	0	0
Sn	0	0	0	0	0	0	3	2	3	2	1	-	-	-	-	0	0	4	3	1	5	6
Sb	0	0	0	0	1	0	0	0	0	0	0	-	-	-	-	0	0	1	2	1	0	1
Ba	565	759	810	807	736	553	197	114	364	287	292	492	276	385	444	248	338	308	315	438	325	323
La	16	12	25	26	29	33	13	9	22	17	10	9	9	12	4	18	13	14	15	16	16	16
Ce	40	36	60	66	70	70	42	28	57	46	28	41	34	43	42	38	41	44	48	36	40	47
Pb	30	12	9	24	22	20	28	24	17	15	18	18	16	17	15	12	14	21	17	36	20	22
Th	9	6	10	13	14	16	5	3	9	6	5	7	7	10	7	5	7	7	7	8	8	7
U	1	3	3	1	1	3	0	2	3	1	3	-	-	-	-	1	3	1	0	1	1	1

Table 5. Moromoro granitoid complex normative compositions (Kelsey, 1865) and geochemical indices.

	LA BOCANA UNIT										MARCABELÍ PLUTON						
Sample	**111**	**280A**	**280B**	**281A**	**281B**	**283**	**329**	**330**	**331**	**332**	**GR01**	**SH4A**	**SH4C**	**SH4E**	**SH4I**	**54G**	**70G**
Quartz	37.84	22.69	21.74	23.31	19.57	14.76	17.63	15.46	26.08	28.70	34.52	35.74	34.99	37.19	32.22	26.03	32.05
Corundum	3.44	1.61	2.04	2.83	2.60	3.26	1.33	1.59	2.65	2.11	1.45	2.79	2.46	2.35	1.74	0.04	1.59
Orthoclase	18.99	7.06	7.23	7.63	7.84	7.99	6.42	6.90	7.57	7.13	23.14	18.01	15.55	17.30	16.29	9.92	16.41
Albite	24.66	7.73	7.49	7.09	8.98	9.33	16.45	15.90	7.96	7.64	36.92	26.63	28.53	24.86	31.60	27.32	31.34
Anorthite	7.30	3.23	3.27	2.35	3.62	5.38	4.41	4.17	1.48	1.03	1.60	8.00	9.63	8.83	10.33	20.56	10.81
Hypersthene	5.16	5.64	6.11	4.71	5.05	6.53	2.37	3.87	2.62	2.10	1.49	5.89	5.96	6.55	5.57	11.82	5.65
Enstatite	2.39	2.67	2.86	1.88	2.18	2.98	0.96	1.68	1.03	0.80	0.25	2.47	2.54	2.74	2.74	6.10	2.83
Ferrosilite	2.77	2.96	3.25	2.83	2.86	3.55	1.41	2.19	1.58	130	1.24	3.42	3.42	3.81	2.83	5.72	2.82
Magnetite	0.56	0.59	0.63	0.55	0.58	0.69	0.28	0.45	0.31	0.26	0.21	0.70	0.69	0.78	0.56	1.22	0.55
Chromite	0.01	0.01	0.01	0.01	0.01	0.01	0.00	0.00	0.01	0.01	0.01	0.01	0.01	0.01	0.01	0.01	0.01
Ilmenite	0.70	0.71	0.70	0.59	0.72	0.70	0.33	0.59	0.35	0.31	0.06	0.93	0.86	1.02	0.64	1.90	0.60
Apatite	0.26	0.21	0.11	0.11	0.13	0.09	0.30	0.42	0.17	0.20	0.12	0.38	0.38	0.28	0.26	0.47	0.24
Diff. index	81.48	37.48	36.46	38.03	36.39	32.28	40.51	38.26	41.61	43.48	94.58	80.38	79.08	79.34	80.11	63.27	79.80
Colour index	6.43	6.94	7.45	5.86	6.35	7.93	2.98	4.91	3.29	2.67	1.76	7.53	7.51	8.36	6.78	14.95	6.81
mg number	46.44	48.01	47.95	41.01	43.44	46.82	40.92	43.35	40.17	38.22	19.53	41.89	43.00	41.72	49.93	50.39	51.12

	EL PRADO PLUTON				
Sample	**323A**	**323B**	**324**	**326A**	**326B**
Quartz	15.85	15.65	0.00	15.25	16.03
Corundum	1.05	1.09	0.00	0.98	1.04
Orthoclase	9.11	9.21	0.00	10.84	9.82
Albite	13.29	13.52	0.00	14.21	14.07
Anorthite	5.36	5.35	0.00	4.31	4.59
Kaliophilite	0.00	0.00	5.47	0.00	0.00
Acmite	0.00	0.00	0.28	0.00	0.00
N Meta silicate	0.00	0.00	0.55	0.00	0.00
K Meta silicate	0.00	0.00	74.93	0.00	0.00
Hypersthene	3.91	3.76	0.00	3.10	3.17
Enstatite	2.06	1.97	0.00	1.46	1.50
Ferrosilite	1.84	1.79	0.00	1.64	1.68
Olivine	0.00	0.00	1.15	0.00	0.00
Forsterite	0.00	0.00	0.53	0.00	0.00
Fayalite	0.00	0.00	0.62	0.00	0.00
Magnetite	0.37	0.36	0.00	0.33	0.34
Chromite	0.00	0.00	0.00	0.00	0.00
Ilmenite	0.45	0.44	0.12	0.42	0.42
Apatite	0.17	0.18	18.45	0.19	0.20
Calcite	0.00	0.00	-17.26	0.00	0.00
SiO_2 deficiency	0.00	0.00	-25.27	0.00	0.00
Diff. index	38.25	38.38	5.47	40.31	39.92
Colour index	4.72	4.56	1.55	3.85	3.94
mg number	53.14	52.73	52.59	47.52	47.47

Figure 9. QAP ternary diagram (after Streckeisen, 1976) based on the CIPW normative values for Moromoro complex (Q = Quartz, Or = Orthoclase, Pl = Anorthite + Albite).

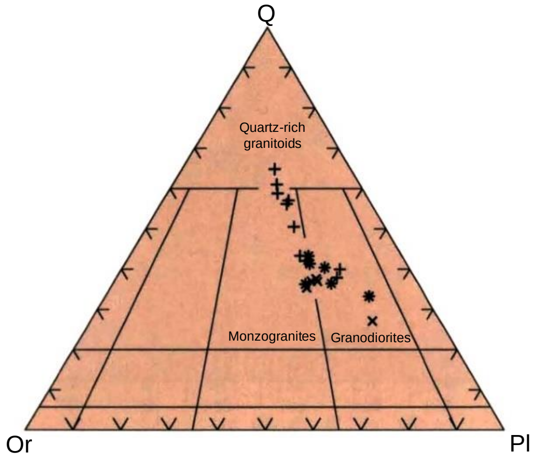

Figure 10. Aluminosity index v. SiO_2 for Moromoro complex. I-type and S-type fields after Chappell and White (1974).

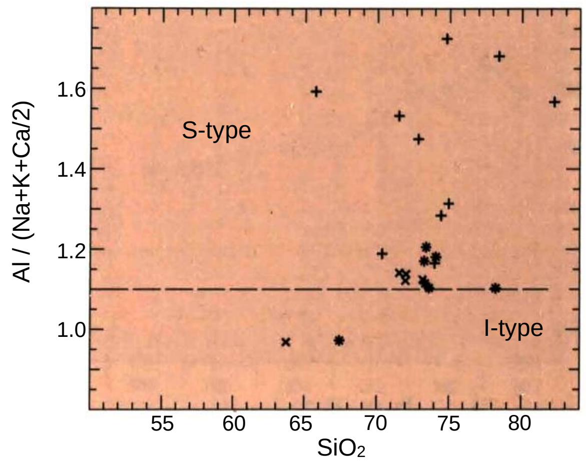

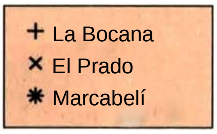

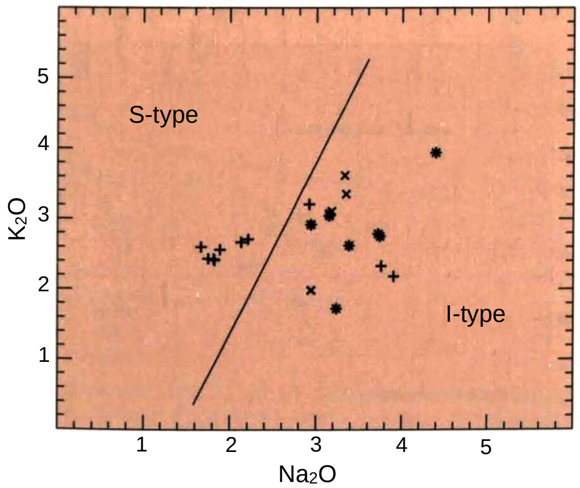

Figure 11. K_2O v. Na_2O diagram for Moromoro complex. I-type and S-type granite fields after Chappell and White (1974).

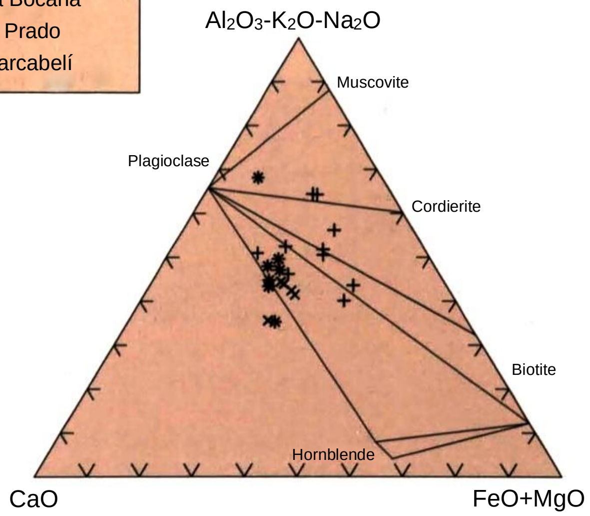

Figure 12. ACF ternary diagram for Moromoro complex.

The use of MORB (mid-ocean ridge basalt) normalised trace element 'spider-diagrams' to infer modification of the parent basalt magma composition by either subduction-related metasomatism and/or contamination by crustal material has been discussed by Pearce (1983). Metasomatic alteration causes enrichment in large ion lithophile (LIL) elements such as Sr, K, Rb, Ba and Th, together with P and light rare earth elements. Crustal contamination results in enrichment of a variety of elements, including Ta and Nb, with decreasing enrichment towards the more immobile elements so that Y and the heavy rare earths are hardly affected. In the absence of modification by either of the above processes the analyses should display flat patterns on the 'spider diagrams' with individual values close to unity for 'typical tholeiitic MORB', greater than 1 for 'primitive MORB' and less than 1 for 'evolved MORB'. Although the present data set does not include the full suite of elements used by Pearce (1983) it provides sufficient elements to determine the general form of the normalised curves.

The 'spider diagrams' for the Quebrada Plata unit and the Arenillas and Taqui units are shown in Figures 23 and 24 respectively. In both diagrams the curves are similar and notably flat. In Figure 23, data for the Quebrada Plata unit indicate little or no modification by either subduction-related metasomatism or crustal contamination, although the scattered, often high values for Ba and Th have not been explained. Low values for Rb, Nb and Ce indicate concentrations below XRFS detection. The general between-sample scatter, and slight enrichment of Cr and Ni suggest the effects of crystal fractionation. Figure 24 shows evidence of a degree of LIL enrichment in the Arenillas and, possibly, the Taqui units, suggesting minor subduction-related metasomatic modification. Nevertheless, the general picture is of ocean ridge basalt formed in an oceanic rather than a back-arc setting.

Figure 13. ROCK/ORG normalised spider diagram (after Pearce et al., 1984) for Marcabelí pluton, Moromoro complex.

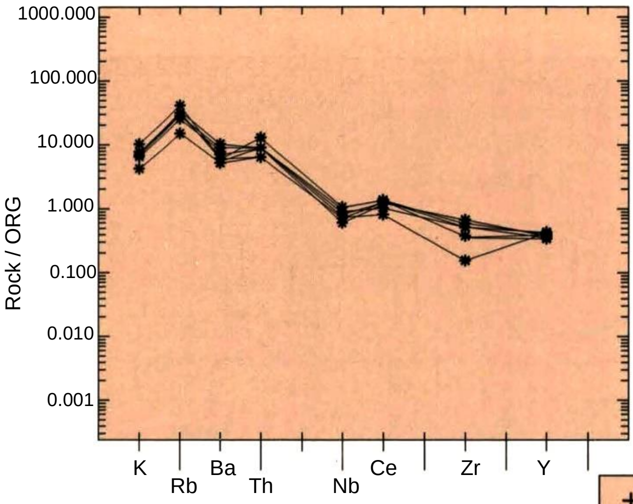

Figure 14. ROCK/ORG normalised spider diagram (after Pearce et al., 1984) for La Bocana unit, Moromoro complex.

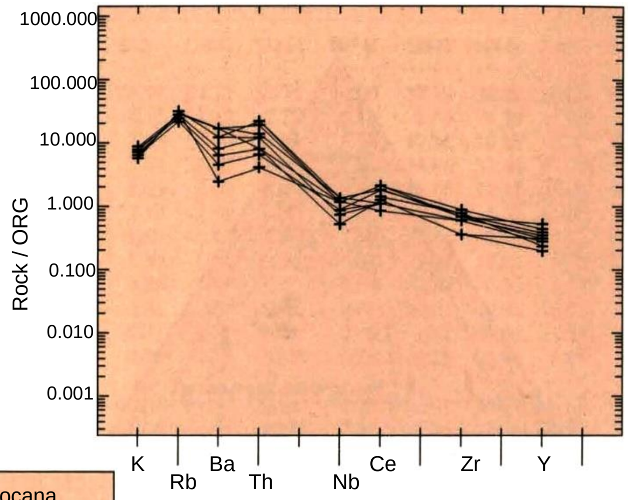

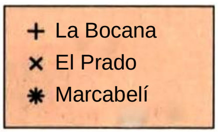

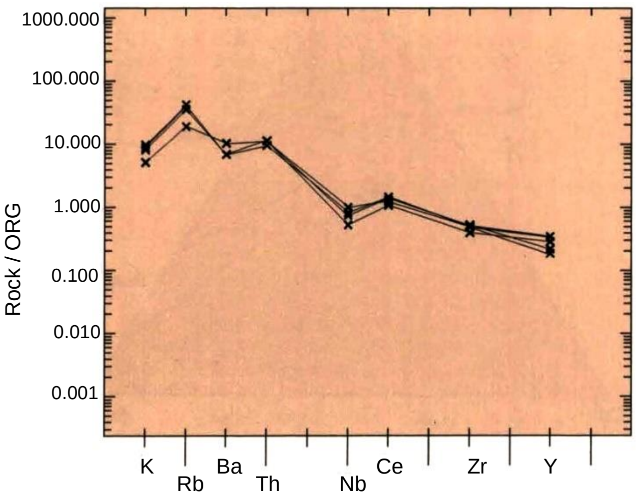

Figure 15. ROCK/ORG normalised spider diagram (after Pearce et al., 1984) for El Prado pluton, Moromoro complex.

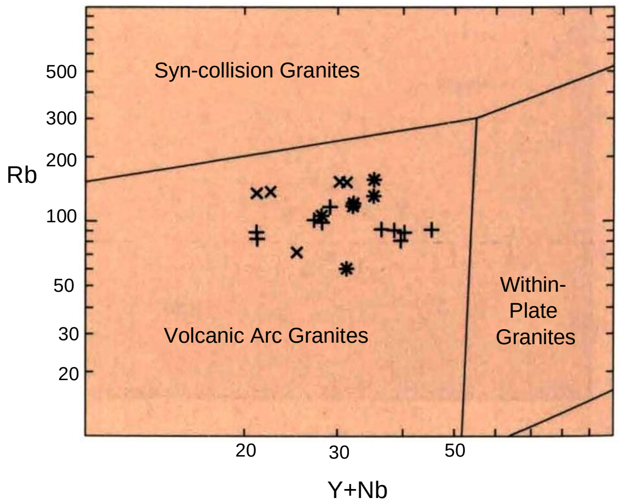

Figure 16. Rb v. Y + Nb diagram (after Pearce et al., 1984) for Moromoro complex.

Pearce (1983) and Pearce and Cann (1973) described the use of plots involving the immobile elements Zr, Ti and Y to discriminate different types of oceanic basalts and to distinguish between continental and oceanic arc basalts. In terms of the Zr/Y v. Zr diagrams (Figure 25), the Piedras mafic complex samples fall largely within the area of overlap between fields of MORB (mid-ocean ridge basalt) and (dominantly) oceanic island arc basalts. In the Ti v. Zr plot (Figure 26) the majority of the analyses plot in the area of overlap between the low-K tholeiite and the ocean-floor basalt fields, but they also define a trend of increasing Ti and Zr indicating ocean-floor character. In Figure 27 all but two of the samples plot within the ocean-floor basalt field. The spread of values in Figure 25 and 26 may reflect fractionation of Zr and Ti poor phases such as olivine.

These data, taken in conjunction with the intrusive character of these rocks and their association with granites of S-type character in a possible continental arc setting, are consistent with the emplacement of relatively unmodified, mantle-derived basaltic magmas.

Palenque mélange division (Raspas ophiolitic complex and unnamed serpentinite units)

The whole-rock analyses obtained from the Raspas ophiolitic complex (Río Panupali unit 7 analyses; El Toro unit 7 analyses) and various of the unnamed serpentinite bodies, including that from the Quebrada Plata unit, complex (8 analyses), are listed in Table 8. The normative compositions of these rocks, together with various geochemical indices, are given in Table 9. The geochemistry of the Arenillas and Taqui units has been discussed in the previous section.

Table 6. Piedras mafic complex whole-rock analyses

	QUEBRADA PLATA UNIT											ARENILLAS UNIT[1]			TAQUI UNIT[1]
Sample	**148**	**149**	**150**	**203**	**206**	**217**	**271**	**275**	**276A**	**339**	**349**	**295**	**333**	**347**	**384**
SiO_2	48.01	47.37	49.35	48.32	48.98	49.35	49.76	49.20	49.47	49.78	48.55	49.08	49.84	49.55	48.27
TiO_2	1.72	1.66	1.39	0.95	1.39	1.17	1.35	0.90	0.99	0.92	0.48	1.81	0.95	1.07	1.96
Al_2O_3	13.77	15.78	16.19	16.51	14.41	14.90	14.65	15.68	15.61	15.76	15.92	14.19	16.49	16.01	16.54
Fe_2O_3T	11.33	10.76	8.80	8.62	10.80	9.92	10.69	9.18	9.64	8.92	6.51	12.23	8.70	9.49	11.24
MnO	0.19	0.17	0.45	0.14	0.23	0.18	0.26	0.15	0.16	0.15	0.10	0.19	0.14	0.16	0.17
MgO	9.15	8.44	8.06	9.38	8.89	8.54	8.58	8.65	8.53	8.41	11.51	8.23	7.84	7.12	6.64
CaO	10.68	10.90	11.43	11.74	10.48	11.83	10.82	12.38	11.78	11.73	12.88	11.07	12.72	14.15	11.26
Na_2O	2.73	2.88	2.82	2.31	2.82	2.59	2.60	2.54	2.58	3.03	1.71	2.74	2.16	2.08	3.00
K_2O	0.08	0.11	0.13	0.09	0.11	0.05	0.20	0.07	0.09	0.24	0.09	0.08	0.38	0.35	0.64
P_2O_5	0.21	0.17	0.20	0.10	0.13	0.13	0.12	0.09	0.10	0.11	0.05	0.17	0.11	0.14	0.28
LOI	2.21	1.95	1.88	2.12	2.32	1.81	1.63	1.71	1.61	1.50	2.51	0.98	0.75	0.62	0.56
Total	100.08	100.19	100.70	100.28	100.56	100.47	100.66	100.55	100.56	100.55	100.31	100.77	100.08	100.74	100.56
As	4	15	1	0	1	0	4	4	3	3	4	1	1	2	18
W	4	3	2	1	0	3	1	1	1	1	1	3	2	2	5
Bi	0	0	0	0	0	0	0	0	0	0	0	0	1	0	0
V	250	231	195	154	237	204	235	182	185	172	104	294	175	203	202
Cr	325	250	290	323	264	290	271	340	330	348	764	253	422	307	202
Co	34	33	30	38	33	35	36	37	37	36	35	37	34	33	33
Ni	114	87	98	144	60	88	61	86	67	102	200	66	125	98	101
Cu	279	184	3	14	54	6	122	3	32	44	5	48	26	48	17
Zn	64	68	32	49	84	57	125	47	49	55	38	65	58	66	86
Rb	0	1	2	1	1	1	1	1	2	1	2	2	5	5	18
Sr	95	124	150	127	105	96	104	96	138	136	96	89	105	165	440
Y	32	27	22	16	27	21	24	18	19	16	10	31	18	20	27
Zr	93	99	88	52	74	61	72	47	52	49	20	82	44	52	134
Nb	4	3	6	1	2	2	2	2	1	0	1	2	2	1	11
Mo	0	2	3	1	1	0	2	1	0	4	0	0	0	3	0
Ag	3	3	3	2	3	3	3	3	2	3	4	4	4	4	4
Sn	0	0	0	0	0	0	0	0	0	0	0	0	0	0	0
Sb	0	0	0	0	1	0	0	0	0	0	0	0	0	0	0
Ba	31	34	60	24	34	21	35	25	44	41	14	43	95	109	201
La	6	6	7	4	4	4	1	3	0	2	1	3	4	3	9
Ce	13	11	9	0	3	2	12	8	6	3	10	9	9	10	26
Pb	1	0	0	0	0	0	3	0	1	0	2	3	3	0	4
Th	2	1	0	1	2	0	0	1	0	0	1	0	2	1	1
U	0	0	0	0	0	1	1	1	2	0	0	0	1	1	0

[1] As tectonic inclusions within the Palenque mélange division

Río Panupali unit

For comparative purposes the analytical data obtained from greenschists of the Río Panupali unit have been plotted together with that of the Piedras mafic complex (Figures 17-22 and 25-27). Based on these diagrams the Río Panupali unit is broadly similar to the Piedras mafic complex and is composed of ocean floor MORB (mid-ocean-ridge) basalts/basaltic andesites. In all of the geochemical plots however, the Río Panupali analyses, with the notable exception of one sample (298), stand out as a separate subgroup and, compared with the Piedras mafic complex are poorer in MgO (<6.0 wt%), Cr and Ni but richer in Fe (total) K, Rb, Ba, Ce (but not Nb) P, Zr, Ti (>1.5 wt%) and Y (Figures 20-28). It is possible that these characteristics reflect modification by crystal fractionation, giving an iron-enriched tholeiitic trend on the Ti/Zr plot (Figure 26), increasing K_2O (Figure 17) and increasing Ti and Zr to values beyond the normal basalt range (Figure 26). In the MORB-normalised trace element plot (Figure 28) this is again suggested by the strong Cr-depletion to values below detection. However, it is not clear whether the modest LIL-enrichment shown by this diagram is due to fractionation or indicates metasomatic enrichment in the magma source region.

As noted above, the greenschist sample 298 is anomalous compared with the rest of the Río Panupali analyses and, based the geochemical data, appears to belong to the Piedras mafic complex (Quebrada Plata unit) which also contains some greenstones (e.g. Table 6, 206). Such rocks are especially common along the Zanjón-Naranjo fault zone and are thought to represent the products of retrograde dynamothermal metamorphism. Given the location of sample 298 close to this fault zone it is therefore possible that, in the extreme east, (tectonic) inclusions of greenschists derived from the Piedras mafic complex exist within what is at present mapped as the Río Panupali unit. More detailed field mapping and geochemical data are required to test this possibility.

Table 7. Piedras mafic complex normative mineral compositions (Kelsey, 1965) and geochemical

	QUEBRADA PLATA UNIT											ARENILLAS UNIT[1]			TAQUI UNIT[1]
Sample	**148**	**149**	**150**	**203**	**206**	**217**	**271**	**275**	**276A**	**339**	**349**	**295**	**333**	**347**	**384**
Orthoclase	0.48	0.65	0.77	0.53	0.65	0.30	0.59	0.21	0.27	0.71	0.27	0.24	1.13	1.03	1.89
Albite	23.30	24.54	23.94	19.63	23.94	21.99	10.98	10.73	10.90	12.79	7.23	11.56	9.16	8.77	12.68
Anorthite	25.29	30.01	31.23	34.55	26.42	28.98	13.83	15.56	15.35	14.32	17.73	13.06	17.13	16.60	14.87
Diopside	21.69	18.92	19.66	18.75	20.19	23.55	10.20	11.97	10.94	11.62	11.18	11.23	11.45	14.58	9.91
Diopside (CaMg)	14.87	12.88	14.04	13.77	13.74	16.20	6.87	8.40	7.54	8.17	9.07	7.23	7.97	9.57	6.18
Hedenbergite	6.82	6.05	5.62	4.98	6.45	7.35	3.34	3.57	3.39	3.45	2.11	4.00	3.48	5.01	3.73
Hypersthene	10.46	3.50	11.00	10.72	12.45	12.24	8.45	4.07	5.85	1.71	6.19	6.40	7.01	4.30	0.18
Enstatite	6.86	2.27	7.54	7.58	8.09	8.05	5.43	2.73	3.86	1.15	4.89	3.92	4.67	2.69	0.11
Ferrosilite	3.60	1.22	3.46	3.14	4.36	4.19	3.03	1.33	1.99	0.56	1.30	2.48	2.34	1.61	0.07
Olivine	10.21	14.43	6.42	9.70	8.66	6.37	2.32	4.44	3.57	5.93	4.74	3.51	1.55	1.99	6.54
Forsterite	6.47	9.06	4.26	6.66	5.43	4.05	1.44	2.89	2.27	3.86	3.66	2.07	1.00	1.20	3.71
Fayalite	3.75	5.38	2.16	3.04	3.22	2.32	0.88	1.55	1.29	2.06	1.08	1.44	0.55	0.79	2.83
Magnetite	2.48	2.36	1.92	1.88	2.36	2.16	1.16	1.00	1.05	0.97	0.71	1.33	0.95	1.03	1.22
Chromite	0.07	0.05	0.06	0.07	0.06	0.06	0.03	0.04	0.04	0.04	0.08	0.03	0.05	0.03	0.02
Ilmenite	3.29	3.17	2.65	1.81	2.65	2.23	1.28	0.85	0.94	0.87	0.46	1.71	0.90	1.01	1.86
Apatite	0.50	0.41	0.48	0.24	0.31	0.31	0.14	0.11	0.12	0.13	0.06	0.20	0.13	0.17	0.33
Diff. index	23.77	25.19	24.71	20.16	23.59	22.29	11.57	10.93	11.16	13.50	7.49	11.80	10.29	9.80	14.57
Colour index	48.21	42.44	41.71	42.92	46.36	46.62	23.44	22.37	22.38	21.13	23.36	24.21	21.91	22.95	19.72
mg number	65.30	64.63	68.09	71.71	65.73	66.73	65.16	68.70	67.34	68.72	80.47	61.06	67.74	63.61	57.92

[1] As tectonic inclusions within the Palenque mélange division

El Toro unit and unnamed serpentinites

According to Pearce et al. (1984a) 'MORB-type' and 'supra-subduction zone' (i.e. back-arc) ophiolites can be distinguished by using Ti as a discriminant element. Most of the present analyses, and especially those of the El Toro unit, have very low Ti contents, often below detection limit (<0.01 %) (Table 8).

It might be assumed that such samples can be classified as 'supra-subduction zone' ophiolites. Hence, as shown in Figure 29, the majority of the serpentinites, including those of the Quebrada Plata unit, plot as supra-subduction zone ophiolites but two samples (RB35G and 284, Table 8) plot within the 'MORB-type' field. The implications of this plot are uncertain.

Figure 17. K_2O v. SiO_2 classification diagram (after Ewart, 1982) for Piedras complex (Quebrada Plata, Arenillas and Taqui units) and Raspas ophiolitic complex (Río Panupali unit).

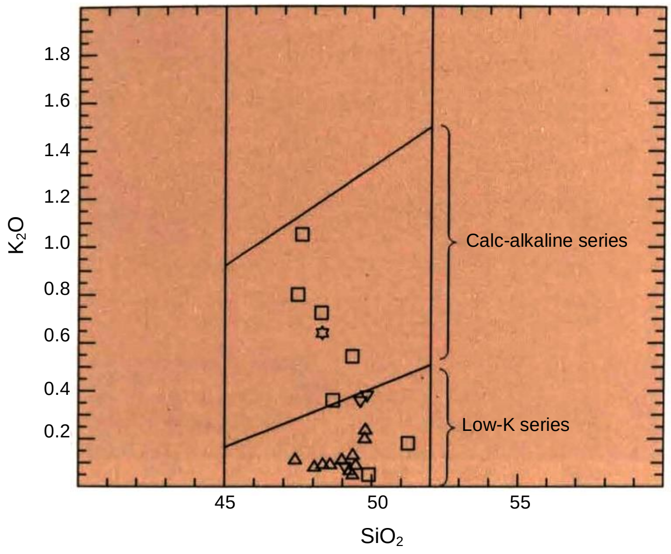

Figure 18. Na_2O+K_2O v. SiO_2 classification diagram (after Le Bas et al., 1986) for Piedras complex (Quebrada Plata, Arenillas and Taqui units) and Raspas ophiolitic complex (Río Panupali unit).

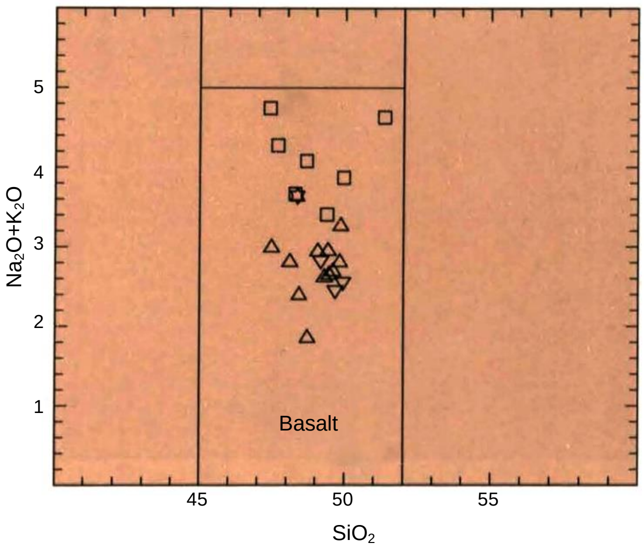

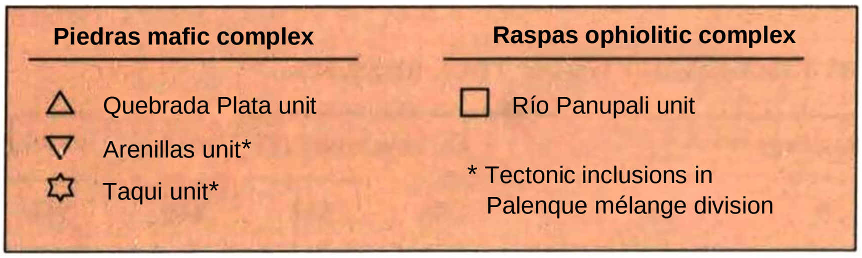

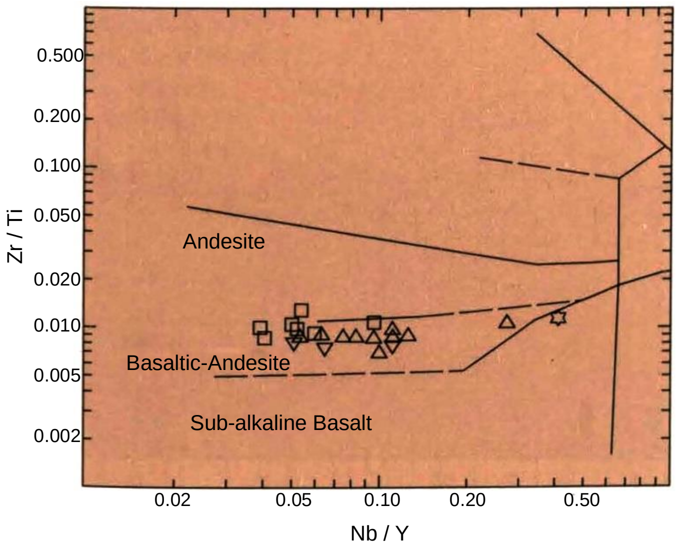

Figure 19. Zr/Ti v. Nb/Y classification diagram (after Winchester and Floyd, 1977) for Piedras complex (Quebrada Plata, Arenillas and Taqui units) and Raspas ophiolitic complex (Río Panupali unit).

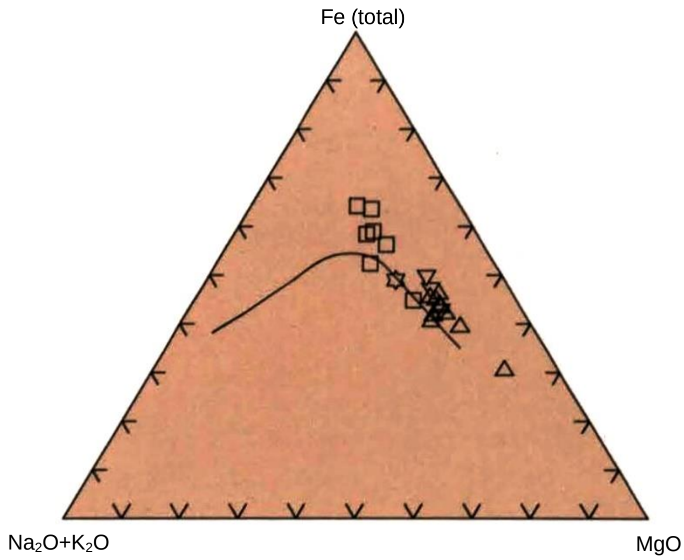

Figure 20. AFM ternary diagram for Piedras complex (Quebrada Plata, Arenillas and Taqui units) and Raspas ophiolitic complex (Río Panupali unit).

Figure 21. TiO_2 and Sr v. MgO diagrams for Piedras complex (Quebrada Plata, Arenillas and Taqui units) and Raspas ophiolitic complex (Río Panupali unit).

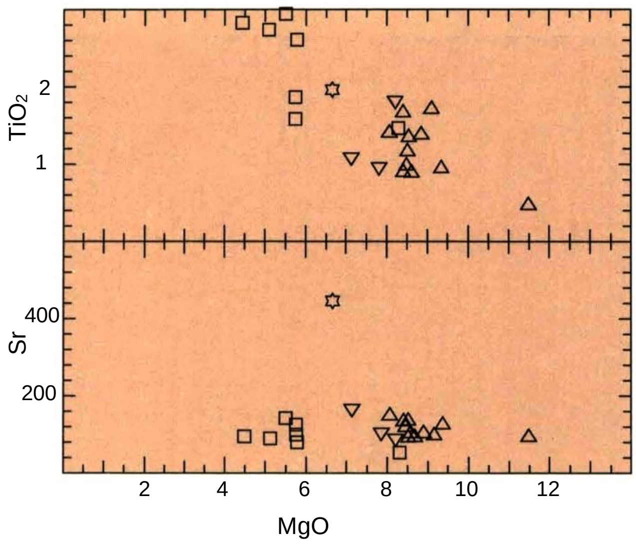

Figure 22. Zr and Y v. MgO diagrams for Piedras complex (Quebrada Plata, Arenillas and Taqui units) and Raspas ophiolitic complex (Río Panupali unit).

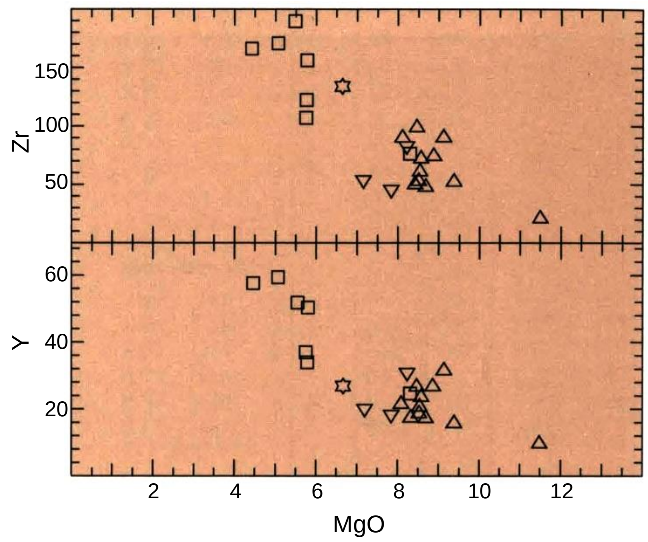

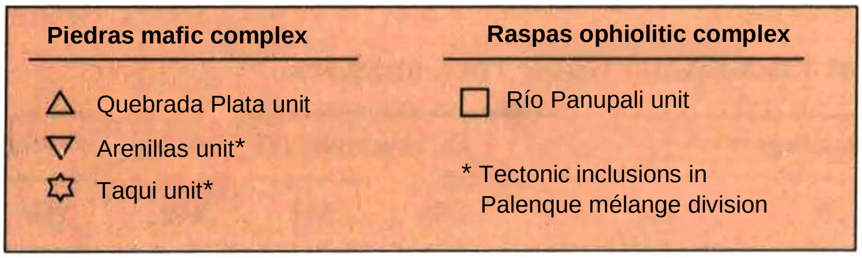

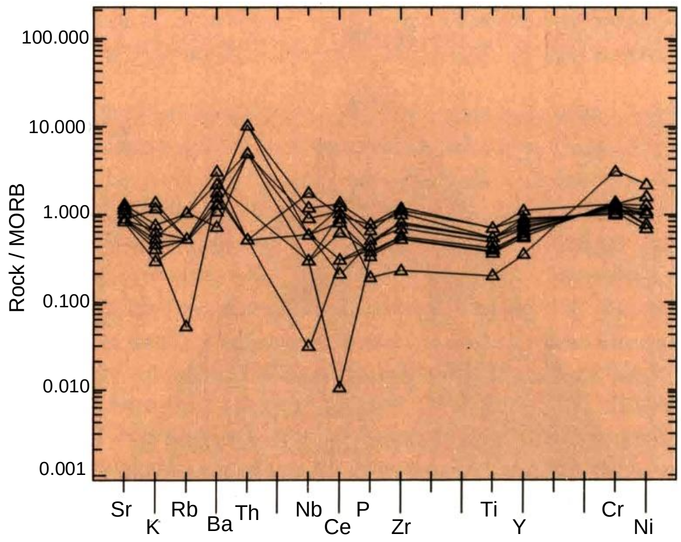

Figure 23. ROCK/MORB normalised spider diagram (after Pearce, 1983) for Quebrada Plata unit, Piedras complex

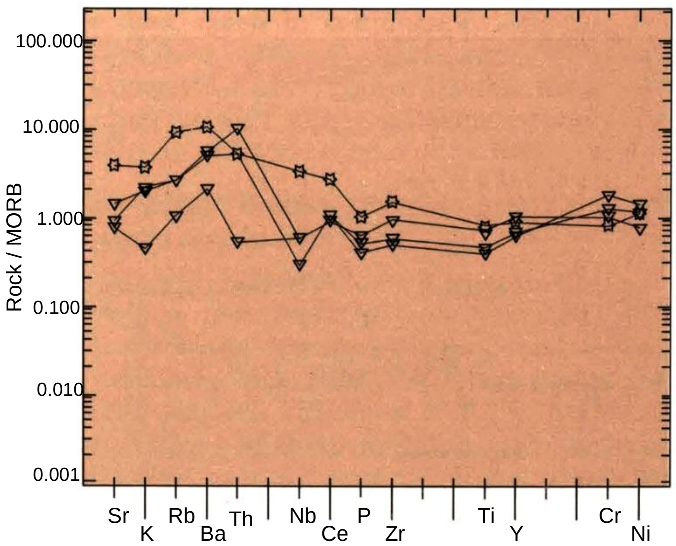

Figure 24. ROCK/MORB normalised spider diagram (after Pearce, 1983) for Arenillas and Taqui units, Piedras complex

Figure 25. Zr/Y v. Zr discriminant plot (after Pearce, 1983) for Piedras complex (Quebrada Plata, Arenillas and Taqui units) and Raspas ophiolitic complex (Río Panupali unit)

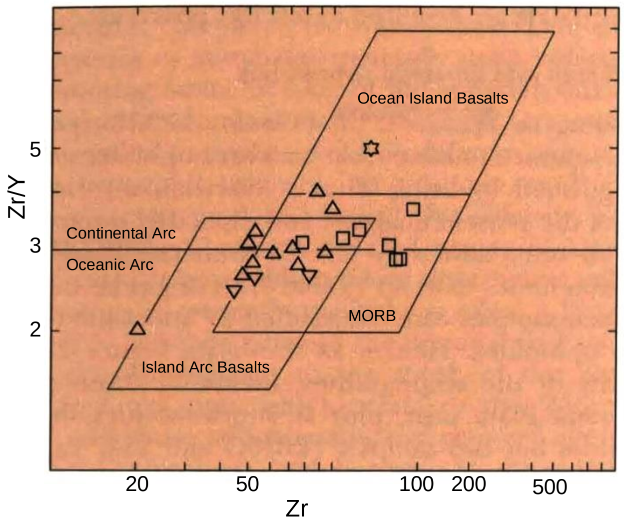

Figure 26. Ti v. Zr discriminant plot (after Pearce and Cann, 1973) for Piedras complex (Quebrada Plata, Arenillas and Taqui units) and Raspas ophiolitic complex (Río Panupali unit)

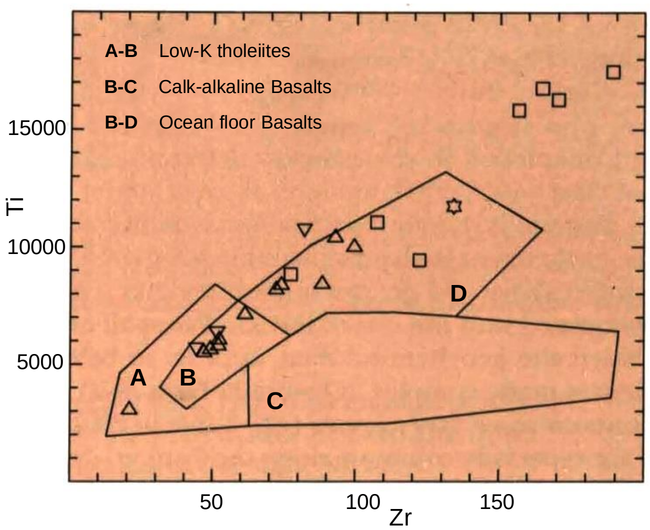

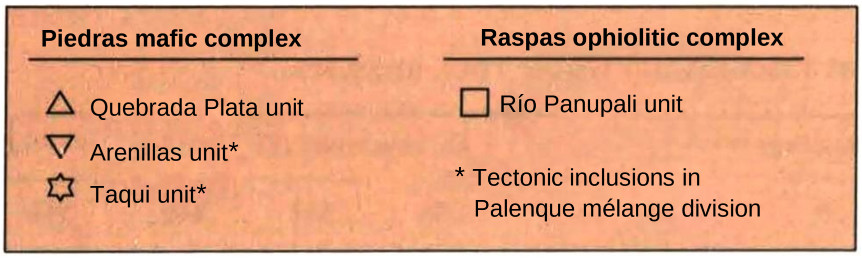

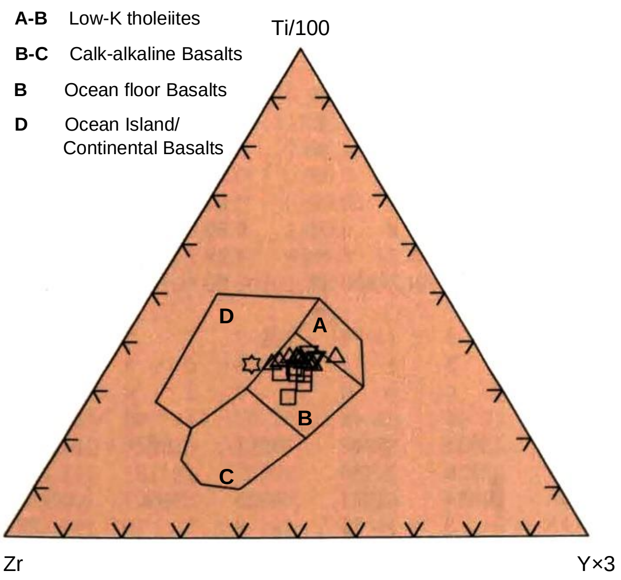

Figure 27. Zr – Ti/100 – Y×3 discriminant plot (after Pearce and Cann, 1973) for Piedras complex (Quebrada Plata, Arenillas and Taqui units) and Raspas ophiolitic complex (Río Panupali unit)

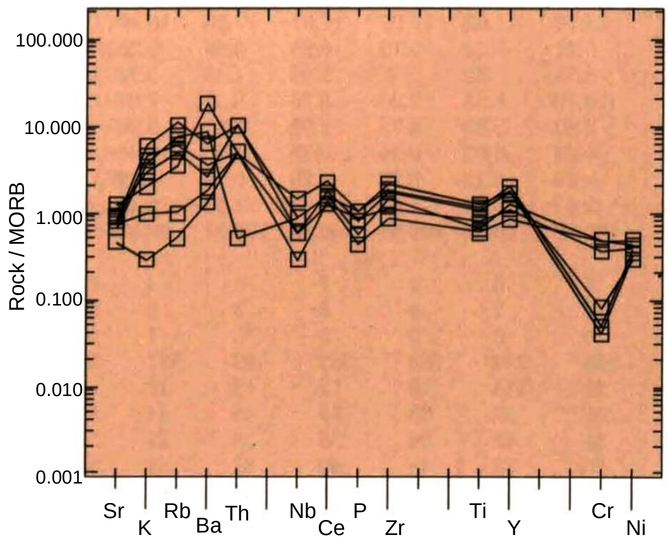

Figure 28. ROCK/MORB normalised spider diagram (after Pearce, 1983) for Río Panupali unit, Raspas ophiolitic complex.

Table 8. Palenque mélange division (inclusions) whole-rock analyses

	RÍO PANUPALI UNIT (RASPAS OPHIOLITIC COMPLEX)							EL TORO UNIT (RASPAS OPHIOLITIC COMPLEX)						
Sample	**270**	**298**	**301B**	**357**	**358**	**359**	**360**	**335**	**341**	**342**	**343**	**346**	**363A***	**363B***
SiO_2	49.33	49.90	48.60	48.21	47.57	47.34	51.31	40.61	41.17	41.34	41.15	41.30	40.85	41.11
TiO_2	1.87	1.47	2.92	2.72	2.80	2.60	1.57	0.00	0.00	0.00	0.00	0.00	0.00	0.00
Al_2O_3	14.49	13.66	14.10	12.94	13.30	12.71	12.98	1.68	1.75	1.92	1.14	1.08	1.30	1.14
Fe_2O_3T	13.18	11.02	15.22	17.01	17.26	16.49	12.66	8.63	8.58	8.34	8.47	9.01	8.55	8.62
MnO	0.21	0.16	0.16	0.23	0.30	0.25	0.17	0.12	0.12	0.12	0.12	0.12	0.10	0.10
MgO	5.73	8.32	5.49	5.09	4.43	5.77	5.74	38.38	39.53	39.54	41.86	43.73	37.12	38.05
CaO	10.10	8.33	7.89	8.70	8.36	7.27	8.68	0.03	1.57	1.47	1.15	0.78	0.52	0.18
Na_2O	2.87	3.82	3.72	2.93	3.21	3.94	4.46	0.00	0.06	0.04	0.03	0.13	0.00	0.00
K_2O	0.54	0.05	0.36	0.73	1.06	0.81	0.18	0.00	0.01	0.01	0.00	0.01	0.01	0.01
P_2O_5	0.24	0.12	0.29	0.28	0.29	0.22	0.15	0.00	0.02	0.02	0.03	0.02	0.01	0.01
LOI	2.42	3.24	1.84	2.04	1.73	2.46	1.30	11.36	7.10	7.84	6.42	4.68	11.66	11.49
Total	100.98	100.09	100.59	100.88	100.31	99.86	99.20	100.81	99.91	100.64	100.37	100.86	100.12	100.71
As	1	6	1	7	5	4	5	14	10	3	4	2	2	6
W	2	2	4	5	5	2	1	2	3	3	1	3	3	2
Bi	0	0	0	0	0	1	0	0	0	0	0	0	0	0
V	265	239	384	365	409	377	257	56	48	46	42	37	40	50
Cr	91	114	19	12	12	10	120	2940	3053	3034	3062	3311	3026	3051
Co	35	35	33	39	46	44	31	132	127	128	135	142	131	136
Ni	36	42	26	35	34	29	38	1531	1645	1654	1791	1883	1867	1785
Cu	36	83	48	40	35	58	39	37	13	3	11	3	16	26
Zn	105	61	119	143	165	132	87	49	37	37	36	44	39	47
Rb	10	1	7	15	20	12	2	0	0	1	0	0	1	0
Sr	125	53	140	89	96	77	102	1	5	5	3	2	3	2
Y	34	25	52	60	58	51	37	0	0	0	0	0	0	0
Zr	107	77	189	170	165	156	122	2	1	0	0	1	1	4
Nb	2	1	5	3	3	2	2	0	0	0	0	0	0	0
Mo	0	0	1	2	1	0	3	0	0	0	1	0	1	0
Ag	3	4	4	4	5	5	4	0	1	1	2	2	0	0
Sn	0	0	0	4	4	1	0	0	0	0	0	0	0	0
Sb	0	0	0	2	0	0	0	1	0	0	0	0	0	0
Ba	52	27	375	167	123	71	36	11	16	17	13	18	23	16
La	3	2	7	7	5	8	3	0	0	0	0	0	0	0
Ce	12	13	22	15	14	16	17	19	10	0	0	4	17	5
Pb	0	0	0	1	2	2	3	0	2	0	0	5	1	0
Th	2	1	1	0	2	1	1	0	0	1	0	1	0	1
U	1	0	0	0	0	0	0	0	0	0	0	0	0	0

* Serpentinite lens within Quebrada Plata unit, Piedras mafic complex

STRUCTURE

General

In complete contrast to the NNE-SSW regional strike of the Ecuadorian Andes the structural grain of the El Oro metamorphic complex is east-west and is dominated by the presence of numerous, generally steep, sub-parallel, anastomosing faults. In spite of the apparent uniformity of the various structural elements, the El Oro metamorphic complex comprises rocks of different ages, origins and metamorphic histories and it follows that the structures preserved must also reflect this diversity. Further work is required before a detailed structural/kinematic framework can be established but nevertheless sufficient information is currently available to allow a broad distinction to be made between the dominantly Late Triassic structures, present to the south of the Zanjón-Naranjo fault zone, which relate to the 'Moromoro event' and those of uncertain, but younger age (? Late Jurassic-Cretaceous), which occur to the north and relate to the 'Palenque event'.

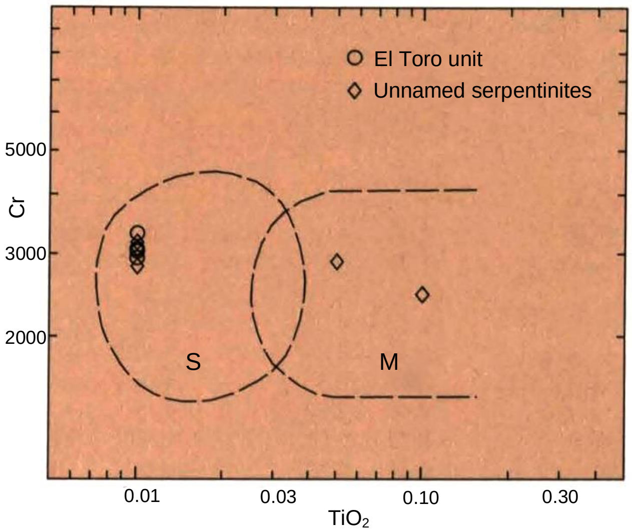

Figure 29. Cr v. TiO_2 discriminant plot (after Pearce et al., 1984a) for El Toro and other serpentinites of Palenque division. S = supra-subduction zone ophiolites; M = MORB ophiolites.

Table 8. (*continued*) Palenque mélange division (inclusions) whole-rock analyses

	UNNAMED SERPENTINITES							
Sample	**RB35G**	**231**	**284**	**303**	**305**	**397**	**398**	**400**
SiO_2	40.69	38.21	42.06	40.16	40.19	40.73	41.33	41.69
TiO_2	0.10	0.01	0.05	0.01	0.00	0.00	0.01	0.00
Al_2O_3	3.13	1.17	3.22	2.51	1.38	1.36	1.86	1.49
Fe_2O_3T	8.09	7.86	7.98	8.31	7.44	7.83	7.46	6.96
MnO	0.12	0.10	0.12	0.11	0.08	0.09	0.10	0.09
MgO	36.44	38.53	35.65	36.38	38.50	39.11	37.50	39.03
CaO	1.23	0.87	2.60	0.83	0.03	0.17	0.47	0.05
Na_2O	0.02	0.00	0.04	0.00	0.00	0.00	0.00	0.00
K_2O	0.06	0.01	0.02	0.01	0.01	0.01	0.01	0.01
P_2O_5	0.02	0.04	0.05	0.00	0.00	0.00	0.00	0.01
LOI	10.80	13.85	8.02	11.85	11.58	11.63	11.30	11.53
Total	100.70	100.65	99.81	100.17	100.21	100.93	100.04	100.86
As	1	7	292	11	20	2	6	5
W	2	5	5	3	2	3	5	3
Bi	1	1	0	0	0	0	0	0
V	67	44	70	63	33	38	49	39
Cr	2461	3083	2898	3167	2823	3093	3103	3187
Co	111	122	102	118	132	125	124	118
Ni	1405	1685	1262	1629	1769	1791	1617	1537
Cu	21	5	55	44	6	0	5	3
Zn	38	31	52	51	46	37	41	31
Rb	2	0	0	1	0	1	2	2
Sr	2	2	10	6	1	2	14	4
Y	2	0	1	1	0	0	1	0
Zr	2	0	0	1	0	1	3	1
Nb	0	0	1	0	0	0	1	0
Mo	2	0	0	0	1	0	0	0
Ag	1	0	2	0	0	0	0	0
Sn	0	0	0	0	0	0	0	0
Sb	1	5	4	6	6	1	1	2
Ba	22	12	15	27	17	10	17	38
La	1	0	0	0	0	0	0	0
Ce	5	12	0	13	19	13	6	14
Pb	1	1	3	1	2	1	0	2
Th	1	1	1	0	0	1	2	0
U	0	0	0	0	0	0	0	0

Table 9. Palenque mélange division (inclusions) normative mineral compositions (Kelsey, 1965) and geochemical indices.

	RÍO PANUPALI UNIT							EL TORO UNIT						
Sample	**270**	**298**	**301B**	**357**	**358**	**359**	**360**	**335**	**341**	**342**	**343**	**346**	**363A***	**363B***
Corundum	0.00	0.00	0.00	0.00	0.00	0.00	0.00	0.80	0.00	0.00	0.00	0.00	0.18	0.39
Orthoclase	1.59	0.15	1.06	2.15	3.15	2.41	0.54	0.00	0.03	0.03	0.00	0.03	0.03	0.03
Albite	12.09	16.22	15.75	12.38	13.64	16.81	19.12	0.04	0.25	0.17	0.13	0.55	0.04	0.04
Anorthite	12.48	10.03	10.36	9.98	9.42	7.36	7.53	0.07	2.24	2.50	1.48	1.16	1.26	0.44
Diopside	9.67	8.39	6.87	8.91	8.80	8.41	11.40	0.00	1.26	0.83	0.99	0.55	0.00	0.00
Diopside (CaMg)	5.18	5.58	3.51	4.02	3.63	4.10	6.17	0.00	1.15	0.76	0.91	0.50	0.00	0.00
Hedenbergite	4.49	2.81	3.35	4.89	5.17	4.30	5.23	0.00	0.11	0.07	0.08	0.05	0.00	0.00
Hypersthene	8.77	6.02	7.23	9.69	5.10	0.56	3.83	16.00	10.11	10.79	8.93	6.57	16.39	16.70
Enstatite	4.40	3.81	3.45	4.04	1.93	0.26	1.94	14.36	9.11	9.75	8.10	5.95	14.68	14.98
Ferrosilite	4.37	2.20	3.78	5.65	3.16	0.31	1.89	1.64	1.00	1.04	0.83	0.62	1.71	1.71
Olivine	0.44	4.59	2.72	0.76	3.78	8.29	3.55	26.12	31.19	30.45	33.91	37.41	24.94	25.36
Forsterite	0.21	2.80	1.23	0.30	1.35	3.57	1.71	23.21	27.82	27.25	30.47	33.56	22.10	22.52
Fayalite	0.23	1.78	1.49	0.46	2.43	4.73	1.84	2.92	3.37	3.21	3.44	3.85	2.83	2.84
Magnetite	1.43	1.20	1.66	1.85	1.88	1.81	1.40	0.93	0.94	0.90	0.92	0.97	0.93	0.93
Chromite	0.01	0.01	0.00	0.00	0.00	0.00	0.01	0.31	0.33	0.32	0.33	0.35	0.33	0.33
Ilmenite	1.77	1.40	2.77	2.58	2.76	2.49	1.51	0.00	0.00	0.00	0.00	0.00	0.00	0.00
Apatite	0.28	0.14	0.34	0.33	0.34	0.26	0.18	0.00	0.02	0.02	0.04	0.02	0.01	0.00
Diff. index	13.68	16.37	16.81	14.53	16.78	19.22	10.66	0.04	0.28	0.20	0.13	0.58	0.07	0.07
Colour index	22.09	21.61	21.25	23.78	22.23	21.56	21.70	43.37	43.82	43.31	45.08	45.85	42.58	43.31
mg number	50.32	63.76	45.66	41.08	37.42	44.91	51.37	91.20	91.48	91.70	92.01	91.88	91.00	91.14

* Serpentinite lens within Quebrada Plata unit, Piedras mafic complex

	UNNAMED SERPENTINITES							
Sample	**RB35G**	**231**	**284**	**303**	**305**	**397**	**398**	**400**
Corundum	0.84	0.00	0.00	0.49	0.65	0.51	0.49	0.69
Orthoclase	0.35	0.06	0.06	0.03	0.03	0.03	0.03	0.03
Albite	0.17	0.00	0.17	0.04	0.04	0.04	0.04	0.04
Anorthite	5.95	3.15	4.29	2.06	0.07	0.42	1.17	0.09
Diopside	0.00	0.70	1.59	0.00	0.00	0.00	0.00	0.00
Diopside (CaMg)	0.00	0.64	1.45	0.00	0.00	0.00	0.00	0.00
Hedenbergite	0.00	0.06	0.14	0.00	0.00	0.00	0.00	0.00
Hypersthene	28.33	18.92	13.59	15.06	17.42	15.06	17.35	17.67
Enstatite	25.50	17.16	12.22	13.51	15.88	13.69	15.78	16.22
Ferrosilite	2.84	1.76	1.37	1.55	1.54	1.38	1.58	1.45
Olivine	51.08	60.91	24.93	25.09	24.84	26.95	24.07	24.62
Forsterite	45.50	54.72	22.18	22.26	22.44	24.26	21.68	22.42
Fayalite	5.58	6.19	2.75	2.82	2.40	2.69	2.39	2.20
Magnetite	1.75	1.70	0.87	0.90	0.81	0.84	0.81	0.75
Chromite	0.53	0.66	0.31	0.34	0.30	0.33	0.33	0.34
Ilmenite	0.19	0.02	0.05	0.01	0.00	0.00	0.01	0.00
Apatite	0.05	0.09	0.06	0.00	0.00	0.00	0.00	0.01
Diff. index	0.52	0.06	0.23	0.07	0.07	0.07	0.07	0.07
Colour index	81.88	82.91	41.34	41.40	43.37	43.19	42.58	43.39
mg number	91.30	91.95	91.23	91.07	92.34	92.09	92.13	92.89

Structure south of Zanjón-Naranjo fault zone, the 'Moromoro event'

The dips in the unmetamorphosed to weakly metamorphosed El Tigre unit are variable but normally steep to moderate and generally to the north. Numerous bedding-parallel faults occur throughout the unit and where observed, the associated lineations/slickensides are horizontal or have gentle, east-west plunges (Plate 20). Many of these faults are marked by irregular, concordant/discordant, quartz veins and lenses. In areas of high strain, zones of bedding-parallel cleavage may be developed but these are generally restricted to narrow incompetent shale/lutite horizons where a horizontal/subhorizontal (transpressional), dextral shear sense can sometimes be established. Elsewhere, structures tend to be of a more brittle nature, especially in the massive, quartzose horizons, where quartz-filled tensional features, some of which are demonstrably dextral, are commonly developed and are typically oblique to the main east-west, structural trend of the unit. In some areas, for example to the west of Marcabelí (**Marcabelí 617/9581**), the El Tigre unit is overturned but we have been unable to confirm that the entire unit is inverted (cf. Feininger, 1978) and suggest that such phenomena may be associated with local thrusts/flower structures which often develop near surface, in association with regional strike-slip zones (Sylvester, 1988).

Structurally the La Victoria unit is similar to the El Tigre unit but, as evidenced by the metamorphic mineral assemblages, this unit was deformed at higher temperatures. The contact between the two units corresponds to a steep, complex, east-west-trending, tectonic zone across which there is an increase in metamorphic grade and intensity of, generally subhorizontal, ductile shearing. Throughout the La Victoria unit, cleavage and bedding, where still recognisable, are normally parallel and, with notable exceptions, they are usually steep and to the north.

Lineations, which typically have shallow (<30°), easterly or westerly plunges, are preserved on many surfaces (Plates 20, 21 and 22). Both within the La Victoria unit and in parts of the Moromoro granitoid complex, especially in the south, macroscopic and microscopic kinematic indicators such as winged inclusions, boudinaged quartz veins, rotated porphyroblasts/megacrysts, tight-to-isoclinal Z-folds and/or kink bands (often with steep-to-vertical fold axes), S-C mylonite fabrics and mica fish are common (for review of kinematic indicators see Hammer and Passchier, 1991): all give a consistent sense of dextral movement (Plates 23-26). In the sense of Lister and Snoke (1984), much of the La Victoria unit (and parts of the El Tigre unit) consists of Type II S-C mylonites.

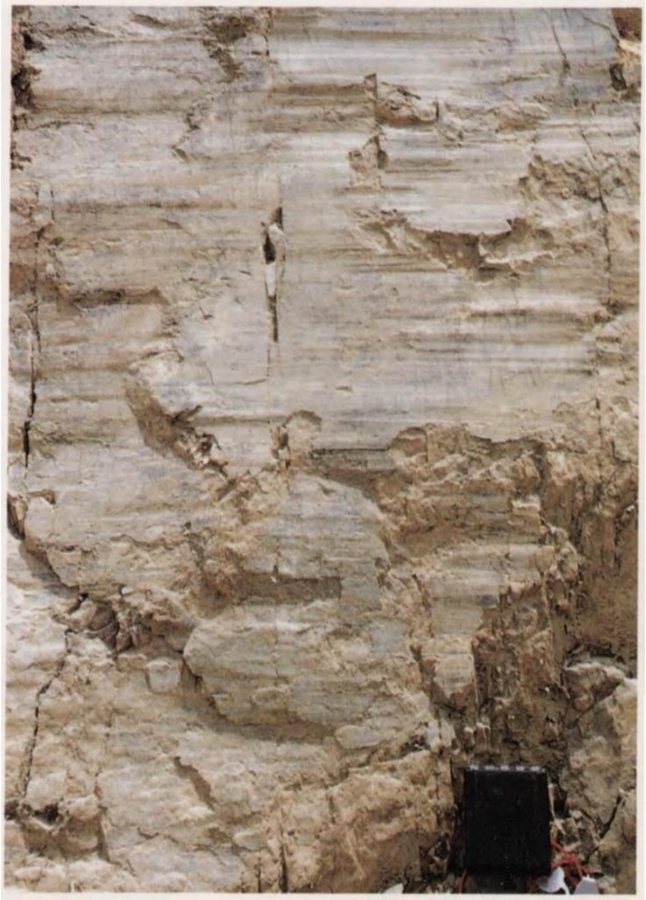

Plate 20. Horizontal (dextral) slickensides on vertical surface, El Tigre unit, Tahuín division, new Arenillas-Alamor road.

The high fault density and its anastomosing pattern, the evidence from mineral lineations and shear sense indicators, all strongly support the interpretation that, during the 'Moromoro event', these rocks were deformed and metamorphosed in a regional zone of dextral transpression. The dominant sense of movement was approximately horizontal and parallel to faulting (i.e. strike-slip in the sense of Sylvester, 1988). In the west, to the north of La Victoria and exposed along the main Arenillas road, thrusts of mylonitic schists have been mapped which are highly oblique to the normal, east-west structural trend of the La Victoria unit. These mylonitic rocks are not well exposed but have a variable, often gentle, westerly dipping, bedding-parallel cleavage and westerly plunging, mineral lineations. Boudinaged and sigmoidally Z-folded quartz veins suggest tectonic transport from west to east. These structures may correspond to contractional strike-slip duplexes, such as are commonly formed at restraining/compressional bends (Woodcock, 1986; Crowell, 1979).

Plate 21. Mylonitic L-S tectonites, La Victoria unit, Tahuín division, Río Moromoro.

Plate 22. Mylonitic L-S tectonites, La Victoria unit, Tahuín division, north of Las Lajas.

In the south, the east-west-trending Marcabelí and El Prado plutons are generally unfoliated. However, the northern part of the Marcabelí pluton is cut by a series of generally steep, dextral shear zones (Plate 14) and within the La Victoria unit, particularly in the west, a number of strongly foliated, isolated, faulted-bounded lenses belonging to the Moromoro granitoid complex, are present. The main outcrop of the Moromoro granitoid complex is variably deformed. In some areas, coarse, but fairly penetrative, foliations and/or discreet, ductile S-C (dextral) mylonite fabrics are preserved (Plate 26) but often these granitoids have an irregular or weakly developed (nebulitic) gneissic foliations or linear fabrics, due to the alignment of biotite/biotite schlieren and/or flattened and elongated xenolithic material (Plates 4 and 5).

Elsewhere, for example in the La Florida area in the west, the La Florida pluton is unfoliated and apparently undeformed (Plates 10 and 11). Together these observations suggest that the magmatic activity associated with the 'Moromoro event' may have been either relatively long-lived or episodic in nature since it appears to include a variety of syn-to late- and possibly post-tectonic plutons.

Structural dips within the elongate, east-west-striking Quebrada Plata unit are variable but generally steep. The southern contact of this unit with the Moromoro granitoid complex was possibly intrusive but is now faulted. Since the amphibolites along this contact are not brecciated, nor apparently have they been significantly retrogressed, it is probable that it was formed close to peak metamorphic conditions during the 'Moromoro event'.

Plate 23. Boudinaged quartz veins indicating dextral movement, low-grade portion of La Victoria unit, Tahuín division, Río Moromoro

Plate 24. Dextral winged inclusion, high-grade portion of La Victoria unit, Tahuín division, Río Moromoro

Zanjón-Naranjo fault zone

Along the Zanjón-Naranjo fault zone the northern margin of the Quebrada Plata amphibolite unit has been widely retrogressed to greenschist. In several areas (e.g. along the Río Naranjo, west of Zaracay) a distinctive, banded tectonite, which has a strongly developed, steep-to-vertical, amphibole (actinolite), mineral lineation has been produced (Plate 17). Late, semiductile, conjugate sets of (Z) kink bands indicate downthrow to the north. These tectonites suggest that movement along this segment of the fault was probably dominantly of a high temperature, ductile nature, however, in the extreme west, near the disputed frontier with Perú, tectonic breccias have been observed. Regionally, this fault zone defines the southern tectonic limit of the Palenque mélange division and the Raspas ophiolitic complex, and therefore represents an important structure within the El Oro metamorphic complex. Although the overall sense and timing of the major movements are uncertain, they postdate those of the Late Triassic 'Moromoro event' and are assumed to relate to those of the 'Palenque event'.

Structure north of the Zanjón-Naranjo fault zone, the 'Palenque event'

To the north of the Zanjón-Naranjo fault zone is the Palenque mélange division. The age of formation of the mélange, its structuring and associated metamorphism are not well constrained but occurred during what is here referred to as the 'Palenque event'. The fine grained, generally incompetent, matrix sediments of the Palenque division have been plastically deformed and their structure is dominated by the presence of steep-to-vertical, bedding-parallel, east-west-trending faults which probably have a complex history of movement. Bedding/cleavage relationships are also parallel and although variable, in both direction (i.e. to the north or south) and amount, are generally steep. Macroscopic, kinematic indicators and lineations are relatively rare at outcrop level but, where observed, they suggest a dextral sense of shear with fairly gentle plunges.

In the south and east, strongly deformed, steeply dipping, sometimes silicified, black (± graphite) phyllonites and quartzose mylonites occur sandwiched between the Zanjón-Naranjo fault zone and the Raspas ophiolitic complex. In the west dips are more variable, but generally they are to the south along the Tahuín dam (thrust) fault. Elsewhere, contacts between the matrix sediments and the various tectonic inclusions within the Palenque mélange division are often steep and, in some cases, subhorizontal dextral shear can be demonstrated.

Plate 25. Boudinaged pegmatitic vein and small-scale Z-folds (right centre) indicating dextral movement, high-grade portion of La Victoria unit, Tahuín division, Quebrada Primavera.

Plate 26. Dextral S-C (Type 1) mylonite, La Bocana unit, Moromoro Complex, Río Moromoro.

In the Quera Chico, Limón Playa, Arenillas and Taqui units (?)older, ductile structures are preserved. However, especially in the amphibolite units, younger, irregular, brittle fractures and semibrittle, often steep, east-west-trending shear zones are present. It is tentatively suggested that these structures formed during, or following, the incorporation of these older, competent rocks into the Palenque mélange division. Available K-Ar and U/Pb dates indicate that a thermal event affected the Arenillas and Limón Playa units at about 74-80 Ma and some of these structures may relate to this event (see also Aspden et al., 1992).

Few detailed structural observations are available for the Raspas ophiolitic complex. Mora (1988) confirmed the common occurrence of mylonitic textures in both the Río Panupali and La Chilca units and in the west, a series of southwesterly dipping imbricate thrust faults, which have southerly plunging mineral lineations, have been mapped within the Río Panupali unit. In spite of the often steep internal and contact structures, the emplacement of the Raspas ophiolitic complex from its original depth of formation (about 9Kb, Duque, 1992), to its present structural level, must have involved several kilometres of vertical movement (for models of blueschist emplacement see Platt, 1987 and 1986).

Structural limits of the El Oro metamorphic complex

The northern limit of the main outcrop of the El Oro metamorphic complex coincides with the Jubones fault, which was previously considered to separate the older metamorphic rocks to the south from the 'Upper Cretaceous marine island arc volcanics … of the Western Cordillera … to the north' (Baldock, 1982). However, since inliers of metamorphic rocks, similar to those found within the El Oro metamorphic complex, have been reported to the north of the Jubones fault it is unlikely that this structure is of major regional significance. Nevertheless, the fault is of local importance and probably has a complex history, which included a normal component of movement with significant downthrow to the north. The fact that the Jubones fault is parallel to other east-west-trending faults within the Palenque mélange complex suggests a common origin but, the presence of highly contorted black phyllites, numerous quartz veins and areas of silicification along its length may relate to younger (possibly Late Cretaceous) movements. Structural dips are variable but generally steep to vertical and both gentle, east-west-plunging and steep, northerly plunging, mineral lineations have been observed.

In the east, near to Uzhcurrumi, the Jubones fault is cut by undeformed granodiorites, of probable Palaeocene age (A. Egüez, Quito Politecnic, personal communication). Similar rocks intrude the El Oro metamorphic complex along much of its eastern margin and along the Piñas-Portovelo fault zone basement lithologies have, in places (e.g. to the south of Piñas), been cataclastically deformed and brecciated by younger (reactivated), normal faulting with downthrow to the north.

The south-eastern limit of the El Oro metamorphic complex is defined by a series of NNE-SSW-trending, 'horse-tail' faults of the Guayabal fault zone. This zone is undoubtedly complex and has probably been affected by several periods of movement which involved not only the metamorphic basement lithologies, but also those of the Cretaceous Alamor basin sequence and younger Tertiary formations and intrusions (Kennerley and Almeida, 1975). Regionally, the main Guayabal fault defines the western margin of the Neogene Catamayo 'graben' (E. Salazar, RTZ plc, Quito, personal communication), a north-south-trending structure that separates the main outcrop of the El Oro metamorphic complex from similar metamorphic lithologies of the Cordillera Real to the east (Aspden and Litherland, 1992; Kennerley and Almeida, 1975). The metamorphic rocks that have been affected by this fault zone have been cataclastically deformed and the more competent, quartz-rich lithologies are typically strongly fractured and/or brecciated. Overall, the sense of movement along the zone is thought to be dextral but also includes an eastward-directed thrust component.

In the south the El Oro metamorphic complex is unconformably overlain by the Cretaceous sediments of the Alamor basin. The development of the basin was probably controlled by extensional faults, repeated movements along which have resulted not only in the brecciation of the metamorphic basement but also of the younger basinal sediments.

Associated younger structures

A number of young, (?)Neogene, cross-cutting, approximately NNE-SSW-trending lineaments have been mapped using airphotographs and SAR images. Where the presence of these lineaments has been confirmed in the field they are associated with diffuse zones of brittle fracture. In the Zaruma mining district and the Cerro Pelado area similarly trending faults represent important controls for mineralisation (Van Thournout et al., 1991; A. Egüez, Quito Politecnic, personal communication).

GEOLOGICAL INTERPRETATION

Regional context within the Northern Andes

The metamorphic rocks of the El Oro Province are interpreted to form part of an accretionary prism complex that probably extends the length of the Northern Andes but much of which is covered by younger strata and especially the extensive, Tertiary/Quaternary volcanic deposits that are widely developed in both Ecuador and Colombia. In Ecuador, it is suggested that the eastern limit of this complex coincides with the Baños-Las Aradas fault zone, a regional structure that defines the western limit of the Cordillera Real and which continues as the Romeral fault in Colombia (Aspden et al., 1992a). For the purposes of this account, the western limit of the accretionary complex is taken as the Calacalí-Pallatanga fault zone (Aspden et al., 1987). However, to the west of this line, the Cordillera Occidental and Coastal Plain are also composed of allochthonous material (Van Thournout et al., 1992; Megard, 1989; Aspden et al., 1987a; McCourt et al., 1984), and hence further accreted crust extends to the present-day trench axis.

In Ecuador the accretionary complex between the Baños-Las Aradas and the Calacalí-Pallatanga fault has been previously (in part) referred to as the Chaucha-Arenillas terrane (Litherland and Aspden, 1992) (see also Feininger, 1987). It is now apparent that the 'Chaucha-Arenillas terrain' contains a variety of rocks of different ages and origins and in our view the accretionary prism model provides a more realistic, conceptual framework in which to discuss, not only the metamorphic rocks of the El Oro Province, but also, the geology of the entire belt. While such a discussion is beyond the scope of the present report, Figure 30 shows the main outcrops of 'metamorphic basement' in Ecuador that are located between the Baños-Las Aradas and Calacalí-Pallatanga fault zones. These are the occurrences which we would now include within the accretionary complex. Terrain further west, and not discussed herein, also forms part of the larger accretionary prism.

Similarly, further to the north in Colombia, the ophiolitic sequence of the Amaime terrane and the associated high-pressure assemblages of Barragán and Jambaló (Aspden and McCourt, 1986; Feininger, 1982) would also form part of the accretionary complex, as would the 'metamorphic' rocks of the Amotape-Tahuín terrane in north-west Perú (Megard, 1989).

Origin of the El Oro metamorphic complex

The rocks of the El Oro metamorphic complex to the north and south of the Zanjón-Naranjo fault are both considered to be part of the same accretionary mass and essentially to have had the same origin. However, many of the rocks which occur as inclusions within the Palenque mélange division to the north of this fault have been tectonically derived from those to the south (or their analogues elsewhere). The southern block is of course a more coherent unit than the mélange and the following partial 'pre-accretionary complex' geological history can be established.

The Tahuín semi-pelitic sediments, of probable lower Palaeozoic age, within the southern block were metamorphosed during the Late Triassic. This metamorphism, a temperature-dominated event, was accompanied by dextral shearing, migmatite formation, the emplacement of the dominantly S-type, syn- to late-tectonic granites (Moromoro complex) and the intrusion of mafic magma (Piedras complex).

Several of the rock types within the El Oro metamorphic complex can be correlated with lithologies from the Cordillera Real, the exception being the high-pressure/low temperature ophiolitic material of the mélange. Immediately to the east in the Cordillera Real, the Loja division (Aspden and Litherland, 1992), like the El Oro rocks, comprises a variably metamorphosed semi-pelitic sequence that is estimated to be of Palaeozoic age. Late Triassic S-type granites and migmatites are present within the Loja division (Noble et al., 1994) and it has been suggested that these were also formed during a period of dextral shearing (Aspden et al., 1992 and 1992a).

The conclusion reached is that the Moromoro complex and Tahuín division of the El Oro Province are the equivalents of the Loja division of the Cordillera Real. In both areas mafic amphibolite bodies are spatially associated with the granitoids; field observations in the Cordillera Real and U/Pb zircon results in the El Oro complex confirm that these rock types are of a similar age. It is therefore possible to suggest that the excess heat contained by the mafic magmas may have contributed to crustal anatexis and hence the development of the regional migmatite/S-type granite belt (Castro et al., 1991). However, Reavy (1989), who reports many features from the Portuguese Hercynian belt that are identical to those seen in the El Oro metamorphic complex, concludes that although the high thermal gradients encountered in narrow 'plutonometamorphic' zones probably result from a combination of factors, they are intrinsically linked to the presence of high strain zones in the crust (see also Strong and Hanmer, 1981, and Pitcher, 1979).

Geochemically the Piedras complex is oceanic in character and could represent suprasubduction (gabbroic) magmas emplaced into an active regional shear zone. Autometamorphism by aqueous fluids penetrating along the shear system could account for the amphibolite/greenschist mineralogy (Honnorez et al., 1984).

In summary, the structural and petrological data from the El Oro metamorphic complex indicate that the emplacement of granitoid of predominantly S-type character, migmatite formation and the intrusion of a linear belt of gabbroic magma were associated with regional shearing and took place under high-temperature/low-pressure metamorphic conditions (see also D'Lemos et al., 1992; Hutton and Reavy, 1992; Krohe, 1991). Based on the geochemical evidence, the Moromoro complex (and those granitoids of the Loja division in the Cordillera Real) can be classified as volcanic arc granites and such tectonic settings are also considered to be favourable environments for the development of low-pressure/high-temperature metamorphism of the type preserved in the Tahuín division (Yardley, 1989; Miyashiro, 1972; but see also Strong and Hanmer, 1981; Wickham, 1987).

Age of accretionary complex and rotation of the El Oro metamorphic complex

The age of formation of the accretionary complex, of which the El Oro metamorphic complex forms a part, is poorly constrained. However, about 140 Ma ago, following the cessation of Jurassic (c. 190-145 Ma) volcano-plutonic activity which affected the whole of the Northern Andes (Aspden et al., 1992, 1987a), there was an important change in the geodynamic framework of Ecuador. This change resulted in deformation, uplift and erosion to the east of the Baños-Las Aradas fault zone (Figure 30). Reset K/Ar mineral ages and a reset Rb/Sr whole-rock isochron, obtained from the older Jurassic batholiths, are interpreted to relate to this event which, in the Cordillera Real, included an important element of (?)dextral shearing along steep-to-vertical, NNE-SSW-trending zones.

Part of the accretionary complex may have an older history, but it is suggested that its main components were probably assembled during this event. From about 140 Ma onwards, it is envisaged that the granitoids of the El Oro metamorphic complex were tectonically derived, either from the western margin of the Cordillera Real (Loja division), or from its southern extension into northern Perú, (Olmos Arch of Cobbing et al., 1981), and incorporated into the accretionary prism.

In the south, the El Oro metamorphic complex is overlain unconformably by the sediments of the Alamor basin which range from Lower to Upper Cretaceous in age. The Alamor structure which extends into northwestern Perú as the Lancones basin, began subsiding in the Aptian (c. 110 Ma) (Baldock, 1982; Cobbing et al., 1981), a date which provides a minimum age for this portion of the accretionary prism. Palaeomagnetic data from the Lancones basin (Mourier et al., 1988) suggest progressive (in situ), up to 90°, clockwise rotation during the Early to Late Cretaceous. This rotation sense is consistent with a dextral shear regime and would also account for the east-west trend of the El Oro metamorphic complex since these rocks, which formed the 'basement' of the Lancones/Alamor basin, must also have been rotated.

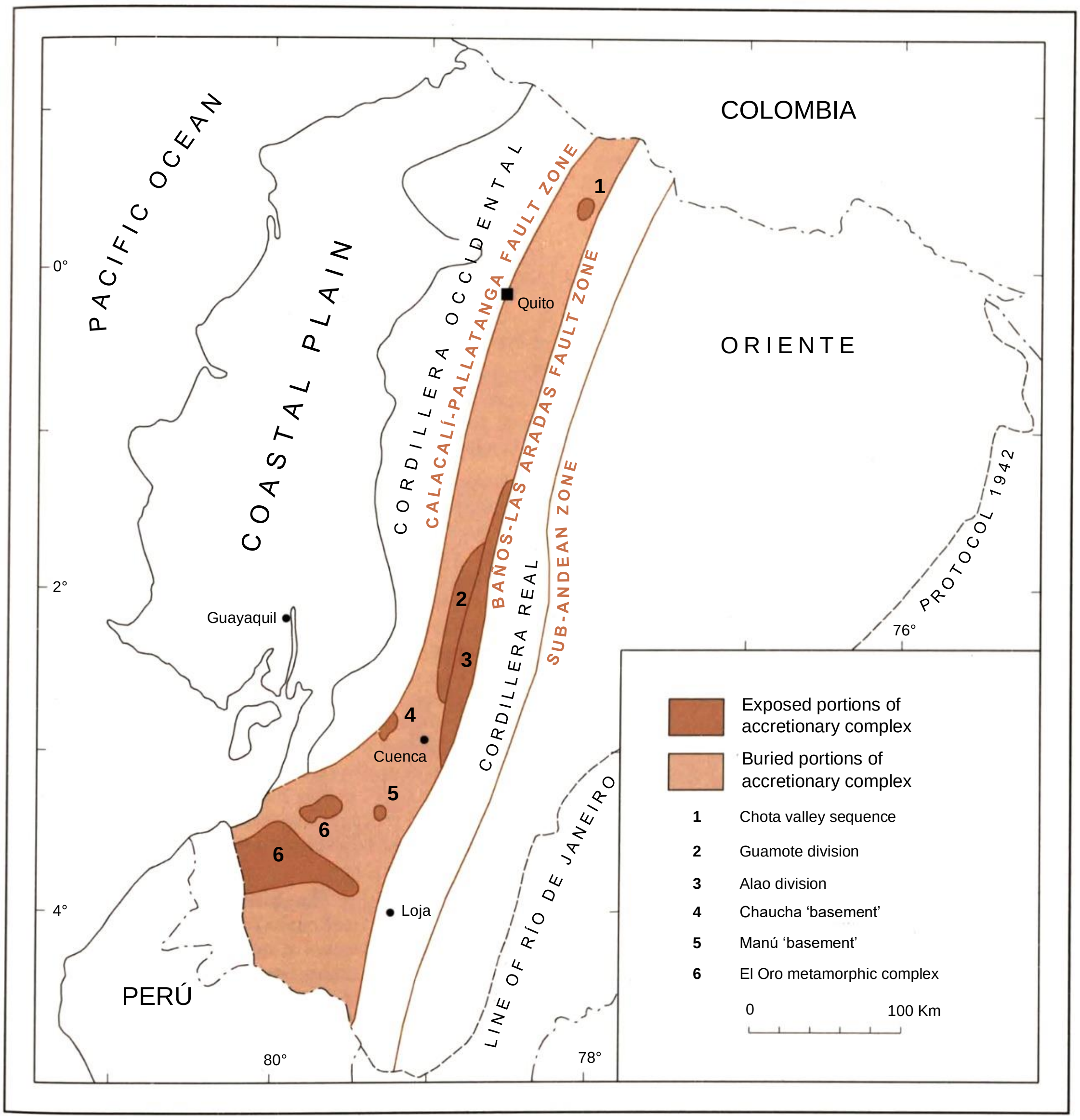

Figure 30. Sketch of eastern portion of Northern Andean accretionary complex, Ecuador segment.

The Calacalí-Pallatanga fault zone represents the western limit of the accretionary prism described here. Although this boundary is reasonably well defined geographically, the timing of the accretion of the allochthonous Cordillera Occidental along it is uncertain. However, it is generally agreed that it took place either in the Late Cretaceous (c. 70 Ma) (Aspden et al., 1992; Megard, 1989) or sometime during the Lower Tertiary (pre. 38 Ma) (Van Thournout et al., 1992; Daly, 1989).

Further work is required, and in particular the 'matrix' of the accretionary complex should be dated in order to establish its age of formation. Based on the observations discussed above, it is tentatively suggested that the majority of the complex was assembled between the latest Jurassic and Late Cretaceous (c. 140-170 Ma), but it is possible that this range will be extended as more information becomes available.

ECONOMIC GEOLOGY

General

The principal mineral of economic importance in the El Oro Province is gold, which has been worked since pre-Colombian time. Reliable production figures are not available but probably between 2 and 3 tons of gold are extracted annually. Most of the known areas of economic mineralisation are located close to, but outside of, the limits of the El Oro metamorphic complex. The general distribution of these occurrences is of interest (Figure 31) since there is a spatial relationship to the complex.

The mesothermal/epithermal polymetallic veins of the Portovelo/Zaruma and Ayapamba mining districts (INEMIN-AGCD-ABOS, 1988; UNDP, 1972; Billingsley, 1926) account for most of the hard rock gold production. Recent discoveries in and around Cerro Pelado, including that of a free gold-bearing breccia pipe, are also now being worked by various groups using artisanal methods. To the north of Cerro Pelado, near Bella María, the Los Lilenes Group (Ecuminas/Odin) is extracting about 0.25 ton/annum of gold from the Río Calaguro alluvial deposit, and to the east, in the vicinity of Cerro Azul, gold-bearing polymetallic quartz veins are reportedly being worked. To the west of Cerro Azul, at Cerro Los Cangrejos, minor gold showings have been recorded and, in the Río Daucay, upstream of Playas de Daucay, a north-south-trending, approximately 1m wide, polymetallic vein is currently being exploited. In the extreme east, small quantities of gold are worked from the Ligzhu epithermal deposit (E. Pillajo, personal communication). In addition, a number of shallow, now abandoned, adits that are typically associated with small, weakly mineralised (? gold-bearing) fractures near intrusive contacts, are present in the Uzhcurrumi area, along the Chilla road and about 1km south of the small village of Cerro Azul on the Paccha road.

All of the above occurrences are spatially associated with the Tertiary volcano-plutonic complex and it may be significant that most of this mineralisation appears to concentrate close to the contact zone between these rocks and those of the El Oro metamorphic basement.

METALLIC MINERAL OCCURRENCES

The location of the occurrences referred to below are shown in Figure 31.

Cerro Pelado area

Several active and abandoned mines are present in the Cerro Pelado area, three of which were visited with Dr. R. A. Jemielita who contributed to the following brief descriptions.

a. El Antimonio mine (**La Avanzada 6272/95043**). This abandoned mine and pilot crushing plant is located in the Quebrada Guayabo. The main adit trends approximately east-west and is located within a granular-textured, sheared granite (Limón Playa unit, Palenque division) which contains xenoliths of mica schist (<0.5m diameter). The shear fabric is approximately vertical and strikes east-west. The mineralised vein is about 40cm wide and comprises massive and vuggy quartz with coarse stibnite. Float blocks of tourmaline breccia are common and a small intrusive breccia vein was observed just upstream of the main adit. The area was mined by the Ecuaba Company for antimony, but gold and silver assays of up to 14g/ton have been obtained from the vein however, average assay values are less than 1g/ton. Several other adits/exploratory tunnels occur upstream of the main adit.

b. El Guayabo mine (**La Avanzada 6274/95052**). This abandoned mine (ex-Ecuaba) is in the upper reaches of the Quebrada Guayabo at an altitude of about 700m. The country rock comprises sheared, in part graphitic, black phyllites and quartzose schists (Palenque mélange division matrix) which are steeply dipping, generally with an east-west strike. Several adits are present on the west side of the river valley and the vein, which is exposed in the river, trends N15°E and dips 50° NE. The vein consists of quartz, arsenopyrite, pyrite with average gold assays of about 7g/ton and with up to 150000 tons of ore reserves. In the adit visited, the vein(s) vary from about 0.1 to 1.0m wide and are banded with rather massive sulphides.

In places the main vein appears to be approximately parallel to the country rock fabric.

c. Cerro Pelado mine (**La Avanzada 6278/96063**). The recently discovered Cerro Pelado deposit appears to be located in flat-lying rhyodacitic volcanics which overlie metamorphic basement. The mine is near the summit of Cerro Pelado at an altitude of about 1280m and consists of a breccia pipe which is being worked for free gold by artisanal methods. When the area was visited in early 1992, an approximately 100m-deep ‘glory-hole’ had been excavated in the breccia pipe which is generally coarse-grained, with elongate and angular clasts of strongly sericitised, grey (?)mica schists clasts set in a very open, vuggy matrix. The clasts are often coated with vuggy, crystalline, transparent to milky quartz, mixed with iron oxides. Visible gold is quite common. Originally the breccia pipe was exposed on a narrow ridge with a surface outcrop of about 26×20m, however it becomes wider at depth and the vertical extent of the mineralisation is unknown.

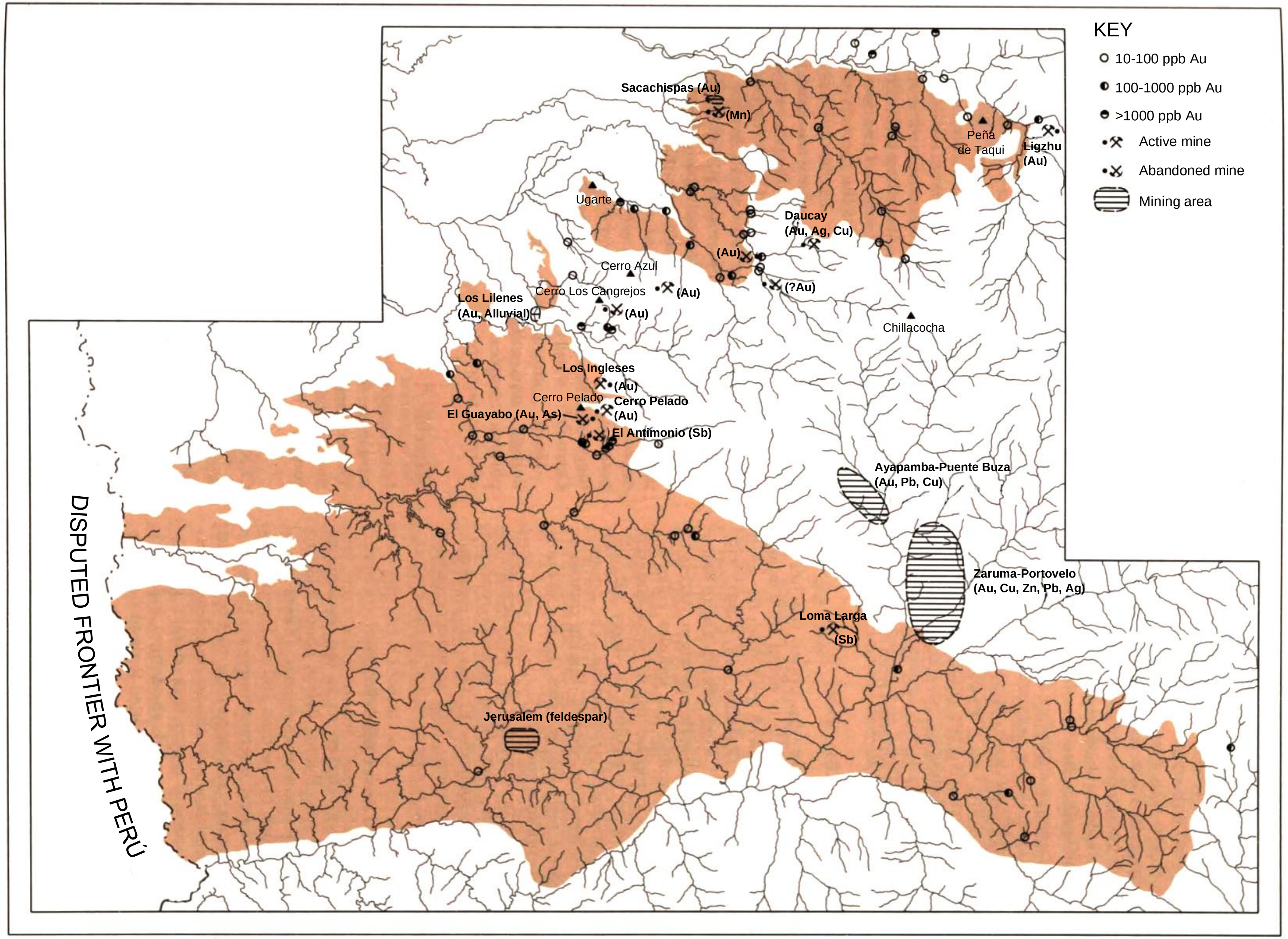

Figure 31. Areas of established mining and distribution of anomalous stream sediment gold values (>10ppb)

Several other small-scale workings occur within the Cerro Pelado area (e.g. Los Ingleses). These have not been visited but reportedly they consist mainly of polymetallic, auriferous quartz veins. Blocks of hydrothermally altered (silica, sericite and tourmaline) intrusive breccias are also common in several rivers which drain the Cerro Pelado area but, as yet, no assay values of economic interest have been reported from these rocks.

Loma Larga mine (Zaruma c. 645/9588)

The Loma Larga mine is in the upper reaches of Quebrada Lozumbe at an altitude of about 1000m and access is by means of an unsurfaced track from the small settlement of Loma Larga (**Zaruma 646/9590**). The mine was visited in early 1991 when attempts were being made to rehabilitate this small-scale operation. Access to the main adit was not possible but samples collected from the mine dump comprise quartz vein material which carries massive to crystalline to vuggy stibnite, hosted in a brittly fractured (?)quartzite. The country rocks are east-west-trending, steeply dipping quartzites and strongly sheared, mylonitic granites (La Bocana unit of the Moromoro granitoid complex).

Stibnite-bearing quartz veins, that are also presumably related to a shear zone have been recently reported from the area of the Quebrada El Oso, an east-bank tributary of the Río Moromoro. This occurrence cannot be confirmed since it has not been visited by the Project.

Manganese mine (Santa Rosa c. 6365/96296)

This ‘mine’, sometimes referred to as the Sacachispas mine is situated in Estero Puerto Balsas, about 1km to the south of San Ramón/Sacachispas (**Santa Rosa 636/9630**) at an altitude of less than 100m. The country rocks comprise silicified metasediments (Palenque mélange division matrix) and according to Harrington (1957) the ‘mine’, which is now almost completely overgrown, consists of lenses of quartz that contain appreciable quantities of massive, pink, rhodonite and black psilomelane. The largest lens identified is about 6m long and 2m wide and it is therefore probably of no commercial interest except, possibly, for ornamental purposes.

Sacachispas gold mining area (Santa Rosa 637/9630)

In Estero Sacachispas minor quantities of alluvial and hard-rock gold are worked intermittently by artisanal miners. The host rock consists of weathered, sericite-quartz schists (Palenque mélange division matrix) which carry concordant/discordant, irregular quartz veins and stringers that contain iron oxides (?after pyrite) and minor quantities of free gold.

Alluvial gold

Apart from the Los Lilenes operation, various rivers in the area of the El Oro metamorphic complex are, or reportedly have been, worked for gold.

The main rivers of interest are the Ríos Amarillo and Calera which drain the Portovelo/Zaruma and Ayapamba mining districts. However, although rich pockets of alluvial gold do occur, the quantities of alluvium are insufficient to be of serious commercial interest. Small-scale, intermittent operations also exist in the Río Santa Rosa and in the Ríos Naranjo/Arenillas, to the east of Piedras and downstream of the Tahuín dam. According to Wallis (1944), most of the north bank tributaries of the Río Naranjo are gold-bearing, and he reports the recovery of a single nugget which weighed 6½ ounces from the Quebrada Las Damas. Minor gold showings have also been panned during the present study in the Río Raspas, to the west of La Chilca, the Río Chico and the Quebrada Chontas. In the area around Valle Hermoso and Palenque many of the rivers carry alluvial gold, which is worked informally, and on an irregular basis, by small groups of miners.

In addition to these known occurrences, the largely unconsolidated, Tertiary and Quaternary sedimentary deposits of the coastal plain are also considered to have potential for alluvial gold mining operations. However, the most likely prospective areas, in the region near to Cerro Pelado and Cerro Azul, are often heavily cultivated.

Much of the alluvial gold is assumed to have been derived from, or is associated with, the Tertiary volcano-plutonic complex which intrudes and/or overlies much of the metamorphic complex in the east.

Magnetite

Large quantities of magnetite octahedra occur as black sand in the Río Arenillas, downstream of the Tahuín dam. The magnetite is probably derived from the weathering of the serpentinised harzburgites of the El Toro unit (Raspas complex) but is unlikely to be of commercial interest.

Chromium, nickel and platinum group metals (PGM)

Within the Palenque mélange division various ultramafic bodies occur. The largest is the El Toro unit of the Raspas ophiolitic complex. These rocks are generally associated with high Cr and Ni values and may have PGM potential.

NON-METALLIC MINERAL OCCURRENCES

Jerusalem feldspar mine (Marcabelí c. 622/9580)

The Jerusalem feldspar mine consists of a series of small open-pit operations that are situated about 1-2km to the south of Marcabelí. The workings are located within the Marcabelí pluton and consist of weathered, leucocratic, pegmatitic feldspar veins which are being extracted for use in the ceramic industry by Cerámica Andina CA.

According to company records approximately 4000 to 5000 tons of material are produced annually and reserves are estimated at about 80000 tons.

Quarrying operations

There are a number of generally small quarries within the El Oro metamorphic complex that are often worked intermittently to supply local and/or provincial needs. The main rock type exploited is the amphibolite of the Piedras mafic complex, especially the Quebrada Plata unit, to the south of the Zanjón-Naranjo fault zone. This material has been widely used throughout the El Oro Province for roadstone.

The serpentinised harzburgite of the El Toro unit (Raspas complex) has also been extensively quarried for hardcore in the area of El Toro (**La Avanzada 611/9600**), and was used in the construction of the Tahuín dam. These quarries were recently re-opened to provide roadstone and roadmetal for the Santa Rosa-Huaquillas highway project.

To the east of Pasaje, on the main road to Cuenca (**Machala 637/9632**), a new quarry has recently been opened in the Palenque mélange complex (matrix) and is taking material for use in land-fill schemes in Machala.

Brick clays

The weathering products of the Marcabelí pluton are especially suited to brick and roof tile making since numerous, small-scale operations are situated within its outcrop, particularly in and around the towns of Balsas and Marcabelí.

Sand and gravel

Sand and gravel are taken from a number of rivers for use in local construction. Potentially large tonnages of sand are available in the lower reaches of the Quebradas Palmales/Chiquita. The former is worked intermittently to supply both local and provincial requirements.

Ornamental stone

The various granites of the La Bocana granitoid complex (e.g. La Florida pluton) may have potential for ornamental stone but deep weathering and the presence of biotite ± muscovite could limit their usefulness. Equally, within the Palenque mélange division there are various serpentinites/serpentinised harzburgite bodies. The largest is the El Toro unit which may be of some interest.

STREAM SEDIMENT SAMPLING PROGRAMME

Introduction

Although the main focus of the El Oro Project was geological mapping, a routine stream sediment sampling programme was also conducted in order to provide a regional geochemical database.

A total of 172 stream sediment samples were collected by wet sieving in the field, using 175 mesh heavy duty nylon sieves. The samples were prepared in Quito by Bondar Clegg (Inc.) and analysed in their Vancouver laboratory for the following elements: Al, Fe (total), Mn, Mg, Ca, Na, K, V, Cr, Co, Ni, Cu, Zn, As, Sr, Y, Mo, Ag, Cd, Sn, Sb, Te, Ba, La, W, Pb, Bi, and Au. Analyses were carried by ICP except for Au, which was determined by Fire Assay. The detailed locations of the stream sediments samples are given in Table 10 and the geochemical results obtained are listed in Table 11. The sample sites (with the exception of AB1 and AB53) are plotted in Figure 32. In some rivers, panned concentrates were also collected (see Table 11) but analytical data are not available for these samples.

The geochemical data have not been subjected to statistical analysis but selected results, for ‘trace elements’ of economic interest, are mentioned below.

Gold and silver

Gold analyses ranged from less than 5ppb (detection limit) to 7166 ppb and a considerable number of samples, especially those collected from drainages close to the contact of the El Oro metamorphic complex with the Tertiary volcano-plutonic complex, carried values of more than 10ppb (Figure 31). A group of very high values was obtained from the south of Cerro Pelado (AB62, 3358ppb; AB64, 7166ppb; AB69, 5133ppb) (see also AB65 and AB66) and from the south of Cerro Los Cangrejos (AB76, 1069ppb; AB77, 2895ppb) (see also AB75). Further to the north, a sample from the Estero de la Poza Negra contained 1560ppb (AB94) (see also AB95, AB12, AB13, AB15 and AB16) and two samples from north bank tributaries of the Río Jubones, the Ríos Vivar (AB2) and Mollepungu (AB3) had values of 1198ppb and 1389ppb, respectively.

Elsewhere, minor amounts of gold are associated with the Río Naranjo and its tributaries, particularly in the east (up to 113ppb in AB60 from the Quebrada Platanillo), and in the south-east, values of 30 to 124ppb were recorded from the Quebradas del Batén (AB49), Chaupi (AB104) and El Belén (AB105). The following ‘isolated’ values (>100 ppb) were also obtained: 416ppb (AB86, Río Santa Rosa); 258ppb (AB19, tributary of Río Chillayacu which drains the Ligzhu deposit, Figure 31); 116ppb (AB85, Estero Tomás); 111ppb (AB52, Río El Ari) and 110ppb (AB103, Quebrada El Salado).

The majority of silver analyses were below 0.2ppm (detection limit) but ranged up to 15.2ppm, with the highest values of coming from the Ríos Mollepungu (AB3, 15.2ppm) and Vivar (AB2, 11.1ppm). The Cerro Pelado samples (AB62, AB64, AB66 and AB69) carried between 1.8 and 9.5ppm of silver and those from Cerro Los Cangrejos (AB75, AB76 and AB77) between 1.5 and 2.9ppm.

Table 10. Stream sediment samples and heavy minerals concentrates.

SAMPLE	MAP SHEET	RIVER	COORDINATES	SAMPLE	MAP SHEET	RIVER	COORDINATES
AB-001 F**	Uzhcurrumi	Q. Santa Martha	6638-96355	**AB-063 F**	La Avanzada	Q. Zabayán	6278-96028
AB-002 F P	Uzhcurrumi	R. Vivar	6544-96358	**AB-064 F P**	La Avanzada	R. Santa Rosa Trib.	6291-96037
AB-003 F P	Uzhcurrumi	R. Mollepungu	6494-96340	**AB-065 F**	La Avanzada	R. Santa Rosa Trib.	6271-96034
AB-004 F P	Uzhcurrumi	R. Muyuyacu	6481-96348	**AB-066 F**	La Avanzada	R. Santa Rosa Trib.	6269-96035
AB-005 F P	Uzhcurrumi	R. Quera	6478-96328	**AB-067 F**	La Avanzada	R. Santa Rosa Trib.	6316-96041
AB-006 F P	Chilla	R. Quera	6497-96309	**AB-068 F**	La Avanzada	R. Santa Rosa Trib.	6326-96038
AB-007 F P	Uzhcurrumi	R. Cune	6535-96323	**AB-069 F**	La Avanzada	R. Santa Rosa	6288-96034
AB-008 F P	Chilla	Q. Carabota	6569-96289	**AB-070 F**	La Avanzada	Q. La Chilca	6221-96046
AB-009 F P	Uzhcurrumi	Q. Carabota	6549-96322	**AB-071 F P**	La Avanzada	R. Santa Rosa Trib.	6193-96041
AB-010 F P	Uzhcurrumi	R. Casacay	6438-96319	**AB-072 F**	La Avanzada	R. Santa Rosa Trib.	6181-96042
AB-011 F P	Uzhcurrumi	R. Huizho	6407-96316	**AB-073 F**	La Avanzada	R. Santa Rosa Trib.	6177-96053
AB-012 F P	Santa Rosa	R. Negro Trib.	6334-96220	**AB-074 F**	La Avanzada	Q. La Pereira	6170-96071
AB-013 F P	Santa Rosa	Q. Las Pavas	6352-96191	**AB-075 F P**	La Avanzada	R. Viron Chico Trib.	6289-96127
AB-014 F P	Santa Rosa	R. Dumari	6376-96167	**AB-076 F P**	La Avanzada	R. Viron Chico Trib.	6290-96123
AB-015 F P	Santa Rosa	R. Daucay Trib.	6384-96169	**AB-077 F**	La Avanzada	R. Viron Chico Trib.	6268-96127
AB-016 F P	Chilla	R. Colorado	6407-96181	**AB-078 F P**	Santa Rosa	R. Chico	6260-96167
AB-017 F P	Chilla	R. Chilola	6405-96173	**AB-079 F**	La Avanzada	Q. La Garganta	6180-95988
AB-018 F P	Chilla	Q. Cerro Azul	6405-96169	**AB-080 F P**	La Avanzada	Q. Sambotambo	6349-95970
AB-019 F P	Chilla	R. Chillayacu Trib.	6622-96289	**AB-081 F P**	La Avanzada	R. Piedras	6204-95980
AB-020 F P	Chilla	R. Palenque	6402-96265	**AB-082 F P**	La Avanzada	Q. De Cañas	6153-95967
AB-021 F P	Chilla	R. Papayacu	6392-96255	**AB-083 F P**	La Avanzada	R. Piedras Trib.	6206-95964
AB-022 F P	Marcabelí	R. Balsas Trib.	6306-95858	**AB-084 F**	La Avanzada	R. Naranjo Trib.	6236-95973
AB-023 F P	Marcabelí	R. Balsas Trib.	6302-95859	**AB-085 F P**	La Avanzada	Est. Tomás	6185-96097
AB-024 F P	Marcabelí	R. Marcabelí	6183-95779	**AB-086 F P**	La Avanzada	R. Santa Rosa	6163-96089
AB-025 F P	Marcabelí	Q. Agua Negra	6182-95810	**AB-087 F P**	La Avanzada	R. Santa Rosa Trib.	6181-96083
AB-026 F P	Marcabelí	Q. Balsas	6286-95848	**AB-088 F P**	Santa Rosa	Est. Culebrero Trib.	6257-96194
AB-027 F P	Marcabelí	R. Balsas Trib.	6278-95838	**AB-089 F**	Santa Rosa	Est. La Quebrada	6262-96198
AB-028 F P	Marcabelí	Q. Milagro	6286-95852	**AB-090 F P**	La Avanzada	R. Panupali	6324-95971
AB-029 F P	Marcabelí	Q. La Esperanza	6278-95851	**AB-091 F**	Santa Rosa	R. Colorado	6353-96235
AB-030 F P	Marcabelí	R. Marcabelí	6205-95824	**AB-092 F P**	Santa Rosa	R. Raspas	6354-96238
AB-031 F	Puyango	Q. Los Zábalos	6010-95720	**AB-093 F P**	La Avanzada	R. Raspas	6208-96025
AB-032 F P	Puyango	Q. Los Zábalos	6010-95715	**AB-094 F P**	Santa Rosa	Est. De La Poza Negra	6299-96226
AB-033 F P	Puyango	Q. Las Palmas	6056-95722	**AB-095 F P**	Santa Rosa	Est. Zapato	6309-96220
AB-034 P	Puyango	R. Puyango Trib.	6042-95718	**AB-096 F P**	Zaruma	R. Ambocas	6648-95814
AB-035 F	Puyango	Q. El Inca	6002-95719	**AB-097 F**	Zaruma	Q. Limoncillo	6647-95818
AB-036 F P	La Avanzada	R. Zaracay	6271-95959	**AB-098 F**	Marcabelí	Q. El Duende	6386-95855
AB-037 F P	Marcabelí	R. del Oro	6185-95878	**AB-099 F**	Marcabelí	Q. El Caucho	6382-95859
AB-038 F P	Marcabelí	Q. Primavera	6239-95901	**AB-100 F**	Zaruma	Q. Alejanita	6395-95881
AB-039 F P	Marcabelí	Q. Valle Hermoso	6219-95906	**AB-101 F**	Marcabelí	Q. De Nalacapa	6385-95893
AB-040 F P	Marcabelí	Q. De Guerras	6342-95785	**AB-102 F P**	Chaguarpamba	R. Yaguachi	6557-95760
AB-041 F P	Marcabelí	R. Zaracay	6289-95928	**AB-103 F**	Zaruma	Q. El Salado	6512-95858
AB-042 F P	Marcabelí	Q. Guayacán	6133-95919	**AB-104 F**	Zaruma	Q. Chaupi	6615-95775
AB-043 F P	Marcabelí	Q. San Luis	6132-95918	**AB-105 F**	Chaguarpamba	Q. El Belén	6612-95729
AB-044 F P	Las Lajas	Q. Las Lajas Trib.	6081-95853	**AB-106 F P**	Las Lajas	Q. El Guarumo	6018-95899
AB-045 F P	Paccha	R. Moro-Moro	6403-95965	**AB-107 F**	Las Lajas	Q. El Guarumo	6016-9587
AB-046 F	Zaruma	R. Lozumbe	6476-95877	**AB-108 F P**	Marcabelí	Q. Bruno	6115-95946
AB-047 F P	Zaruma	Q. Del Trapiche	6574-95811	**AB-109 F P**	Marcabelí	Q. Bruno Trib.	6117-95945
AB-048 F P	Zaruma	Q. Naranjo	6583-95805	**AB-110 F**	Marcabelí	Q. Bruno Trib.	6121-95946
AB-049 F	Zaruma	Q. Del Batén	6599-95763	**AB-111 F**	Arenillas	Q. Tahuín Chico	6055-95951
AB-050 F	Zaruma	Q. Naranjo Trib.	6582-95798	**AB-112 F**	Las Lajas	Q. Canoas	6050-95942
AB-051 F	Zaruma	Q. Usulaca	6514-95838	**AB-113 F**	Las Lajas	Q. Cañas	6047-95925
AB-052 F P	Santiago	R. El Ari	6773-95798	**AB-114 F P**	Arenillas	Q. Las Palmas	6111-96045
AB-053 F**	Catamayo	Q. De La Concha	6745-95661	**AB-115 P**	Arenillas	R. Arenillas	6095-96006
AB-054 F P	Paccha	Q. Chontas	6423-95962	**AB-116 F P**	Chilla	R. Casacay	6502-96218
AB-055 F	La Avanzada	Q. Plata	6349-95958	**AB-117 F P**	Chilla	R. Gallo Cantana	6501-96217
AB-056 F P	La Avanzada	R. Naranjo Trib.	6338-95965	**AB-118 F**	Chilla	R. Casacay Trib.	6492-96228
AB-057 F	La Avanzada	R. Naranjo Trib.	6326-95963	**AB-119 F**	Chilla	Est. Dumari	6490-96237
AB-058 F	La Avanzada	R. Naranjo Trib.	6322-95963	**AB-120 F**	Chilla	R. Casacay Trib.	6488-96247
AB-059 F P	La Avanzada	R. Naranjo Trib.	6282-95967	**AB-121 F P**	Chilla	R. Casacay Trib.	6479-96254
AB-060 F	La Avanzada	Q. Platanillo	6355-95966	**AB-122 F**	Chilla	Est. Dumari	6451-96283
AB-061 F P	La Avanzada	Q. De Damas	6258-95983	**AB-123 F P**	Chilla	R. Casacay Trib.	6452-96292
AB-062 F P	La Avanzada	R. Santa Rosa	6285-96031				

Table 10. Stream sediment samples and heavy minerals concentrates. *Continued*

SAMPLE	MAP SHEET	RIVER	COORDINATES	SAMPLE	MAP SHEET	RIVER	COORDINATES
AB-124 F	Chilla	R. Colorado Trib.	6393-96198	**AB-149 F**	Chilla	R. Huizho Trib.	6405-96299
AB-125 F	Chilla	R. Colorado	6397-96199	**AB-150 F**	Uzhcurrumi	R. Tobar	6404-96319
AB-126 F	Chilla	R. Raspas Trib.	6396-96211	**AB-151 F**	Chilla	Q. Trancaloma	6604-96255
AB-127 F	Chilla	R. Raspas Trib.	6397-96216	**AB-152 F**	Chilla	R. Chillayacu	6614-96284
AB-128 F	Chilla	R. Raspas Trib.	6398-96217	**AB-153 F**	Chilla	R. Chillayacu Trib.	6598-96287
AB-129 F	Chilla	R. Raspas	6398-96218	**AB-154 F**	Chilla	Q. El Pindo	6590-96297
AB-130 F	Chilla	R. Raspas Trib.	6395-96216	**AB-155 F**	Santiago	R. Naranjo	6739-95795
AB-131 F	Chilla	Est. San Antonio	6397-96231	**AB-156 F**	Santiago	R. Suares	6698-95799
AB-132 F	Chilla	Est. San Antonio	6398-96231	**AB-157 F**	Santiago	R. Suares Trib.	6699-95799
AB-133 F	Chilla	Est. San Antonio	6398-96233	**AB-158 F**	Santiago	R. Granadillo	6681-95802
AB-134 F	Chilla	Est. San Antonio	6399-96237	**AB-159 F**	Santiago	R. Ambocas	6673-95806
AB-135 F	Chilla	R. Quera Trib.	6528-96261	**AB-160 F**	Santiago	R. Ambocas Trib.	6671-95810
AB-136 F	Chilla	R. Quera Trib.	6522-96265	**AB-161 F**	Santiago	Q. Tabloncillo	6668-95817
AB-137 F	Chilla	R. Quera	6522-96266	**AB-162 F**	Santiago	Q. Luzumbe	6672-95827
AB-138 F	Chilla	R. Quera Trib.	6510-96281	**AB-163 F**	Catamayo	Q. Del Sharve	6713-95733
AB-139 F	Chilla	R. Quera Trib.	6511-96284	**AB-164 F**	Catamayo	Q. Del Verde	6692-95746
AB-140 F	Chilla	R. Casacay	6519-96180	**AB-165 F**	Catamayo	Q. Del Sharve	6682-95752
AB-141 F	Chilla	R. Casacay Trib.	6518-96180	**AB-166 F**	Catamayo	Q. Del Sharve	6674-95759
AB-142 F	Chilla	R. Gallo Cantana Trib.	6502-96194	**AB-167 F**	Zaruma	Q. San Joaquín	6663-95762
AB-143 F	Chilla	R. Gallo Cantana	6500-96194	**AB-168 F**	Zaruma	Q. Rumipotrero	6631-95788
AB-144 F	Chilla	Est. Dumari	6484-96195	**AB-169 F**	Las Lajas	Q. Lajas Trib.	6023-95801
AB-145 F	Chilla	R. Huizho Trib.	6423-96281	**AB-170 F**	Las Lajas	Q. El Guineo Trib.	5987-95854
AB-146 F	Chilla	R. Huizho Trib.	6413-96295	**AB-171 F**	Las Lajas	Q. El Guineo Trib.	5985-95851
AB-147 F	Uzhcurrumi	Est. Las Minas	6400-96391	**AB-172 F**	Las Lajas	Q. Palmales	6068-95888
AB-148 F	Uzhcurrumi	R. Huizho	6402-96318	**AB-173 F**	Las Lajas	Q. Palmales	6067-95887

** Samples fall outside of area covered by Figure 32.
F Stream sediment sample see Appendix for Analytical results.
P Heavy mineral concentrate (analytical data not available)
Est. Estero
Q. Quebrada
R. Río
Trib. Tributary

Arsenic, antimony, bismuth and tellurium

Arsenic analyses ranged from less than 5ppm (detection limit) to more than 2000ppm but the majority of samples contained less than 30ppm. In general, there appears to be a good correlation between arsenic and gold and the highest values were recorded from samples collected from near to the contact of the El Oro metamorphic complex and the Tertiary volcano-plutonic complex. The Cerro Pelado area (AB62, AB63, AB64, AB65, AB66 and AB69) had values between 40 and more than 2000ppm whereas samples collected from near to Cerro Los Cangrejos (AB75, AB76, AB77 and AB78) ranged from 49 to more than 2000ppm. Sample AB86, from the Río Santa Rosa, contained 98ppm and, in the north, values of 170ppm (AB2) and 496ppm (AB3) were recorded from the Ríos Vivar and Mollepungu. Arsenic values greater than 50ppm were also obtained from the following rivers: Río Colorado (AB16, 206ppm); Río El Ari (AB52, 101ppm); Río Raspas (AB129, 53ppm); Quebrada Carabota (AB9, 51ppm) and an unnamed tributary to the Río Casacay (AB140, 51ppm).

Antimony analyses were generally less than 5ppm (detection limit) but values of between 51 and 286ppm (AB62, AB64, AB65, AB66 and AB69) were recorded from the Cerro Pelado area and 91ppm (AB2) and 46 ppm (AB3) from the Ríos Vivar and Mollepungu. Elsewhere, antimony values were less than 10ppm with the exception of the following rivers: Quebrada Limoncillo (AB97, 17ppm); Río Yaguachi (AB102, 18ppm); Quebrada El Salado (AB103, 21ppm); Quebrada Chaupi (AB104, 15ppm); Quebrada El Belén (AB105, 12ppm) and Río Quera (AB137, 12ppm).

Bismuth analyses were similar to those of antimony and the majority of samples contained less than 5ppm (detection limit). The only significant values recorded were from the Cerro Pelado area (AB62, AB64 and AB69, 57-104ppm) and the Ríos Vivar and Mollepungu (AB2 and AB3, 23-25ppm). Only one other sample (AB77, 17ppm) from the Cerro Los Cangrejos area, carried more than 10ppm of bismuth.

Only four samples contained more than 10ppm (detection limit) of tellurium. Three of these came from the Cerro Pelado area (AB62, AB64 and AB69, 28-47ppm) and the other one was collected from the Quebrada de Cañas (AB82, 14ppm).

Table 11. Stream sediment sample geochemistry

Sample	Al PCT	FeTot PCT	Mn PCT	Mg PCT	Ca PCT	Na PCT	K PCT	V PPM	Cr PPM	Co PPM	Ni PPM	Cu PPM	Zn PPM	As PPM
AB-001*	2.32	4.99	0.08	0.28	0.81	0.09	0.15	148	85	9	6	43	73	28
AB-002	2.64	6.97	0.06	0.38	0.25	0.02	0.26	96	48	11	7	8067	107	170
AB-003	2.49	6.85	0.05	0.50	0.37	0.09	0.26	133	160	53	11	2629	93	496
AB-004	3.71	3.80	0.06	0.59	0.43	0.06	0.31	92	94	12	9	58	63	24
AB-005	2.45	2.48	0.08	0.30	0.21	0.03	0.40	47	112	15	22	53	41	11
AB-006	2.14	2.72	0.05	0.49	0.19	0.04	0.49	46	300	9	25	46	56	8
AB-007	2.65	3.02	0.05	0.53	0.22	0.04	0.42	56	265	10	26	39	51	6
AB-008	4.64	3.69	0.06	0.68	0.20	0.02	0.30	73	100	12	12	30	75	15
AB-009	2.05	2.74	0.04	0.45	0.33	0.09	0.27	100	158	10	11	54	42	51
AB-010	2.43	2.85	0.04	0.70	0.46	0.08	0.46	61	261	8	25	30	54	10
AB-011	2.97	3.51	0.04	0.56	0.17	0.04	0.69	53	224	9	25	29	74	15
AB-012	2.43	3.45	0.05	0.51	0.43	0.08	0.25	107	187	10	18	37	46	20
AB-013	2.22	4.10	0.04	0.32	0.16	0.03	0.27	157	207	11	14	47	33	10
AB-014	3.40	7.19	0.05	0.47	0.34	0.06	0.17	348	143	13	15	75	51	10
AB-015	3.39	3.48	0.03	0.77	0.06	0.02	0.71	54	130	13	38	62	41	22
AB-016	3.14	3.10	0.04	1.11	0.89	0.12	0.37	73	236	18	29	187	50	206
AB-017	3.15	4.94	0.05	0.81	0.61	0.13	0.30	150	161	16	23	38	98	55
AB-018	2.75	7.60	0.05	0.72	0.70	0.13	0.25	322	192	14	21	36	48	22
AB-019	1.90	4.34	0.05	0.36	0.60	0.05	0.22	132	68	10	6	14	64	37
AB-020	2.80	2.74	0.04	0.80	0.49	0.07	0.48	63	172	9	19	23	53	16
AB-021	2.62	3.24	0.05	1.81	0.35	0.04	0.51	58	299	18	144	28	59	16
AB-022	1.92	2.18	0.04	0.42	0.10	0.02	0.47	31	100	7	15	11	42	13
AB-023	1.13	1.39	0.03	0.22	0.03	0.01	0.29	17	168	4	11	8	27	8
AB-024	1.05	1.26	0.03	0.17	0.04	0.05	0.27	14	245	4	10	8	25	6
AB-025	0.92	1.26	0.02	0.16	0.03	0.02	0.25	15	219	4	11	8	21	10
AB-026	1.51	2.03	0.09	0.32	0.17	0.05	0.35	28	212	7	11	10	36	5
AB-027	1.43	1.69	0.05	0.22	0.05	0.01	0.33	20	143	7	11	9	31	15
AB-028	1.18	2.03	0.07	0.22	0.05	0.02	0.35	36	219	6	14	12	39	7
AB-029	0.71	0.84	0.02	0.09	0.02	<0.01	0.15	12	203	3	6	8	16	<5
AB-030	1.13	1.52	0.03	0.23	0.04	0.02	0.32	18	267	5	14	9	30	<5
AB-031	1.77	1.93	0.02	0.19	0.08	0.02	0.41	24	378	6	17	12	33	8
AB-032	1.42	1.69	0.02	0.18	0.04	0.01	0.38	17	353	5	16	10	28	11
AB-033	1.19	1.46	0.02	0.19	0.05	0.01	0.31	13	122	6	13	9	35	10
AB-034	1.15	1.39	0.02	0.10	0.06	0.01	0.26	15	266	4	11	8	24	6
AB-035	1.67	1.92	0.02	0.19	0.07	<0.01	0.39	18	196	7	15	12	33	7
AB-036	1.23	1.75	0.03	0.26	0.06	0.02	0.35	20	281	5	25	10	44	9
AB-037	1.29	1.66	0.03	0.28	0.05	0.02	0.35	21	188	5	13	10	34	9
AB-038	2.00	2.25	0.03	0.34	0.07	0.03	0.54	31	396	7	20	12	44	<5
AB-039	1.65	2.07	0.03	0.38	0.15	0.05	0.51	29	342	6	19	12	41	11
AB-040	1.58	2.15	0.04	0.24	0.07	<0.01	0.41	18	76	8	16	12	45	10
AB-041	1.53	1.93	0.03	0.35	0.06	0.03	0.43	24	269	6	16	11	38	8
AB-042	3.07	2.95	0.05	0.63	0.14	0.02	0.69	49	145	9	21	19	70	10
AB-043	3.27	3.34	0.06	0.62	0.13	0.03	0.69	53	148	10	22	21	75	10
AB-044	1.38	1.91	0.03	0.28	0.05	0.02	0.35	23	157	5	13	9	39	9
AB-045	3.44	4.45	0.06	0.58	0.30	0.04	0.11	99	51	16	15	21	71	20
AB-046	1.42	2.11	0.03	0.27	0.06	0.02	0.36	24	118	6	14	11	44	15
AB-047	1.95	2.46	0.09	0.34	0.15	0.02	0.39	30	103	9	11	10	119	6
AB-048	2.34	2.38	0.06	0.32	0.07	0.02	0.37	37	137	7	14	12	51	8
AB-049	1.46	1.50	0.03	0.17	0.06	<0.01	0.25	16	179	4	12	9	78	10
AB-050	3.17	2.76	0.07	0.50	0.10	0.02	039	28	42	9	13	12	78	7
AB-051	1.10	1.41	0.03	0.21	0.14	0.03	0.28	17	194	5	10	9	61	16
AB-052	3.06	4.54	0.07	0.76	0.42	0.02	0.22	73	38	14	16	31	122	101
AB-053	2.09	3.66	0.08	0.55	3.48	0.01	0.21	101	31	14	18	45	225	26
AB-054	4.38	4.82	0.09	0.61	0.39	0.03	0.14	114	50	18	12	28	96	48
AB-055	2.79	3.07	0.05	0.55	0.17	0.02	0.52	45	174	10	24	22	76	9

* Samples which occur outside the area covered by Figure 32

Table 11. Stream sediment sample geochemistry. *Continued*

Sample	Sr PPM	Y PPM	Mo PPM	Ag PPM	Cd PPM	Sn PPM	Sb PPM	Te PPM	Ba PPM	La PPM	W PPM	Pb PPM	Bi PPM	Au PPB
AB-001	45	9	1	0.2	<0.2	<20	7	<10	112	8	<20	57	<5	12
AB-002	16	8	74	11.1	<0.2	<20	91	<10	54	11	<20	117	23	1198
AB-003	24	14	128	15.2	<0.2	<20	46	<10	153	36	405	89	25	1389
AB-004	31	7	6	<0.2	<0.2	<20	<5	<10	267	12	<20	18	<5	35
AB-005	21	16	6	<0.2	<0.2	<20	<5	<10	190	28	<20	16	<5	<5
AB-006	17	15	7	<0.2	<0.2	<20	<5	<10	155	65	<20	10	<5	<5
AB-007	18	16	5	<0.2	<0.2	<20	<5	<10	141	63	<20	14	<5	26
AB-008	42	8	3	<0.2	<0.2	<20	<5	<10	164	17	<20	14	<5	15
AB-009	22	8	3	<0.2	<0.2	<20	6	<10	103	12	<20	14	<5	15
AB-010	21	35	4	<0.2	<0.2	<20	<5	<10	150	146	<20	12	<5	6
AB-011	19	10	4	<0.2	<0.2	<20	<5	<10	204	26	<20	13	<5	<5
AB-012	23	7	3	<0.2	<0.2	<20	<5	<10	100	15	<20	18	<5	632
AB-013	12	5	4	<0.2	<0.2	<20	<5	<10	101	13	<20	11	<5	646
AB-014	24	6	3	<0.2	<0.2	<20	<5	<10	103	5	<20	44	<5	17
AB-015	11	9	3	<0.2	<0.2	<20	<5	<10	162	17	<20	7	<5	323
AB-016	35	15	2	<0.2	<0.2	<20	<5	<10	173	41	<20	15	<5	511
AB-017	38	7	3	<0.2	<0.2	<20	<5	<10	133	9	<20	13	<5	31
AB-018	37	8	2	<0.2	<0.2	<20	<5	<10	102	8	<20	11	<5	58
AB-019	41	7	2	0.2	<0.2	<20	<5	<10	136	12	<20	13	<5	258
AB-020	25	8	2	<0.2	<0.2	<20	<5	<10	134	22	<20	10	<5	<5
AB-021	14	10	3	<0.2	<0.2	<20	<5	<10	149	25	<20	10	<5	6
AB-022	9	8	2	<0.2	<0.2	<20	<5	<10	97	21	<20	9	<5	<5
AB-023	5	7	2	<0.2	<0.2	<20	<5	<10	69	27	<20	8	<5	<5
AB-024	5	6	4	<0.2	<0.2	<20	<5	<10	65	21	<20	5	<5	16
AB-025	5	4	3	<0.2	<0.2	<20	<5	<10	57	14	<20	6	<5	<5
AB-026	8	10	3	<0.2	<0.2	<20	<5	<10	104	24	<20	14	<5	<5
AB-027	6	8	2	<0.2	<0.2	<20	<5	<10	95	18	<20	10	<5	<5
AB-028	6	21	3	<0.2	<0.2	<20	<5	<10	87	84	<20	12	<5	<5
AB-029	4	4	1	<0.2	<0.2	<20	<5	<10	44	18	<20	4	<5	<5
AB-030	5	6	4	<0.2	<0.2	<20	<5	<10	77	22	<20	6	<5	<5
AB-031	13	6	5	<0.2	<0.2	<20	<5	<10	101	21	<20	12	<5	<5
AB-032	8	4	5	<0.2	<0.2	<20	<5	<10	89	18	<20	8	<5	<5
AB-033	8	6	5	<0.2	<0.2	<20	<5	<10	126	25	<20	11	<5	<5
AB-034	9	3	1	<0.2	<0.2	<20	<5	<10	80	17	<20	7	<5	<5
AB-035	9	5	1	<0.2	<0.2	<20	<5	<10	99	22	<20	13	<5	<5
AB-036	6	9	-	<0.2	<0.2	<20	<5	<10	81	33	<20	8	<5	<5
AB-037	7	8	-	<0.2	<0.2	<20	<5	<10	79	30	<20	8	<5	<5
AB-038	10	8	5	<0.2	<0.2	<20	<5	<10	120	25	<20	10	<5	<5
AB-039	11	9	5	<0.2	<0.2	<20	<5	<10	96	29	<20	8	<5	<5
AB-040	9	6	1	<0.2	<0.2	<20	<5	<10	105	27	<20	14	<5	<5
AB-041	8	7	4	<0.2	<0.2	<20	<5	<10	93	24	<20	10	<5	<5
AB-042	12	32	2	<0.2	<0.2	<20	<5	<10	127	138	<20	12	<5	<5
AB-043	14	29	1	<0.2	<0.2	<20	<5	<10	146	110	<20	16	<5	<5
AB-044	8	7	2	<0.2	<0.2	<20	<5	<10	76	31	<20	7	<5	<5
AB-045	23	6	1	<0.2	<0.2	<20	<5	<10	104	5	<20	11	<5	5
AB-046	8	10	2	<0.2	<0.2	<20	7	<10	88	50	<20	11	<5	<5
AB-047	9	9	1	<0.2	<0.2	<20	<5	<10	120	33	<20	22	<5	<5
AB-048	7	10	2	<0.2	<0.2	<20	<5	<10	106	33	<20	15	<5	<5
AB-049	5	6	3	<0.2	<0.2	<20	<5	<10	72	22	<20	157	<5	124
AB-050	15	13	<1	<0.2	<0.2	<20	<5	<10	138	40	<20	20	<5	<5
AB-051	6	8	3	<0.2	<0.2	<20	<5	<10	62	24	<20	23	<5	<5
AB-052	30	11	1	<0.2	<0.2	<20	<5	<10	122	12	<20	35	<5	111
AB-053	41	12	7	<0.2	0.6	<20	7	<10	177	10	<20	17	<5	<5
AB-054	30	8	1	<0.2	<0.2	<20	<5	<10	148	7	<20	26	<5	8
AB-055	15	22	3	<0.2	<0.2	<20	<5	<10	159	90	<20	11	<5	<5

Table 11. Stream sediment sample geochemistry. *Continued*

Sample	Al PCT	FeTot PCT	Mn PCT	Mg PCT	Ca PCT	Na PCT	K PCT	V PPM	Cr PPM	Co PPM	Ni PPM	Cu PPM	Zn PPM	As PPM
AB-056	3.28	3.35	0.07	1.30	3.11	0.13	0.17	107	211	22	49	36	51	15
AB-057	3.16	3.84	0.06	0.99	1.45	0.07	0.29	93	164	15	44	35	57	49
AB-058	3.57	3.53	0.07	0.72	0.58	0.04	0.41	68	162	14	33	31	83	14
AB-059	2.94	3.48	0.10	0.90	1.40	0.05	0.27	81	226	21	54	33	56	22
AB-060	2.70	3.69	0.07	0.88	1.13	0.04	0.30	90	117	17	40	53	59	13
AB-061	2.11	3.52	0.06	0.73	1.13	0.04	0.06	108	107	21	35	46	49	<5
AB-062	1.68	3.98	0.03	0.32	0.17	0.03	0.27	47	142	9	32	387	126	>200
AB-063	2.55	3.55	0.06	0.90	0.93	0.04	0.15	84	187	18	60	61	69	40
AB-064	1.18	4.56	0.01	0.14	0.05	0.01	0.30	17	98	6	14	676	231	>2000
AB-065	3.24	4.17	0.03	1.07	0.47	0.03	0.22	93	244	23	113	70	98	80
AB-066	2.49	5.21	0.05	0.27	0.08	0.02	0.21	79	87	17	33	91	134	467
AB-067	3.77	3.69	0.04	0.73	0.20	0.02	0.60	65	114	13	30	35	104	16
AB-068	2.57	2.35	0.04	0.56	0.60	0.04	0.12	51	47	10	12	26	38	13
AB-069	1.03	3.07	0.01	0.10	0.05	0.01	0.28	22	103	6	14	544	46	1979
AB-070	2.74	3.31	0.04	0.19	0.10	0.02	0.25	65	78	8	18	27	42	32
AB-071	1.94	3.24	0.07	0.52	0.48	0.03	0.18	65	167	18	55	51	83	20
AB-072	3.34	4.48	0.22	0.59	0.44	0.05	0.33	85	210	24	61	81	106	25
AB-073	1.88	3.87	0.17	1.09	0.24	0.03	0.33	58	537	25	212	32	59	13
AB-074	2.84	4.29	0.14	0.41	0.50	0.07	0.27	98	108	17	46	53	81	<5
AB-075	1.56	2.03	0.03	0.57	0.63	0.07	0.16	49	124	7	13	53	47	100
AB-076	2.58	2.80	0.05	0.62	0.54	0.05	0.25	61	100	14	15	220	292	1150
AB-077	2.20	2.83	0.09	0.41	0.50	0.04	0.27	53	127	13	15	295	205	>2000
AB-078	1.51	1.86	0.03	0.30	0.39	0.04	0.19	39	154	6	12	19	39	49
AB-079	1.92	3.96	0.07	1.34	0.43	0.09	0.33	76	190	19	35	23	69	<5
AB-080	1.76	3.36	0.04	1.76	0.43	0.08	0.13	65	97	19	45	40	78	<5
AB-081	1.85	2.70	0.08	1.34	0.32	0.08	0.39	44	143	14	24	17	65	<5
AB-082	2.67	4.70	0.35	1.33	0.33	0.08	0.54	72	279	18	33	27	76	<5
AB-083	2.39	4.29	0.11	1.51	0.28	0.07	0.54	85	150	17	29	32	89	<5
AB-084	2.31	3.86	0.07	2.67	1.57	0.15	0.20	100	147	28	61	44	71	7
AB-085	0.87	2.35	0.01	0.27	0.07	0.06	0.21	27	130	5	15	18	67	5
AB-086	2.18	4.05	0.04	1.56	0.27	0.08	0.22	64	145	19	63	72	145	98
AB-087	1.33	3.68	0.02	0.38	0.10	0.08	0.26	54	121	9	23	30	82	<5
AB-088	1.15	1.37	0.02	0.64	0.21	0.09	0.27	19	193	5	16	8	34	<5
AB-089	1.28	1.09	0.01	0.51	0.13	0.14	0.49	14	231	3	13	7	22	<5
AB-090	2.48	3.50	0.05	2.19	0.67	0.11	0.18	72	149	18	61	37	73	<5
AB-091	2.67	2.88	0.05	2.06	0.36	0.09	0.27	57	163	14	40	32	71	17
AB-092	2.63	2.98	0.04	2.35	0.38	0.11	0.32	59	269	15	85	31	70	<5
AB-093	1.65	2.97	0.06	1.25	0.68	0.10	0.09	63	165	20	41	40	59	28
AB-094	1.49	2.32	0.02	0.84	0.18	0.07	0.26	33	196	9	32	20	51	10
AB-095	2.35	3.33	0.05	1.36	0.43	0.11	0.23	85	186	13	26	22	50	<5
AB-096	1.76	2.40	0.04	0.73	0.08	0.03	0.30	33	181	7	18	15	16	7
AB-097	4.04	4.67	0.05	1.13	0.12	0.02	0.39	74	132	15	26	35	140	15
AB-098	1.09	1.80	0.05	0.51	0.17	0.05	0.29	19	290	6	17	10	13	7
AB-099	1.18	1.60	0.04	0.68	0.01	0.03	0.39	18	141	7	15	9	19	10
AB-100	0.75	1.34	0.03	0.37	0.03	0.02	0.21	14	68	5	10	8	13	<5
AB-101	1.84	2.33	0.04	0.97	0.08	0.05	0.48	27	257	9	21	13	58	<5
AB-102	2.24	3.90	0.06	1.01	0.69	0.07	0.29	100	208	13	22	33	118	22
AB-103	3.01	4.68	0.11	1.90	0.60	0.06	0.50	96	139	20	27	41	110	30
AB-104	3.29	2.65	0.06	1.59	0.60	0.11	0.49	38	187	8	19	17	119	17
AB-105	2.04	2.39	0.04	0.81	0.21	0.03	0.28	43	185	7	19	12	112	17
AB-106	1.20	2.08	0.04	0.33	0.15	0.03	0.41	26	139	5	13	12	38	<5
AB-107	1.57	2.43	0.04	0.41	0.08	0.03	0.53	29	186	6	16	12	45	<5
AB-108	1.53	2.78	0.04	0.24	0.12	0.02	0.33	41	192	6	17	17	44	<5
AB-109	2.90	4.32	0.07	0.42	0.21	0.02	0.43	74	110	12	24	33	72	<5
AB-110	4.10	4.92	0.07	0.75	0.22	0.03	0.54	81	119	18	36	41	105	<5

Table 11. Stream sediment sample geochemistry. *Continued*

Sample	Sr PPM	Y PPM	Mo PPM	Ag PPM	Cd PPM	Sn PPM	Sb PPM	Te PPM	Ba PPM	La PPM	W PPM	Pb PPM	Bi PPM	Au PPB
AB-056	35	24	1	<0.2	<0.2	<20	<5	<10	74	54	<20	6	<5	24
AB-057	23	20	3	<0.2	<0.2	<20	7	<10	119	50	<20	9	<5	<5
AB-058	18	20	2	<0.2	<0.2	<20	7	<10	154	64	<20	13	<5	<5
AB-059	28	15	3	<0.2	<0.2	<20	<5	<10	154	33	<20	8	<5	<5
AB-060	25	28	<10	<0.2	<0.2	<20	<5	<10	124	91	<20	16	<5	113
AB-061	24	12	<1	<0.2	<1.0	<20	<5	<10	54	3	<20	5	<5	36
AB-062	16	8	<10	4.8	<1.0	<20	51	28	107	26	<20	153	57	3558
AB-063	24	10	<10	<0.2	<1.0	<20	<5	<10	85	11	<20	8	<5	40
AB-064	11	8	<10	9.0	<1.0	<20	93	43	105	34	<20	296	104	7166
AB-065	18	10	<10	<0.2	<1.0	<20	147	<10	146	16	<20	22	<5	184
AB-066	9	12	<10	1.8	<1.0	<20	286	<10	85	24	<20	123	<5	249
AB-067	25	14	<10	<0.2	<1.0	<20	<5	<10	170	28	<20	19	<5	7
AB-068	20	11	<1	<0.2	<1.0	<20	<5	<10	116	11	<20	12	<5	11
AB-069	8	6	<10	9.5	<1.0	21	59	47	107	31	<20	153	87	5133
AB-070	11	8	<1	<0.2	<1.0	<20	<5	<10	80	31	<20	21	<5	34
AB-071	23	9	<10	<0.2	<1.0	<20	<5	<10	140	14	<20	11	<5	37
AB-072	23	12	<10	<0.2	<1.0	<20	<5	<10	239	25	<20	18	<5	16
AB-073	17	8	<10	<0.2	<1.0	<20	<5	<10	131	24	<20	13	<5	7
AB-074	28	14	<10	<0.2	<1.0	<20	<5	<10	121	23	<20	15	<5	10
AB-075	23	7	<10	1.9	<1.0	<20	<5	<10	66	16	<20	21	<5	283
AB-076	24	9	<10	1.5	<1.0	<20	6	<10	103	13	<20	128	8	1069
AB-077	30	10	<10	2.9	<1.0	<20	6	<10	122	16	<20	251	17	2895
AB-078	21	7	<10	<0.2	<1.0	<20	<5	<10	83	14	<20	18	<5	56
AB-079	16	38	4	0.2	<0.2	<20	<5	<10	136	244	<20	10	<5	<5
AB-080	14	6	5	0.2	0.5	<20	<5	<10	68	9	<20	8	<5	20
AB-081	16	11	4	0.2	0.8	<20	<5	<10	130	30	<20	14	<5	<5
AB-082	24	19	5	0.3	0.3	<20	<5	<10	329	85	<20	14	5	10
AB-083	19	20	4	0.2	<0.2	<20	<5	<10	196	85	<20	16	<5	<5
AB-084	21	12	2	<0.2	<0.2	<20	<5	<10	75	12	<20	<2	<5	10
AB-085	12	4	4	0.3	0.7	<20	<5	<10	62	20	<20	9	<5	116
AB-086	16	10	5	0.7	1.4	<20	5	<10	98	18	<20	30	8	416
AB-087	16	8	3	0.3	1.2	<20	<5	<10	84	29	<20	11	<5	<5
AB-088	16	6	4	<0.2	0.3	<20	<5	<10	77	11	<20	8	<5	38
AB-089	13	4	6	<0.2	<0.2	<20	<5	<10	101	11	<20	7	<5	<5
AB-090	22	9	6	0.3	<0.2	<20	<5	<10	98	14	<20	5	<5	<5
AB-091	21	6	5	0.2	0.5	<20	<5	<10	137	16	<20	16	<5	51
AB-092	23	10	8	<0.2	0.7	25	<5	<10	156	40	<20	15	<5	13
AB-093	21	7	8	0.4	0.7	<20	<5	<10	72	9	<20	16	<5	57
AB-094	12	10	4	0.7	1.1	<20	<5	<10	92	41	<20	18	<5	1560
AB-095	25	7	7	0.3	0.3	<20	<5	<10	115	17	<20	14	<5	425
AB-096	9	9	4	<0.2	0.4	22	9	<10	81	38	<20	19	<5	10
AB-097	13	22	3	0.3	1.4	25	17	<10	131	100	<20	30	<5	50
AB-098	9	7	5	0.3	<0.2	<20	6	<10	78	17	<20	13	<5	<5
AB-099	6	6	3	<0.2	0.8	<20	7	<10	77	19	<20	18	<5	12
AB-100	4	5	2	0.3	0.4	<20	<5	<10	50	20	<20	15	<5	8
AB-101	10	9	6	0.2	0.5	26	8	<10	104	30	<20	17	<5	<5
AB-102	43	9	8	0.6	2.2	<20	18	<10	173	12	<20	22	<5	13
AB-103	27	29	3	0.7	1.5	<20	21	<10	178	105	<20	44	<5	110
AB-104	30	18	3	0.4	1.1	<20	15	<10	104	52	<20	48	<5	30
AB-105	13	10	4	0.4	0.9	<20	12	<10	85	29	<20	40	<5	70
AB-106	11	37	2	<0.2	<1.0	<20	<5	<10	89	117	<20	2	<5	<5
AB-107	12	15	1	<0.2	<1.0	<20	<5	<10	107	68	<20	<2	<5	<5
AB-108	14	33	2	<0.2	<1.0	<20	<5	<10	138	260	<20	7	<5	<5
AB-109	19	30	2	<0.2	<1.0	<20	<5	<10	208	134	<20	17	<5	<5
AB-110	22	31	2	<0.2	<1.0	<20	<5	<10	271	93	<20	18	<5	<5

Table 11. Stream sediment sample geochemistry. *Continued*

Sample	Al PCT	FeTot PCT	Mn PCT	Mg PCT	Ca PCT	Na PCT	K PCT	V PPM	Cr PPM	Co PPM	Ni PPM	Cu PPM	Zn PPM	As PPM
AB-111	1.84	2.80	0.05	0.63	1.44	0.06	0.21	67	150	12	26	20	38	<5
AB-112	1.78	2.79	0.05	0.41	0.54	0.05	0.43	45	205	7	20	17	49	<5
AB-113	2.50	3.34	0.06	0.53	0.70	0.05	0.52	54	202	19	10	18	65	<5
AB-114	1.22	9.25	0.12	5.88	0.42	0.02	0.04	77	1820	164	1696	13	74	<5
AB-115	No fluvial sample													
AB-116	2.16	1.77	0.03	0.57	0.31	0.05	0.28	55	69	8	16	15	68	27
AB-117	1.98	2.21	0.03	0.48	0.12	0.02	0.45	79	131	7	19	22	60	<5
AB-118	1.56	1.93	0.03	0.27	0.04	0.02	0.36	43	197	6	19	20	59	19
AB-119	3.22	2.19	0.04	0.63	0.16	0.04	0.48	64	151	11	30	31	76	24
AB-120	2.10	2.58	0.03	0.29	0.07	0.03	0.32	68	162	12	32	37	88	<5
AB-121	2.24	2.45	0.03	0.42	0.15	0.06	0.40	65	190	9	30	43	85	18
AB-122	2.41	2.10	0.04	0.63	0.31	0.04	0.46	60	131	9	28	32	62	<5
AB-123	2.36	2.40	0.05	0.57	0.18	0.03	0.51	83	98	12	24	37	83	<5
AB-124	3.46	2.11	0.05	1.03	0.66	0.05	0.25	72	160	14	42	51	67	36
AB-125	3.65	2.50	0.07	1.23	0.30	0.02	0.32	96	193	16	39	43	94	<5
AB-126	2.05	1.41	0.03	0.67	0.33	0.05	0.24	50	143	9	23	28	40	40
AB-127	2.71	1.80	0.03	0.86	0.39	0.06	0.29	61	160	11	33	34	53	18
AB-128	2.45	1.72	0.02	0.22	0.05	<0.01	0.16	56	106	4	18	25	49	12
AB-129	3.54	2.11	0.04	0.80	0.25	0.04	0.44	71	132	12	38	48	59	53
AB-130	3.05	2.39	0.06	1.17	0.24	0.03	0.30	66	187	18	81	47	87	33
AB-131	4.02	3.04	0.08	1.66	1.08	0.15	0.13	121	145	30	95	110	58	<5
AB-132	3.36	2.41	0.06	0.88	0.25	0.04	0.56	70	135	15	48	54	76	10
AB-133	3.31	2.40	0.05	0.92	0.25	0.04	0.60	68	150	14	52	45	76	47
AB-134	3.35	2.77	0.05	0.78	0.19	0.03	0.47	83	144	15	51	57	101	37
AB-135	2.43	2.44	0.03	0.73	0.12	0.04	0.38	69	190	18	76	52	81	7
AB-136	2.93	2.50	0.04	0.55	0.06	0.02	0.75	63	135	10	29	28	104	31
AB-137	2.56	2.42	0.03	0.63	0.10	0.03	0.58	65	192	11	44	36	88	34
AB-138	2.59	2.00	0.03	0.55	0.18	0.04	0.43	57	187	11	31	30	50	8
AB-139	2.92	2.08	0.05	0.71	0.34	0.08	0.57	63	226	10	32	30	51	<5
AB-140	3.20	3.32	0.05	0.88	0.50	0.06	0.34	80	129	11	16	22	63	51
AB-141	3.21	2.59	0.04	0.64	0.49	0.13	0.36	92	98	10	17	29	53	9
AB-142	3.66	2.61	0.04	0.83	0.27	0.04	0.55	61	168	10	28	28	66	9
AB-143	2.42	2.82	0.04	0.63	0.14	0.04	0.54	51	184	8	24	25	66	8
AB-144	4.59	2.76	0.04	0.91	0.30	0.04	0.37	75	186	12	33	26	90	11
AB-145	2.37	2.83	0.04	0.40	0.10	0.03	0.54	41	231	8	19	22	61	11
AB-146	2.05	2.85	0.04	0.47	0.16	0.02	0.41	83	155	10	27	27	89	10
AB-147	1.25	2.78	0.06	0.20	0.11	0.01	0.23	35	76	10	20	21	45	34
AB-148	1.68	2.59	0.04	0.42	0.11	0.02	0.37	46	79	9	18	22	58	12
AB-149	1.71	3.10	0.05	0.46	0.14	0.02	0.40	69	126	12	25	29	66	11
AB-150	1.54	2.64	0.07	0.31	0.16	0.03	0.38	45	250	10	20	22	47	7
AB-151	2.85	4.20	0.05	0.50	0.24	0.06	0.17	85	68	14	17	30	58	15
AB-152	2.51	3.04	0.05	0.53	0.38	0.06	0.24	54	55	10	12	16	63	23
AB-153	3.09	2.41	0.03	0.74	1.02	0.25	0.27	76	147	10	19	31	51	19
AB-154	2.44	2.86	0.04	0.83	0.46	0.06	0.38	73	96	13	31	41	51	20
AB-155	2.58	7.05	0.05	0.80	0.36	0.06	0.22	175	136	18	10	28	90	27
AB-156	2.44	3.21	0.05	0.52	0.10	0.04	0.47	59	265	11	16	14	59	20
AB-157	2.40	4.25	0.06	0.51	0.10	0.02	0.38	102	254	12	16	15	62	27
AB-158	2.62	4.71	0.05	0.79	0.23	0.05	0.43	113	204	13	16	19	65	18
AB-159	1.99	2.41	0.04	0.39	0.11	0.04	0.39	36	354	9	17	14	49	14
AB-160	3.04	2.59	0.04	0.64	0.08	0.01	0.42	33	140	11	19	14	71	44
AB-161	2.58	2.76	0.04	0.64	0.18	0.02	0.34	45	146	10	16	15	65	40
AB-162	3.25	3.28	0.04	0.74	0.12	0.02	0.43	43	150	12	23	21	88	48
AB-163	1.50	1.80	0.04	0.21	0.13	0.02	0.41	15	193	8	12	9	112	<5
AB-164	1.46	1.85	0.04	0.39	0.10	0.01	0.29	18	106	9	14	10	49	6
AB-165	1.20	1.52	0.04	0.14	0.05	0.01	0.25	18	168	6	10	10	39	15

Table 11. Stream sediment sample geochemistry. *Continued*

Sample	Sr PPM	Y PPM	Mo PPM	Ag PPM	Cd PPM	Sn PPM	Sb PPM	Te PPM	Ba PPM	La PPM	W PPM	Pb PPM	Bi PPM	Au PPB
AB-111	27	31	<1	<0.2	<1.0	<20	<5	<10	85	169	<20	>2	<5	<5
AB-112	21	64	2	<0.2	<1.0	<20	<5	<10	143	432	<20	6	<5	<5
AB-113	27	56	2	<0.2	<1.0	<20	<5	<10	162	290	<20	11	<5	<5
AB-114	8	5	<1	<0.2	<1.0	<20	<5	<10	39	<1	<20	10	10	<5
AB-115							No fluvial sample							
AB-116	24	5	1	<0.2	<1.0	<20	<5	<10	93	11	<20	8	<5	<5
AB-117	9	16	2	<0.2	<1.0	<20	<5	<10	99	66	<20	6	<5	77
AB-118	8	29	4	<0.2	<1.0	<20	6	<10	113	161	<20	11	<5	<5
AB-119	13	12	3	<0.2	<1.0	<20	<5	<10	150	51	<20	17	<5	7
AB-120	13	17	3	<0.2	<1.0	<20	<5	<10	146	86	<20	10	<5	<5
AB-121	11	17	4	<0.2	<1.0	<20	<5	<10	148	78	<20	11	<5	<5
AB-122	19	44	2	<0.2	<1.0	<20	<5	<10	158	233	<20	8	<5	30
AB-123	11	9	<1	<0.2	<1.0	<20	<5	<10	148	18	<20	4	<5	<5
AB-124	37	9	1	<0.2	<1.0	<20	<5	<10	133	10	<20	15	<5	27
AB-125	27	8	<1	<0.2	<1.0	<20	<5	<10	201	18	<20	19	<5	94
AB-126	22	5	2	<0.2	<1.0	<20	<5	<10	103	10	<20	14	<5	<5
AB-127	25	6	2	<0.2	<1.0	<20	<5	<10	167	22	<20	15	<5	<5
AB-128	5	4	2	<0.2	<1.0	<20	<5	<10	60	16	<20	11	<5	13
AB-129	23	7	3	<0.2	<1.0	<20	9	<10	195	25	<20	18	6	23
AB-130	22	6	1	<0.2	<1.0	<20	<5	<10	128	14	<20	16	<5	6
AB-131	29	11	<1	<0.2	<1.0	<20	<5	<10	33	2	<20	<2	7	6
AB-132	20	10	1	<0.2	<1.0	<20	<5	<10	149	25	<20	8	<5	6
AB-133	19	9	3	<0.2	<1.0	<20	9	<10	151	27	<20	16	9	7
AB-134	18	7	<1	<0.2	<1.0	<20	<5	<10	162	18	<20	8	<5	7
AB-135	17	10	2	<0.2	<1.0	<20	<5	<10	144	48	<20	8	<5	<5
AB-136	11	11	4	<0.2	<1.0	<20	7	<10	187	56	<20	18	5	<5
AB-137	13	13	5	<0.2	<1.0	<20	12	<10	159	65	<20	17	7	<5
AB-138	21	17	2	<0.2	<1.0	<20	<5	<10	216	103	<20	9	<5	13
AB-139	32	11	2	<0.2	<1.0	<20	<5	<10	252	59	<20	7	<5	14
AB-140	35	12	<1	<0.2	<1.0	<20	<5	<10	124	27	<20	19	<5	32
AB-141	51	9	<1	<0.2	<1.0	<20	<5	<10	140	21	<20	12	<5	<5
AB-142	23	12	<1	<0.2	<1.0	<20	<5	<10	156	39	<20	16	<5	<5
AB-143	11	13	1	<0.2	<1.0	<20	<5	<10	122	38	<20	12	<5	29
AB-144	24	9	<1	<0.2	<1.0	<20	<5	<10	192	20	<20	20	<5	<5
AB-145	16	8	2	<0.2	<1.0	<20	<5	<10	144	25	<20	12	<5	<5
AB-146	14	9	1	<0.2	<1.0	<20	<5	<10	133	11	<20	10	<5	<5
AB-147	15	5	<1	<0.2	<1.0	<20	<5	<10	99	14	<20	14	<5	34
AB-148	13	8	<1	<0.2	<1.0	<20	<5	<10	112	16	<20	12	<5	<5
AB-149	11	9	2	<0.2	<1.0	<20	<5	<10	100	12	<20	11	<5	<5
AB-150	14	7	2	<0.2	<1.0	<20	<5	<10	127	12	<20	12	<5	<5
AB-151	25	9	<1	<0.2	<1.0	<20	<5	<10	89	22	<20	17	<5	<5
AB-152	34	8	<1	<0.2	<1.0	<20	<5	<10	177	14	<20	16	<5	<5
AB-153	85	5	1	<0.2	<1.0	<20	<5	<10	122	10	<20	18	<5	15
AB-154	22	9	1	<0.2	<1.0	<20	<5	<10	120	13	<20	11	<5	8
AB-155	32	5	5	0.5	<1.0	<20	<5	<10	87	30	<20	20	6	<5
AB-156	13	13	3	<0.2	<1.0	<20	<5	<10	121	57	<20	15	<5	<5
AB-157	12	16	5	0.3	<1.0	<20	<5	<10	99	79	<20	16	6	<5
AB-158	16	11	5	0.3	<1.0	<20	<5	<10	100	42	<20	11	<5	<5
AB-159	11	8	4	<0.2	<1.0	<20	<5	<10	95	35	<20	13	<5	<5
AB-160	11	24	2	0.2	<1.0	<20	<5	<10	110	124	<20	13	<5	<5
AB-161	13	21	3	0.3	<1.0	<20	<5	<10	99	93	<20	12	<5	<5
AB-162	13	19	4	0.2	<1.0	<20	<5	<10	119	89	<20	14	<5	<5
AB-163	14	5	2	0.2	<1.0	<20	<5	<10	96	27	<20	27	<5	<5
AB-164	8	5	1	<0.2	<1.0	<20	<5	<10	67	30	<20	13	<5	<5
AB-165	5	5	3	0.4	<1.0	<20	<5	<10	118	26	<20	22	<5	<5

Table 11. Stream sediment sample geochemistry. *Continued*

Sample	Al PCT	FeTot PCT	Mn PCT	Mg PCT	Ca PCT	Na PCT	K PCT	V PPM	Cr PPM	Co PPM	Ni PPM	Cu PPM	Zn PPM	As PPM
AB-166	2.04	2.50	0.03	0.38	0.02	0.01	0.37	26	111	10	17	15	64	9
AB-167	3.05	5.59	0.06	0.85	0.30	0.07	0.35	162	251	16	16	18	71	44
AB-168	1.17	1.41	0.03	0.17	0.05	0.02	0.24	20	158	6	9	7	36	12
AB-169	0.43	0.92	0.02	0.08	0.02	0.01	0.11	11	156	3	7	3	12	<5
AB-170	1.33	1.89	0.09	0.30	0.09	0.03	0.39	26	177	7	15	9	34	7
AB-171	1.70	2.46	0.07	0.49	0.09	0.02	0.56	32	175	10	20	12	44	15
AB-172	2.41	2.98	0.05	0.57	0.17	0.05	0.70	47	190	10	22	18	56	16
AB-173	2.40	3.78	0.06	0.75	0.18	0.03	0.60	54	64	13	21	19	79	29

Copper, lead, zinc, cadmium and barium

Copper analyses varied from less than 10ppm, in a few samples, up to a maximum of 8067ppm (AB2) and 2629ppm (AB3) in the Ríos Vivar and Mollepungu. In general copper values were less than 60ppm with the highest concentrations being found in the Cerro Pelado (AB62, AB63, AB64, AB65, AB66 and AB69, 61-676ppm) and the Cerro Los Cangrejos (AB76 and AB77, 220-295ppm) areas. The following rivers also contained copper values greater than 60ppm: Río Colorado (AB16, 187ppm); Estero San Antonio (AB131, 110ppm) (see also AB124, AB125, AB129, AB130, AB132, AB133 and AB134); Río Santa Rosa (AB86, 72ppm); an unnamed tributary of the Río Santa Rosa (AB72, 81ppm) (see also AB71 and AB74); Río Dumari (AB14, 75ppm) (see also AB13) and an unnamed tributary of the Río Daucay (AB15, 62ppm).

The highest lead analyses were obtained from the Cerro Pelado (AB62, AB64, AB66 and AB69, 123-296ppm) and Cerro Los Cangrejos (AB76 and AB77, 128-251ppm) areas. Anomalous lead values were also recorded in the Ríos Vivar and Mollepungu (AB2 and AB3 117-89ppm) and the Quebrada del Batén (AB49, 157ppm). Lesser quantities of lead (>25ppm) were found in the following rivers: Quebrada Santa Martha (AB1, 57ppm – falls outside of area covered by Figure 32, see Table 10 for location); Río Dumari (AB14, 44ppm); Río El Ari (AB52, 35ppm); Quebrada Chontas (AB54, 26ppm); Río Santa Rosa (AB86, 30ppm); Quebrada Limoncillo (AB97, 30ppm); Quebrada El Salado (AB103, 44ppm); Quebrada Chaupi (AB104, 48ppm); Quebrada El Belén (AB105, 40ppm); Quebrada del Sharve (AB163, 27ppm) and Quebrada San Joaquín (AB167, 41ppm).

Zinc analyses varied from 12 to 292ppm but the distribution of the higher values (>100ppm) appears to be more scattered than some of the other elements considered. In the Cerro Pelado and Cerro Los Cangrejos areas values ranged from 104 to 231ppm (AB62, AB64, AB66 and AB67) and 292 to 205ppm (AB76 and AB77) respectively and 107ppm was recorded from the Río Vivar (AB2). In the south-east, the Río Yaguachi, Quebrada Chaupi and Quebrada El Belén (AB102, AB104 and AB105) all contained more than 110ppm of zinc.

The following rivers also carried zinc values more than 100ppm: Quebrada del Trapiche (AB47, 119ppm); Río El Ari (AB52, 122ppm); Quebrada de La Concha (AB53, 225ppm – falls outside area covered by Figure 32, see Table 10 for location); an unnamed tributary of the Río Santa Rosa (AB72, 106ppm); Río Santa Rosa (AB86, 145ppm); Quebrada Limoncillo (AB97, 140ppm); Quebrada El Salado (AB103, 110ppm); an unnamed tributary of the Quebrada Bruno (AB110, 105ppm); an unnamed tributary of Estero San Antonio (AB134, 101ppm); an unnamed tributary of the Río Quera (AB136, 104ppm) and Quebrada del Sharve (AB163, 112ppm).

Cadmium analyses were generally less than 1ppm (or <0.2ppm) (detection limits) and the highest value recorded is 2.2 ppm (AB102) from the Río Yaguachi.

Barium analyses ranged from 33 to 329ppm. The following rivers carried values greater than 200 ppm: Río Muyuyacu (AB4, 267ppm); Río Huizho (AB11, 204ppm); an unnamed tributary of the Río Santa Rosa (AB72, 239ppm); Quebrada de Cañas (AB82, 329ppm); unnamed tributaries of the Quebrada Bruno (AB109 and AB110, 208-271ppm); Río Colorado (AB125, 201ppm) and unnamed tributaries of the Río Quera (AB138 and AB139, 216-252ppm).

Chromium, nickel, cobalt and vanadium

Chromium analyses ranged from 31 to 1820ppm and the two highest values, 1820ppm (AB114) and 537ppm (AB73), both spatially relate to serpentinite bodies in the Palenque mélange division. In the north, several samples collected from rivers which drain these rocks had values greater than 250ppm (AB6, AB7, AB10, AB21, AB92 and AB150). However, it is perhaps surprising that high chromium analyses were also obtained from the following drainages associated with the Tahuín division and/or the Moromoro granitoid complex: Quebrada Los Zábalos (AB31, 378ppm and AB32, 353ppm); an unnamed tributary of the Río Puyango (AB34, 266ppm); Río Zaracay (AB36, 281ppm and AB41, 269ppm); Quebrada Primavera (AB38, 396ppm); Quebrada Valle Hermoso (AB39, 342ppm); Quebrada El Duende (AB98, 290ppm) and Quebrada de Ñalacapa (AB101, 257ppm). In the southeast, chromium values of greater than 250ppm were also recorded from the upper reaches of the Río Ambocas (AB156, AB157 and AB159) and the Quebrada San Joaquín (AB167).

Table 11. Stream sediment sample geochemistry. *Continued*

Sample	Sr PPM	Y PPM	Mo PPM	Ag PPM	Cd PPM	Sn PPM	Sb PPM	Te PPM	Ba PPM	La PPM	W PPM	Pb PPM	Bi PPM	Au PPB
AB-166	6	6	3	<0.2	<1.0	<20	<5	<10	87	38	<20	14	<5	<5
AB-167	25	7	4	0.7	<1.0	<20	<5	<10	94	30	<20	41	<5	<5
AB-168	5	4	2	<0.2	<1.0	<20	<5	<10	61	25	<20	12	<5	<5
AB-169	3	3	2	<0.2	<1.0	<20	<5	<10	33	14	<20	4	<5	<5
AB-170	15	16	2	<0.2	<1.0	<20	<5	<10	103	64	<20	9	<5	<5
AB-171	16	8	2	<0.2	<1.0	<20	<5	<10	115	24	<20	11	<5	<5
AB-172	18	28	3	<0.2	<1.0	<20	<5	<10	150	93	<20	15	<5	<5
AB-173	22	19	1	<0.2	<1.0	<20	<5	<10	148	33	<20	18	<5	<5

Nickel analyses ranged from 6 to 1696ppm but only a few samples had values greater than 100ppm. The highest nickel values recorded, 1696ppm (AB114) and 212ppm (AB73) both relate geographically to serpentinite bodies in the Palenque mélange division (see also possibly AB92 and AB131). However, the 113ppm analysis obtained from AB65 may reflect mineralisation in the Cerro Pelado area.

Cobalt analyses of 164ppm and 53ppm were obtained from the Quebrada del Verde and the Río Mollepungu (AB114 and AB3) respectively. All other samples contained 30ppm (AB131), or less, of this element.

Vanadium analyses were fairly variable up to a maximum of 348ppm but the following rivers contained more than 150ppm: Quebrada Las Pavas (AB13, 157ppm); Río Dumari (AB14, 348ppm); Río Chilola (AB17, 150ppm); Quebrada Cerro Azul (AB18, 322ppm); Río Naranjo (AB155, 175ppm) and Quebrada San Joaquín (AB167, 162ppm).

Molybdenum, tin and tungsten

Molybdenum analyses were all less than 10ppm (detection limit) with the exception of samples AB2 (74ppm) and AB3 (128ppm) collected from the Ríos Vivar and Mollepungu.

Tin analyses were mostly less than 20ppm (detection limit). Samples AB69, AB92, AB96, AB97 and AB101 gave values of between 21 and 26ppm.

Tungsten analyses were all less than 20ppm (detection limit) with the exception of sample AB3 (405ppm), collected from the Río Mollepungu.

Lanthanum and yttrium

Lanthanum analyses varied between less than 1 and 432ppm. All of the high values (>100ppm) appear to be associated with the granitoids of the El Oro metamorphic complex and possibly reflect the presence of a rare earth element-enriched mineral, such as monazite, in these rocks.

In the south-east, the following rivers, which drain the Moromoro granitoid complex, has enhanced lanthanum values (>100ppm): Quebrada Guayacán (AB42, 138ppm); Quebrada San Luis (AB43, 110ppm); Quebrada La Garganta (AB79, 244ppm); Quebrada El Guarumo (AB106, 117ppm); Quebrada Bruno and tributary (AB108, AB109, 260-134ppm); Quebrada Tahuín Chico (AB111, 169ppm); Quebrada Canoas (AB112, 432ppm) and Quebrada Cañas (AB113, 290ppm) (see also in the south-west AB97, AB103 and AB160). In the north-east the following rivers, which drain the Quera Chico (granitoid) unit of the Palenque mélange division, also had lanthanum values of more than 100ppm: Río Casacay and tributary (AB10, AB118, 146 to 161ppm); Río Dumari (AB122, 233ppm) and an unnamed tributary of the Río Quera (AB138, 103ppm).

Yttrium analyses ranged from 3 to 64ppm and, as with lanthanum, the majority higher values (>20 ppm) appear to be associated with the granitoids of the El Oro metamorphic complex. In the south, the following rivers, which drain the Moromoro granitoid complex, carried more than 25ppm of yttrium: Quebrada Guayacán (AB42, 32ppm); Quebrada San Luis (AB43, 29ppm); Quebrada Platanillo (AB60, 28ppm); Quebrada La Garganta (AB79, 38ppm); Quebrada El Salado (AB103, 29ppm); Quebrada El Guarumo (AB106, 37ppm); Quebrada Bruno and tributaries (AB108, AB109 and AB110, 30-33ppm); Quebrada Tahuín Chico (AB111, 31ppm); Quebrada Canoas (AB112, 64ppm); Quebrada Cañas (AB113, 56ppm) and Quebrada Palmales (AB172, 28ppm). In the north-east, the following rivers, which drain the Quera Chico (granitoid) unit of the Palenque mélange division, also had values of yttrium greater than 25ppm: Río Casacay and tributary (AB10 and AB118, 35-29ppm) and the Río Dumari (AB122, 44ppm).

Although, perhaps of limited economic significance, the high values of lanthanum and yttrium in the Quera Chico and La Bocana units are of interest since they suggest a geochemical correlation between these units, which supports deductions made elsewhere in this report.

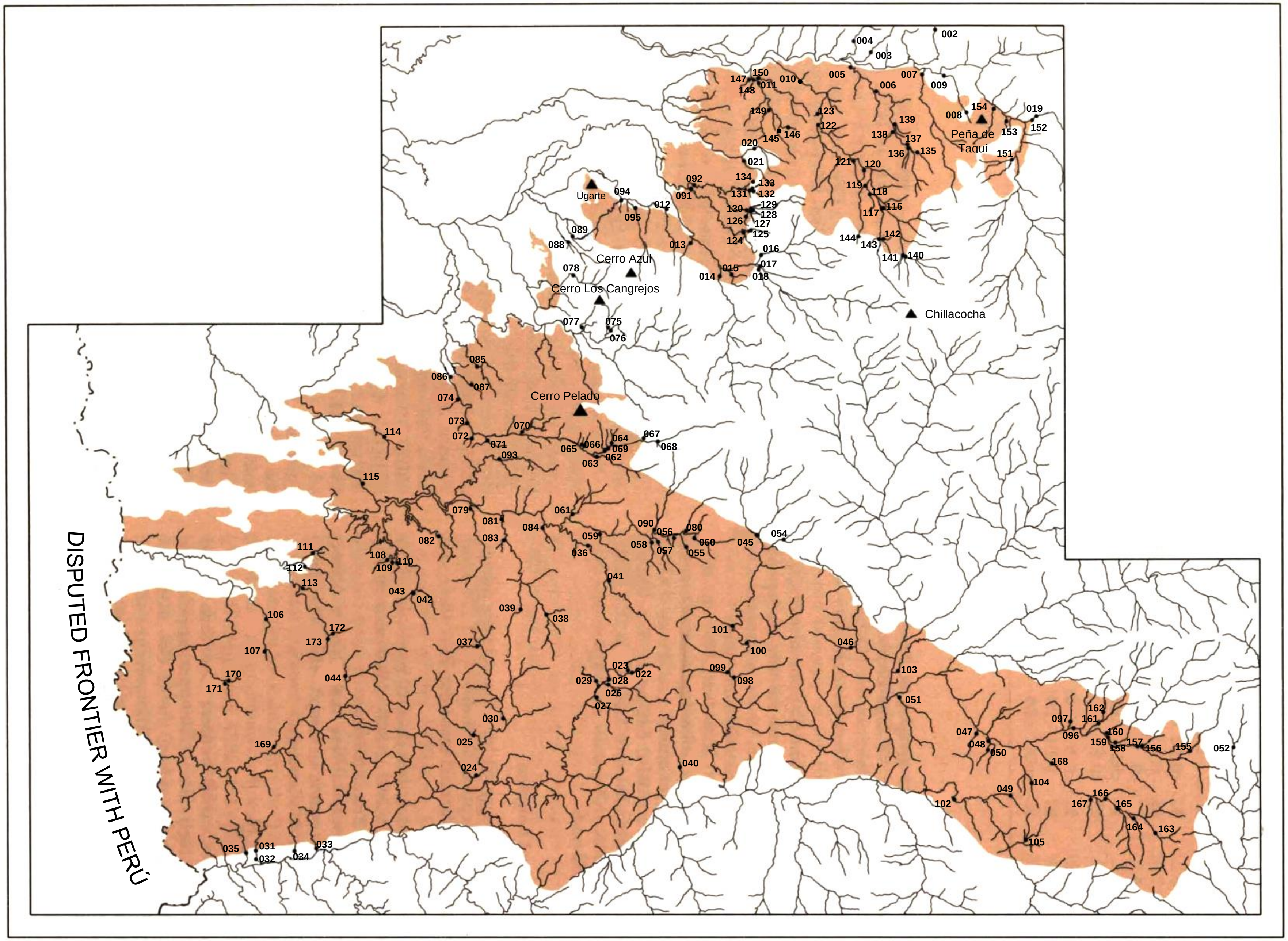

Figure 32. Stream sediment sample location map

REFERENCES

Most of the references listed below are held in the Library of the British Geological Survey at Keyworth, Nottingham. Copies of the references can be purchased subject to the current copyright legislation.

ALMEIDA E. (1977) Límite inferior de metamorfismo del Grupo Tahuín, Provincia de El Oro. Tesis no publicada, Escuela Politécnica Nacional, Quito, 126 pp. (unpublished).

ASPDEN J.A., FORTEY N., LITHERLAND M., VITER F. and HARRISON S.M. (1992a) Regional S-type granites in the Ecuadorian Andes: possible remnants of the breakup of western Gondwana. *Journal of South American Earth Sciences,* Vol. 6, No.3, 123-132.

ASPDEN J.A., HARRISON S.M. and RUNDLE C.C. (1992) New geochronological control for the tectono-magmatic evolution of the metamorphic basement, Cordillera Real and the El Oro Province of Ecuador. *Journal of South American Earth Sciences,* Vol. 6, 112, 77-96.

ASPDEN J.A. and LITHERLAND M. (1992) The geology and Mesozoic collisional history of the Cordillera Real, Ecuador. *In* Andean geodynamics. OLIVER R.A., VATIN-PERIGNON N. and LAUBACHER G. (editors) *Tectonophysics,* Vol. 205, 187-204.

ASPDEN J.A., LITHERLAND M., DUQUE P., SALAZAR E., BERMÚDEZ R., and VITERI F. (1987) Un nuevo cinturón ofiolítico en la Cordillera Real, Ecuador, y su posible significación regional. *Politécnica (Quito), Monografía de Geología,* Vol. XII, No. 2, 81-94.

ASPDEN J.A., LITHERLAND M. and SALAZAR E. (1988) Una interpretación preliminar de la historia colisional del centro y sur del Ecuador y posibles controles para la geología cenozoica y de mineralización polimetálicas. *Politécnica (Quito), Monografía de geología,* Vol. XII, No. 3, 49-76.

ASPDEN J.A., and McCOURT W.J. (1986) A Mesozoic oceanic terrane in the Central Andes of Colombia. *Geology,* Vol. 14, 415-418.

ASPDEN J.A., McCOURT W.J. and BROOK M. (1987a) Geometrical control of subduction-related magmatism: the Mesozoic and Cenozoic plutonic history of Western Colombia. *Journal of the Geological Society of London,* Vol. 144, 893-905.

BALDOCK J.W. (1982) Geología del Ecuador. Boletín de la Explicación del Mapa Geológico (1:1000000) de la República del Ecuador. Ministerio de Recursos Naturales y Energéticos, Dirección General de Geología y Minas, Quito, Ecuador, 54pp.

BERTHÉ D., CHOUKRONE P. and JEGOUZO P. (1979) Orthogneiss, mylonite and non-coaxial deformation of granites, the example of the South American Shear Zone. *Journal of Structural Geology,* Vol. 4, 31-42.

BILLINGSLEY P. (1926) Geology of the Zaruma Gold District of Ecuador. *Transactions of the American Institute of Mining Engineers,* Vol. 74, 255-277

CASTRO A., MORENO-VENTAS I. and DE LA ROSA J.D. (1991) H-type (hybrid) granitoid: a proposed revision of the granite-type classification and nomenclature. *Earth Science Review,* Vol. 31, 237-253.

CHAPPELL B.W. and WHITE A.J.R. (1974) Two contrasting granite types. *Pacific Geology,* Vol. 8, 173-174.

COBBING E.J., PITCHER W.S., WILSON J.J., BALDOCK J.W., TAYLOR W.P., McCOURT J.W. and SNELLING J.T. (1981) The geology of the Western Cordillera of northern Perú. *Overseas Memoir of the Institute of Geological Sciences,* No. 5, 143 pp.

CROWELL J.C. (1979) The San Andres fault system through time. *Journal of the Geological Society of London,* Vol. 136, 293-302.

DALY M.C. (1989) Correlation between Nazca-Farallón plate kinematics and forearc basin evolution in Ecuador. *Tectonics,* Vol. 8, No. 4, 769-790.

D' LEMOS R.S., BROWN M. and STRACHAN R.A. (1992) Granite magma generation, ascent and emplacement within a transpressional orogen. *Journal of the Geological Society of London,* Vol. 149, 487-490.

DUQUE P. (1993) Metamorphic history and structure of the El Oro ophiolitic complex, Ecuador. Andean Geodynamics, ORSTOM/University of Oxford, Oxford 21-23 Sept 1993, Extended Abstracts volume, 359-362.

DUQUE P. (1992) Condiciones de formación de las rocas metamórficas de alta presión de la Formación Raspas. *Boletín Geológico Ecuatoriano,* Vol. 3, No. 1, 63-78.

DUQUE P. (1975) Petrogénesis de unas rocas metamórficas de alta presión en la Provincia de El Oro. Tesis inédita, Escuela Politécnica Nacional, Quito, 66pp. (unpublished).

DUQUE P. and FEININGER T. (1974) Eclogitas y esquistos azules de la Provincia de El Oro, Ecuador. Memorias Simposio sobre ofiolitas. Universidad Nacional Medellín, Colombia, 35-38 (abstract).

EWART A. (1982) The mineralogy and petrology of Tertiary-Recent orogenic volcanic rocks: with special reference to the andesitic-basaltic compositional range. 25-87 in *Andesites.* THORPE, R.S. (editor). (New York: John Wiley and Sons).

FEININGER T. (1987) Allochthonous terranes in the Andes of Ecuador and northwestern Perú. *Canadian Journal of Earth Sciences,* Vol. 24, No. 2, 266-278.

FEININGER T. (1982) Glaucophane schist in the Andes at Jambaló, Colombia. *Canadian Mineralogist,* Vol. 20, 41-47.

FEININGER T. (1980) Eclogite and related high-pressure regional metamorphic rocks from the Andes of Ecuador. *Journal of Petrology,* Vol. 21, 107-140.

FEININGER T. (1978) Geologic map of western El Oro Province. 1:50000. Escuela Politécnica Nacional, Quito, Ecuador.

FEININGER T. and SILBERMAN M.L. (1982) K-Ar geochronology of basement rocks on the northern flank of the Huancabamba deflection, Ecuador. *United States Geological Survey, Open-File Report,* No. 83-206, 21pp.

FORTEY N.J. and GILLESPIE M.G. (1993) Internal Assessment of geochemical analyses of igneous rocks from Ecuador. *Report of the British Geological Survey, Keyworth, Nottingham, UK,* 100pp. (unpublished).

GANSSER A. (1973) Facts and theories on the Andes. *Journal of the Geological Society of London,* Vol. 129, 93-131.

HANMER S. and PASSCHIER C. (1991) Shear-sense indicators: a review. *Geological Survey of Canada, Paper,* No. 90-17, 72pp.

HARRINGTON J. (1957). Varios aspectos de las investigaciones de las posibilidades mineras de las provincias de Azuay y Cañar. Archivo Servicio Nacional de Geología y Minas (Quito), Informe H, 19pp. (unpublished).

HONNOREZ J., MÉVEL C. and MONTIGNY R. (1984) Occurrence and significance of gneissic amphibolites in the Vema fracture zone, equatorial Mid-Atlantic Ridge. *In* Ophiolites and oceanic lithosphere. GASS I.G., LIPPARD S.J. and SHELTON A.W. (editors). *Special Publication of the Geological Society of London,* No. 13, 121-130.

HUTTON D.H.W. and REAVY R.J. (1992) Strike-slip tectonics and granite petrogenesis. *Tectonics,* Vol. 11, No. 5, 960-967.

INEMIN-MISIÓN BELGA (1989) Estudios del yacimiento de cobre porfídico de Chaucha, Ecuador. Open-file report, INEMIN, Quito, 334 pp. (unpublished).

INEMIN-AGCD-ABOS (1988) Inventario, clasificación y metalogenia de las mineralizaciones polimetálicas en el Ecuador. Open-file report, INEMIN, Quito, 278pp. (unpublished).

JAILLARD E., SOLER P., CARLIER G. and MOURIER T. (1990) Geodynamic evolution of the Northern and Central Andes during early to middle Mesozoic times: A Tethyan model. *Journal of the Geological Society of London,* Vol. 147, 1009-1022.

KELSEY C.H. (1965) Calculation of the CIPW norm. *Mineralogical Magazine,* Vol. 34, 275-282.

KENNERLEY J.B. (1980) Outline of the geology of Ecuador. Institute of Geological Sciences. *Overseas Geology and Mineral Resources,* No. 55, 20pp.

KENNERLEY J.B. and ALMEIDA L. (1975) Mapa Geológico del Ecuador, Loja, Hoja 56 (1:100000). Dirección General de Geología y Minas, Quito.

KENNERLEY J.B., ALMEIDA L. and CALLE J. (1973) Mapa geológico del Ecuador, Saraguro, Hoja 55 (1:100000). Dirección General de Geología y Minas, Quito.

KROHE A. (1991) Emplacement of synkinematic plutons in the Variscan Odenwald (Germany) controlled by transtensional tectonics. *Geologische Rundschau,* Vol. 80, No. 2, 391-409.

LE BAS M.J., LE MAITRE R.W., STRECKEISEN A. and ZANETTIN B. (1986) A chemical classification of volcanic rocks based on the total alkali-silica diagram. *Journal of Petrology,* Vol. 27, 745-750.

LEGGETT J.K. (editor) (1982) Trench-forearc geology: sedimentation and tectonics on modern and ancient active plate margins. *Special Publication of the Geological Society of London,* No. 10, 576 pp.

LISTER G.S. and SNOKE A.W. (1984) S-C- mylonites. *Journal of Structural Geology,* Vol. 6, 617-683.

LITHERLAND M., ASPDEN J.A. and JEMIELITA R.A. (1994) The metamorphic belts of Ecuador. *Overseas Memoir of the British Geological Survey,* No. 11.

LITHERLAND M. and ASPDEN J.A. (1992) Terrane-boundary reactivation: a control on the evolution of the Northern Andes. *Journal of South American Earth Sciences,* Vol. 5, No. 1, 71-76.

MARTÍNEZ M. (1970) Geología del basamento Paleozoico en las Montañas de Amotape y posible origen del petróleo en las rocas Paleozoicas del noreste de Perú. *Lima 1° Congreso Latinoamericano de Geología,* No. 2, 105-138.

McCOURT W.J., ASPDEN J.A. and BROOK M. (1984) New geological and geochronological data from the Colombian Andes: continental growth by multiple accretion. *Journal of the Geological Society of London,* Vol. 141, 831-845.

MEGARD F. (1989) The evolution of the Pacific Ocean margin in South America north of the Arica Elbow (18°S). *In* The evolution of the Pacific Ocean margins. ZVI BEN-AVRAHAM (editor). *Oxford Monographs on Geology and Geophysics,* Vol. 8, 208-230.

MIYASHIRO A. (1972) Pressure and temperature conditions and tectonic significance of regional ocean floor metamorphism. *Tectonophysics,* Vol. 13, 141-159.

MIYASHIRO A. (1961) Evolution of metamorphic belts. Journal of Petrology, Vo. 2, 277-311.

MORA I.M. (1988) Petrología estructural de la Formación Raspas, Provincia de El Oro. Tesis no publicada, Escuela Politécnica Nacional, Quito, 159pp. (unpublished).

MOURIER T., LAJ C., MEGARD F., ROPERCH P., MITOUARD P. and FARFÁN-MEDRANO A. (1988) An accreted continental terrane in northwestern Perú. *Earth and Planetary Science Letters,* Vol. 88, 182-192.

MOURIER T. (1988) La transition entre Andes marginales et Andes cordilleraines a ophiolites : évolution sédimentaire, magmatique et structurale du relais de Huancabamba (3° à 8° Lat S ; Nord, Pérou Sud Equateur). Université de Paris-Sud, Centre D'Orsay, PhD thesis, unpublished.

NACSN (1983) North American Commission on Stratigraphic Nomenclature. *American Association of Petroleum Geologists,* Vol. 67, D841-875.

NOBLE S.R., ASPDEN J.A. JEMIELITA R. and LITHERLAND M. (1994) U-Pb geochronology of the Cordillera Real and the El Oro Provinces, Ecuador. *In* Abstracts of the Eighth International Conference on Geochronology, Cosmochronology and Isotope Geology, Berkeley California, 234.

OWENS B. (1992) Palynological Investigation of Ecuador samples collected by M. Woods, 1991. *Internal Report, British Geological Survey, Biostratigraphy and Sedimentology Group,* WH/92/157R, 34 pp.

PEARCE J.A. (1983) Role of sub-continental lithosphere in magma genesis at active continental margins. 230-272 in *Continental basalts and mantle xenoliths*. HAWKESWORTH C.J. and NORRY N.J. (editors). (Nantwich, UK: Shiva Publishing).

PEARCE J.A., HARRIS N.B.W. and TINDLE A.G. (1984) Trace element discrimination diagrams for the tectonic interpretation of granitic rocks. *Journal of Petrology,* Vol. 5, 956-983.

PEARCE J.A., LIPPARD S.J. and ROBERTS S. (1984a) Characteristics and tectonic significance of supra-subduction zone ophiolites. *In* Marginal basin geology. KOKELAAR B.P. and HOWELLS N.F. (editors). *Special Publication of the Geological Society of London,* Vol. 16, 77-96.

PEARCE J.A. and CANN J.R. (1973) Tectonic setting of basic volcanic rocks determined using trace element analyses. *Earth and Planetary Science Letters,* Vol. 19, 290-300.

PITCHER W.S. (1983) Granite type and tectonic environment. 19-40 in *Mountain building processes*. Hsu, K (editor). (London Academic Press).

PITCHER W.S. (1979) The nature, ascent and emplacement of granitic magmas. *Journal of the Geological Society of London,* Vol. 136, 627-662.

PLATT J.P. (1986) Dynamics of orogenic wedges and the uplift of high-pressure metamorphic rocks. *Bulletin of the Geological Society of America,* Vol. 97, 1037-1053.

PLATT J.P. (1987) The uplift of high-pressure-low-temperature metamorphic rocks. *Philosophical Transactions of the Royal Society, London,* No. A321, 87-102.

REAVY R.J. (1989) Structural controls on metamorphism and syn-tectonic magmatism: the Portuguese Hercynian collision belt. *Journal of the Geological Society of London,* Vol. 146, 649-657.

SEVILLA J. (1976) Geología del sector entre Piedras y Marcabelí, Provincia de El Oro. Tesis inédita, Escuela Politécnica Nacional, Quito, 55 pp. (unpublished).

STRECKEISEN A. (1976) To each plutonic rock its proper name. *Earth Science Reviews,* Vol. 12, 1-33.

STRONG D.F. and HANMER S.K. (1981) The leucogranites of southern Brittany: origin by faulting, frictional heating, fluid flux and fractional melting. *Canadian Mineralogist,* Vol. 19, 163-176

SYLVESTER A.G. (1988) Strike-slip faults. *Bulletin of the Geological Society of America,* Vol. 100, 1666-1703

UNDP (1972) Survey of metallic and non-metallic minerals (Phase II). Exploration for metallic minerals in south Ecuador, Loja, the El Oro, Operation No.8, Systematic geochemical exploration and geological reconnaissance. *Technical Report, United Nations Development Programme, New York,* No. 13.

VAN THOURNOUT F., HERTEGEN J. and QUEVEDO L. (1992) Allochthonous terranes in north western Ecuador. *In* Andean geodynamics. OLIVER R.A., VATIN-PERIGNON N., and LAUBACHER G. (editors). *Tectonophysics,* Vol. 205, 205-222.

VAN THOURNOUT F., VALENZUELA G., MERLYN M. and SALEMINK J. (1991) Portovelo-mineralización epitermal en relación con una caldera. *Boletín Geológico Ecuatoriano,* Vol. 2, No. 1, 13-26.

WALLIS F. (1944) Reconnaissance survey of contact between metamorphics and volcanics province of the El Oro. *Río Tinto Zinc (Quito), Internal Report,* 9pp.

WICKHAM S.M. (1987) Crustal anatexis and granitic petrogenesis during low-pressure regional metamorphism: The Trois Seigneurs Massif, Pyrenees, France. *Journal of Petrology,* Vol. 28, No 1, 127-169.

WINCHESTER J.A. and FLOYD P.A. (1977) Geochemical discrimination of different magma series and their differentiation products using immobile elements. *Chemical Geology,* Vol. 20, 325-343.

WOODCOOK N.H. (1986) The role of strike-slip faults at plate boundaries. *Philosophical Transactions of the Royal Society of London,* No. A317, 13-29.

YARDLEY W.D. (1989) An introduction to metamorphic petrology. Longman Earth Science Series (New York: John Wiley and Sons Inc.).

ZAMORA A. and POTHE DE BALDIS E. (1988) Nuevos aportes al conocimiento del Paleozoico del Ecuador. *Minería Ecuatoriana (INEMIN, Quito),* No. 1, 54.

OGMR 67

The El Oro metamorphic complex, Ecuador: geology and economic mineral deposits

J A Aspden, W Bonilla and P Duque

BRITISH GEOLOGICAL SURVEY

The full range of Survey publications is available from the BGS Sales Desk at the Survey headquarters, Keyworth, Nottingham. The more popular maps and books may be purchased from BGS-approved stockists and agents and over the counter at the Bookshop, Gallery 37, Natural History Museum, Cromwell Road, (Earth Galleries), London. Sales Desks are also located at the BGS London Information Office, and at Murchison House, Edinburgh. The London Information Office maintains a reference collection of BGS publications including maps for consultation. Some BGS books and reports may also be obtained from HMSO Publications Centre or from HMSO bookshops and agents.

The Survey publishes an annual catalogue of maps, which lists published material and contains index maps for several of the BGS series.

The British Geological Survey carries out the geological survey of Great Britain and Northern Ireland (the latter as an agency service for the government of Northern Ireland), and of the surrounding continental shelf, as well as its basic research projects. It also undertakes programmes of British technical aid in geology in developing countries as arranged by the Overseas Development Administration.

The British Geological Survey is a component body of the Natural Environment Research Council.

Natural Environment Research Council

ISBN 0-85-272242-7

ISBN 0 85 272242 7

Price code GZ